Enhanced local voltage control of active distribution networks with high penetration of PVs

A Thesis submitted to The University of Manchester for the degree of

Doctor of Philosophy

in the Faculty of Science & Engineering

2021

MELIKE SELCEN AYAZ

SCHOOL OF ENGINEERING

DEPARTMENT OF ELECTRICAL & ELECTRONIC ENGINEERING

Lists of Contents

List of Tables

List of Figures

List of Abbreviations

ADN	Active Distribution Network
APC	Active Power Curtailment
BESS	Battery Energy Storage System
CDF	Cumulative Distribution Function
CIG	Converter Interfaced Generation
DERs	Distributed Energy Resources
DG	Distributed Generator
DNO	Distribution Network Operator
DSO	Distribution System Operator
ENTSO-E	European Network of Transmission System Operators for Electricity
ESS	Energy Storage System
EV	Electric Vehicle
FACTS	Flexible AC Transmission Systems
FC	Fixed Capacitor
HC	Hosting Capacity
IEC	International Electro technical Commission
IEEE	Institute of Electrical and Electronics Engineers
IRENA	International Renewable Energy Agency
kW	Kilowatt
MCS	Monte Carlo Simulation
MPPT	Maximum Power Point Tracking
MVA	Mega Volt Amp
NG	National Grid
OLTC	On Load Tap Changer
PCC	Point of Common Coupling
PDF	Probability Density Function
PEs	Power Electronics
PLL	Phase-Locked Loop
PF-Power	Active Power Dependent Power Factor Control
PV	Photovoltaic
Q-voltage	Voltage Dependent Reactive Power Control

RES	Renewable Energy Source
RMS	Root Mean Square
RPC	Reactive Power Compensation
RWM	Roulette Wheel Mechanism
SP	Stochastic Programming
SG	Synchronous Generator
STATCOM	Static Synchronous Compensator
SVC	Static VAR Compensator
SVR	Static Voltage Regulator
WT	Wind Turbine
WTG	Wind Turbine Generator

Nomenclature

Parameters

I_{ln}	Line nominal current
P_{pvn}	PV system nominal active power
PF_{over}	PV over-excited power factor limit
PF_{pvn}	PV system nominal power factor
PF_{under}	PV under-excited power factor limit
Q_{over}	PV over-excited reactive power limit
Q_{pvn}	PV system nominal reactive power
Q_{under}	PV under-excited reactive power limit
R_l	Line resistance
R_v	PV voltage droop gain
S_{pvn}	PV system nominal apparent power
S_{trn}	Transformer nominal apparent power (kVA)
uk	Transformer short-circuit voltage (%)
V_{hvn}	Transformer high voltage (HV)-side nominal voltage (kV)
V_{lvn}	Transformer low voltage (LV)-side nominal voltage (kV)
V_{max}	Bus voltage magnitude upper limit ($p.u.$)
V_{min}	Bus voltage magnitude lower limit ($p.u.$)
V_{ref}	Bus reference voltage magnitude ($p.u.$)
X_l	Line reactance

Variables

P_{ld}	Load active power
P_{pv}	PV system active power
Q_{ds}	Down-stream reactive power
Q_{ld}	Load reactive power
Q_{lim}	PV system reactive power limit
Q_{pv}	PV system reactive power
Q_{us}	Up-stream reactive power
S_{tr}	Transformer apparent power
V_b	Bus voltage magnitude (*p.u.*)
$\bar{V}_b$	Bus voltage vector
V_g	Grid voltage magnitude (*p.u.*)
$\bar{V}_g$	Grid voltage vector
δ	Bus voltage angle
ΔV_b	Bus voltage magnitude deviation (*p.u.*)
$\bar{I}_l$	Line current vector
φ	Line current angle
α, β	Shape parameters for Beta Distribution Function
NT	Number of time intervals
NP	Number of PV units
P_{pv}	PV system active power
Q_{lim}	PV system reactive power limit
Q_{pv}	PV system reactive power
Q_{us}	Up-stream reactive power
S_{tr}	Transformer apparent power

Abstract

The main goal of this thesis is to overcome voltage related problems with increased penetration of photovoltaics (PVs) in the active distribution networks (ADNs). Hence, the thesis aims to develop a novel voltage controller to act in a decentralized local control strategy to regulate voltage, to enhance the hosting capacity of ADNs. Moreover, the developed problem formulation is extended to consider the stochastic nature of PV power output and load demand for higher accuracy of the results.

In modern power systems, where a considerable number of converter interfaced generation (CIG) units (e.g. PVs) are increasing, the conventional distribution networks face issues from voltage regulation aspects. The network faces overvoltage problems with increased PV generation in peak generation hours (midday). With increased PV generation in the network, especially at peak periods of generation and low demand, there will be a massive amount of reactive power flow from distribution towards the upstream network. This leads to an increase in grid losses on the network, and also requires greater capacity in system components. ADNs are introduced to contribute to the voltage regulation with the high participation of intermittent renewable energy resources in the system, instead of using conventional grid reinforcement.

This thesis proposes a decentralised voltage control strategy to enable a further amount of PVs in the system without exceeding pre-defined limits. The work aims to tackle the problems in previous local voltage control methods in literature (PF-power and Q-voltage methods). Previous methods are not able to overcome the overvoltage issues and tend to increase the grid losses, especially with high penetration of PVs in ADNs. Towards addressing the voltage related concerns, a computationally efficient algorithm is developed to minimize reactive power flow through the network electrical bottlenecks. In the proposed approach, all controllers are implemented locally, where the communication devices are eliminated, mitigating the investment cost significantly.

Another challenge in the future ADNs is related to the stochastic characteristics of PVs and loads, where, the deterministic approaches may not reach to desired accuracy results with the limited number of time-domain simulations. The current state-of-the-art studies need further consideration for PV power output and load demand when defining the uncertainty. With a scenario generation based technique, the system uncertainties, PV generation output and load demand, have been probabilistically modelled and studied with Monte Carlo Simulations. The generation scenarios are reduced to a number of scenarios that is enough to represent the desired variety of samples, and simulations are carried out for these scenarios.

To investigate the practicality and scalability of the proposed approach, the proposed methodology has been applied to 33-nodes (radial) and 69-node (meshed and radial configurations) test feeders. The results prove that the developed controller can increase system hosting capacity by about 20% of the systems base power. Furthermore, network active power losses are considerably decreased by 30% concerning existing methods. Moreover, the transformer tap changer experiences fewer tap operations over a day. Thus, feeder hosting capacity can allocate more PVs in the ADN. Besides, the accuracy of results is improved with the stochastic assessment of uncertain values for each generated scenario. Consequently, a more accurate perspective is gained with the overall outcomes for enhancing hosting capacity in ADNs.

Declaration

No portion of the work referred to in the thesis has been submitted in support of an application for another degree or qualification of this or any other university or other institute of learning.

Copyright Statement

I. The author of this thesis (including any appendices and/or schedules to this thesis) owns certain copyright or related rights in it (the "Copyright") and s/he has given The University of Manchester certain rights to use such Copyright, including for administrative purposes.

II. Copies of this thesis, either in full or in extracts and whether in hard or electronic copy, may be made only in accordance with the Copyright, Designs and Patents Act 1988 (as amended) and regulations issued under it or, where appropriate, in accordance with licensing agreements which the University has from time to time. This page must form part of any such copies made.

III. The ownership of certain Copyright, patents, designs, trademarks and other intellectual property (the "Intellectual Property") and any reproductions of copyright works in the thesis, for example graphs and tables ("Reproductions"), which may be described in this thesis, may not be owned by the author and may be owned by third parties. Such Intellectual Property and Reproductions cannot and must not be made available for use without the prior written permission of the owner(s) of the relevant Intellectual Property and/or Reproductions.

IV. Further information on the conditions under which disclosure, publication and commercialization of this thesis, the Copyright and any Intellectual Property and/or Reproductions described in it may take place is available in the University IP Policy(see http://documents.manchester.ac.uk/DocuInfo.aspx?DocID=24420), in any relevant Thesis restriction declarations deposited in the University Library, The University Library's regulations (see http://www.library.manchester.ac.uk/about/regulations/) and in The University's policy on Presentation of Theses.

Acknowledgements

First of all, I appreciate all the help from my supervisor Vladimir Terzija, for his academic and wellbeing support overall my PhD. Secondly, I would like to take this opportunity to the people that ever assisted my research in the University of Manchester. Special thanks to my colleage Rasoul Azizipanah-Abarghooee for his endless support and encouragement throughout my PhD journey. He deserves a special mention for his belief in me and many discussions throughout my PhD. The completion of this PhD would also have not been thinkable without the generous help, advice, and support of Mostafa Malekpour.

In this journey, I am very thankful to my great family who always supported me with the choices I made in life. Any of the successes I have achieved would not have been accomplished without my biggest source of strength, my mum Fatma, my father Fatih and my sister Beyza. With their unconditional love and support from miles away, they were always there when I needed their support.

This research project would not have been possible without funding, so I would like to acknowledge the Turkish Ministry of higher Education.

I also want to thank all the amazing people I met for the past 4 years in Manchester, and made my PhD journey memorable, especially in the School of Electrical & Electronic Engineering, Ferranti Building. I am very happy that I participated in volunteering activities in IEEE PES Student Branch and CIGRE UK NGN. I would like to take this opportunity to thank Alex, Angeliki, Elif, Jane, Gaoyuan, Gulizar, Negar, Rasoul, Rafat, Onur, Ziyneti and many others helping me to set a work-life balance and always support me in this journey. Thanks to whoever supported and helped me during my journey towards the PhD.

I dedicate this PhD to my mother, who dedicated her PhD to her daughter, 25 years ago...

1. INTRODUCTION

Over the last decade, in the electrical power systems, conventional generation units have gradually been replaced by converter-interfaced generation (CIG) units, with the increased participation of renewable energy sources. The future distribution networks will be constituted by high proportions of solar and wind generation, controllable loads and energy storage systems where the management will be provided smartly. Renewable energy sources are largely installed at the distribution level, introducing new challenges to the distribution systems [1]. To be able to deliver the energy produced by the renewable energy sources efficiently, the power electronic (PE) devices are used. The PE interface technology is used to integrate the renewables e.g. wind and solar, to the power system, which allows the source of generation to provide voltage support to the network. However, this new technology has also brought several challenges for maintaining the power system stability from voltage and frequency aspects [2]. The stochastic characteristics of renewable energy sources (e.g. solar) and loads are expected to change the dynamic behaviour of the system. New active network control strategies are required for the system to cope with the intermittent renewable energy sources, which can lead to the deterioration of power systems steady-state and dynamic performance [3].

The focus of this research project was on challenges brought by the high penetration of PVs for voltage control in Active Distribution Networks (ADNs). With the integration of increased amount of PV power plants over time, voltage control is one of the critical aspects to be considered in the distribution network. Hence, the voltage regulation approaches for ADNs to deal with voltage related problems has become a highly investigated point of research in recent years. Due to the variable and uncertain characteristic of PVs, over-voltage problems arise at

distribution systems, primarily when the peak PV generation occurs. It leads to overloading of system components such as, lines, transformers, whereas also limits the further integration of PVs into the ADNs. To solve these issues, this thesis proposes a novel fully local voltage controller to regulate the voltage with the high integration of PVs. To achieve a simple, practical and decentralised control, this study proposes to control the voltage by partitioning the distribution network into several zones.

Another crucial challenge faced in the ADNs caused by the overvoltage at peak PV generation hours is the limitations on feeder hosting capacity. The hosting capacity is defined as the maximum PV generation that can be integrated into the network without violating standard limits for voltage, protection and power quality and with no feeder upgrades. Remarkably, the use of this novel controller will allow further integration of PVs to the system by enhancing the hosting capacity of the feeder without using communication infrastructure. Finally, a stochastic approach has also been proposed in order to obtain more accurate results to enhance the feeder hosting capacity.

1.1. Background

The rise in global energy consumption has led to a massive climate change, and side effects on the environment, in parallel to the increase of fossil fuel consumption over the last century. The conventional energy sources that release greenhouse gases are evolving to be replaced by more efficient and cleaner sources, for instance, renewables. Wind and solar energy have become recognised energy sources and they are progressively competing with fossil fuel power plants.

The evolvement from synchronous generation (SG) technology towards the new technologies like renewables (e.g., wind and solar) are replacing SGs in the future power systems. The

unequal distribution of SG is represented in Figure 1-1, confirming that SG in the GB network will reduce its capacity over the near future [4].

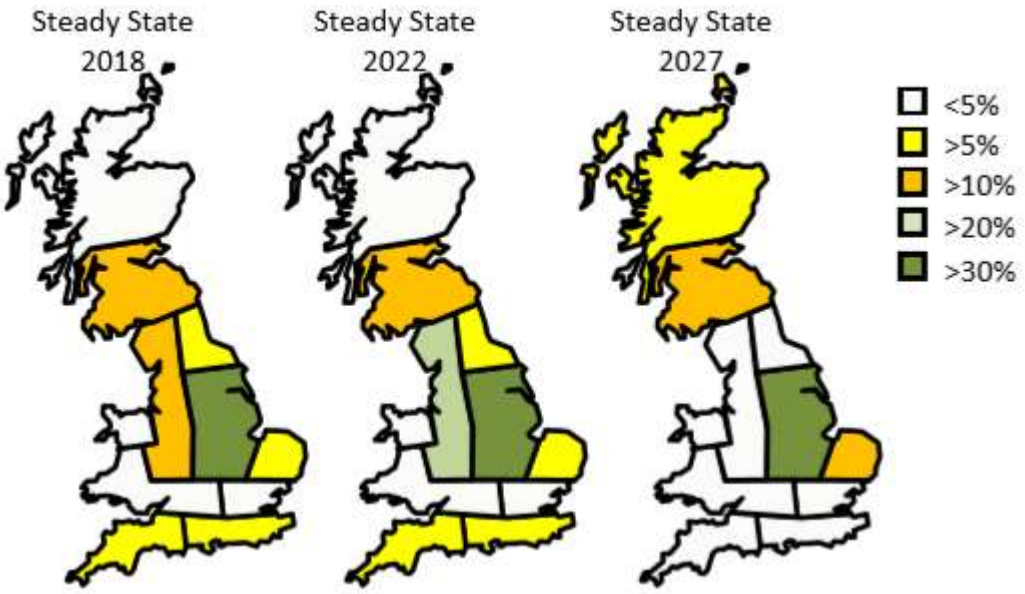

Figure 1-1. Overall Reduction in the SG capacity across UK [4]

According to the International Renewable Energy Agency (IRENA), wind and solar energy accounted for the most increase in generation over ten years scale (2010-2020), with capacities of 623 GW and 586 GW respectively [5]. Figure 1-2 represents the annual PV installations to the grid over the last ten years. There is a significant increase in PV installations over the previous years. Also, in 2019, the highest solar power capacity additions have been reached in a year, at 115 GW (DC) [6].

Table 1-1., illustrates the share of PV capacities globally. According to the statistics shown in Table 1-1 , at least 32 countries operational renewable power capacity exceeded 10 GW by the end of 2019, resulting in a total of 627 GW installed capacity [6].

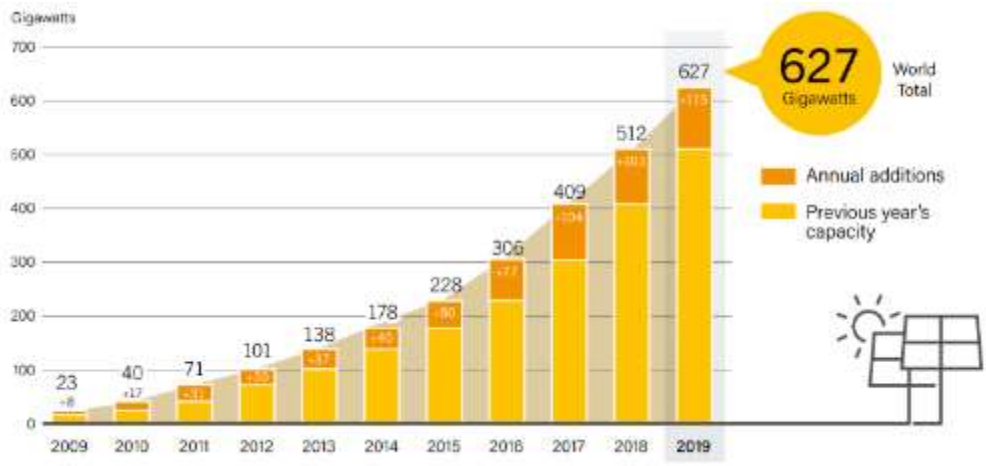

Figure 1-2.Annual PV installations in the past ten years (GW)

Table 1-1. Added PV capacity in the top 10 countries in 2019

Top Countries by Total Capacity			
	Total 2018 (GW)	Added 2019 (GW)	Total 2019 (GW)
China	175.4	30.1	204
United States	62.7	13.3	76
Japan	56	7	63
Germany	45.2	3.8	49
India	32.9	9.9	42.8
Italy	20.1	0.7	20.8
Australia	11	3.7	14.7
United Kingdom	13.1	0.3	13.4
Republic of Korea	8.1	3.1	11.2
Spain	5.2	4.8	9.9
Rest of World	**82.3**	**38.3**	**120.6**
World Total	**512**	**115**	**627**

For the UK, the annual energy demand is projected to increase by 4% by 2035. UK government aims to reduce the greenhouse gas emmissions by at least 68% by 2030, and 100% by 2050 to reach net zero emmissions. PV integration is playing a crucial role to implement this goal. To cope with the challenges of uncertainty, National Grid ESO has introduced four main future energy scenarios namely Consumer transformation, System transformation, Leading the way and Steady progression scenarios [7]. In System Transformation, Consumer Transformation and Leading the Way scenarios, up to 60% electricity generation is expected to be provided by renewables. Across all scenarios, the solar generation is expected to increase to massive penetration levels within the near future, shown in Figure 1-3.

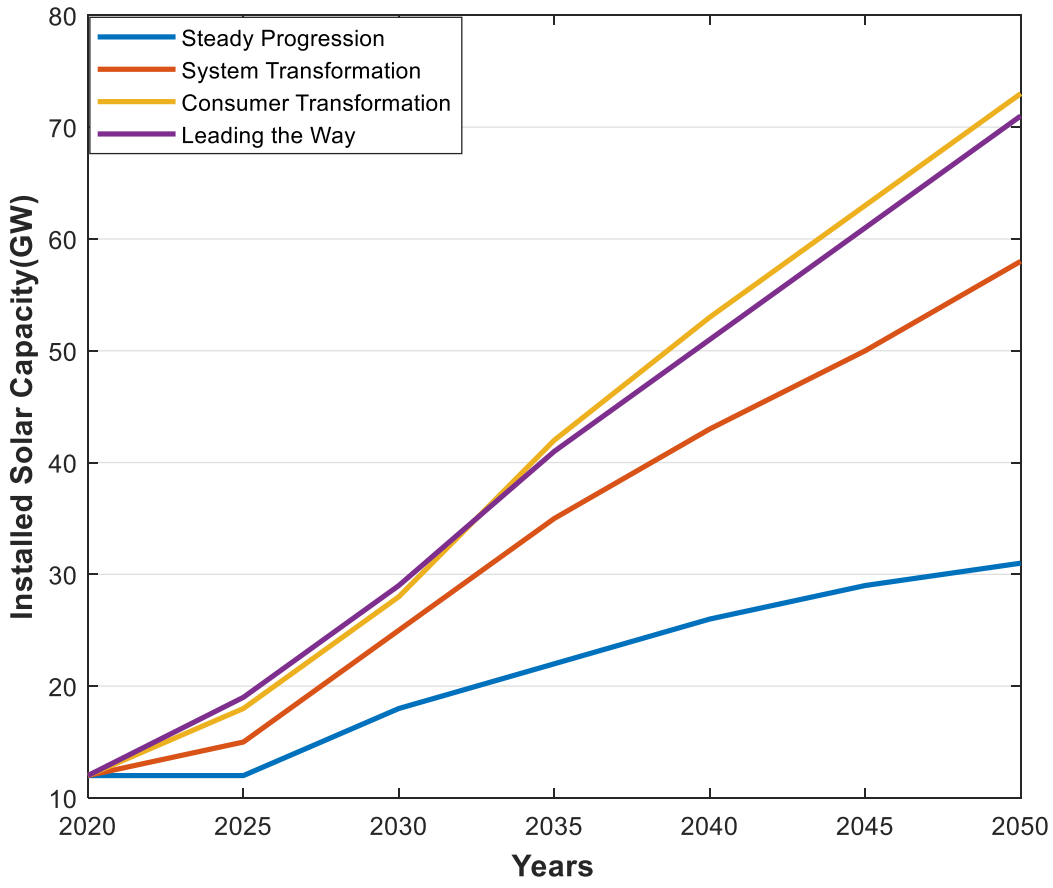

Figure 1-3. Future Scenarios for the solar capacity increase over the years in UK [7]

Voltage control is one of the critical aspects to be considered as the penetration of PVs in the distribution network increases. The PV power plants are mainly connected to the distribution

network in the GB. National Grid in the UK aims to increase voltage support resources in ADNs, primarily through PV inverters [8]. Distribution networks need to be actively managed, along with the consumers they serve, to cope with rapidly changing demands on the system. With the integration of PVs and other PE interconnected devices, there is a move from 'passive' to 'active' network operation.

While the growth in the solar generation is increasing in the power system, this technology brings new challenges to the power grid by the extended integration of PV power plants. Besides the advantages that PE interfaces allow the PVs participation in voltage control, however, there are some technical limitations such as, inverters capability, in this participation. The following chapters will address these challenges. Thus, the consideration of the voltage control should be focused on ADNs. To reach this target, the work focuses on the voltage control studies at the active distribution network.

1.2. Active Distribution Networks

Historically, ADNs were traditionally designed as a passive structure, which means having a unidirectional power flow (from generation to end-user). At present, when there is generation also in the distribution level, the excess power after meeting the consumers' demand, flows back to the upstream network (towards the high voltage). This excessive flow may result in the voltage to surpass the grid code voltage limits [9], which will be covered in Section 2.5.1.

Recently, as the conventional passive distribution systems are shifting towards ADNs, the system flexibility increases for power generation. However, properly deploying this flexibility is challenging as it requires coordination of a large number of assets owned by consumers and producers. This behaviour may introduce reverse power flows in the upstream network and, potentially, cause system component overloads such as, lines, transformers, etc. Furthermore, the distribution networks are shifting towards more complex topologies like meshed

configurations [10]. Understanding the potential future network topologies is required to properly develop strategies to integrate PV generation into the grid.

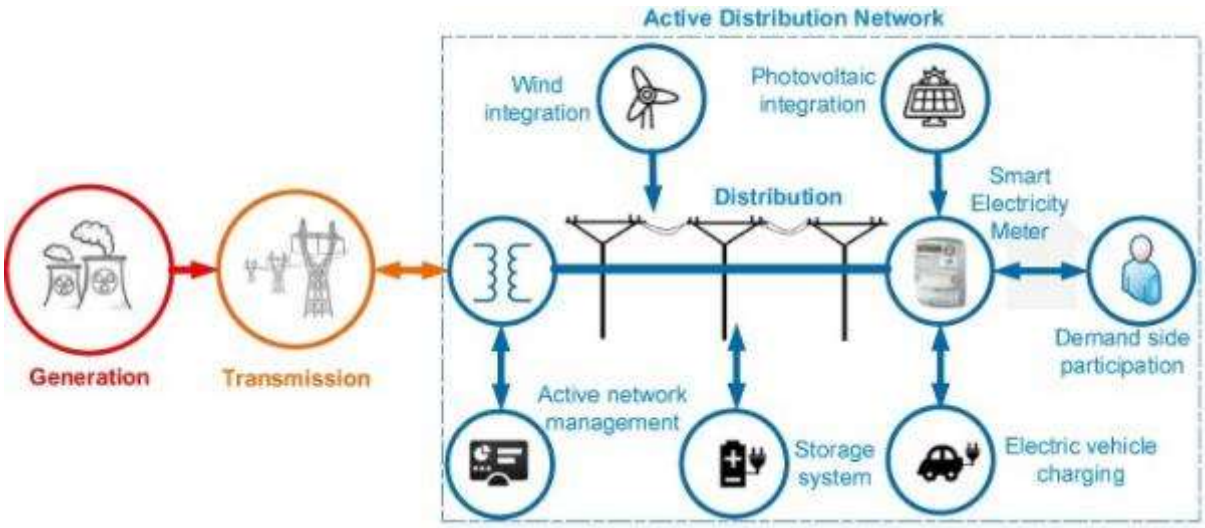

Figure 1-4. Structure of the active distribution networks [3]

Figure 1-4 represents a vision of the future ADNs with the integration of wind turbine, PV, electric vehicle (EV), storage, demand-side participation, and active network management. In distribution level, smart metering and demand side participation will be important aspects. On the other hand, the highlight of this thesis will be only on the high penetration of PVs impact over the ADNs. The increased integration of PV generation may affect the power system with variability & uncertainty during the continuous balancing of the system. Especially with the high PV integration to ADNs, the voltage control issues arise with some complications. Considering that PV peak generation occurs near noon when UK demand is generally low, large PV integration can lead to technical issues like voltage rise and thermal overloading for the system components (lines and transformers). Therefore, the reactive power and voltage control cannot be ignored for the operational behaviour of ADNs in terms of reaching the reliable and secure operation of power systems. Figure 1-5 shows the balance of active and reactive powers related to frequency and voltage in UK, respectively. Where the balance of

frequency is dependent to active power, the balance of voltage is dependent to reactive power. In typical, majorly reactive networks, the voltage is directly proportional to the reactive power, as an increase in reactive power leads to voltage increment and vice versa.

Figure 1-5. Active and reactive power balances [11]

Adequate voltage control can support PV integration, while deferring the need for costly network upgrades. According to the National Grid System operability framework report 2017 [11], additional reactive power absorption is required in most regions to regulate high voltages, especially with the increased power flows from the distribution network. Also, additional reactive power generation is needed in areas where power flows are large and volatile. Depending on the needs of the system, the voltage regulation can be provided from the PV inverters' reactive power capability. Voltage depends on the local balance between the reactive power supply and demand. Thus, the flexibility of PV inverters can be actively exploited by local reactive power management in future distribution networks.

1.2.1 Network Configurations

The distribution system functions to deliver the electrical energy from the transmission system having one path between the substation and each end user. A radial system is the most used architecture of a low voltage distribution system [12]. Radial topology has numerous advantages such as, being cheap, have an uncomplicated design & operation, to allocate more PV units [13]. On the other hand, parallel, ring or interconnected (mesh) systems are usually

preferred in transmission systems for increasing the reliability by providing [12] multiple routes for the end-users in case of fault occurrence. Hence, the grid network tends to be built underground, which significantly increases the cost of construction, repair, and maintenance. The distribution networks commonly have a high resistance to reactance R/X>>1 ratio which may cause voltage drops and rises within the bidirectional current flow. The higher resistance causes a higher voltage drop in the distribution feeder. Their high resistance to reactance (R/X) ratio makes voltage magnitudes to fluctuate more with changes in active power.

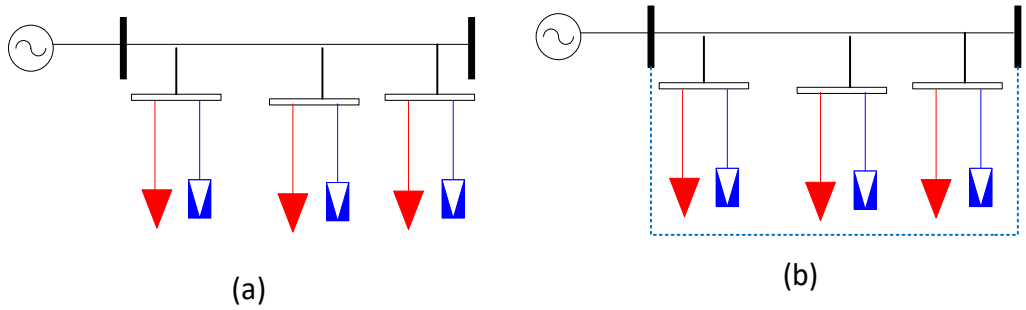

Figure 1-6 Network topologies: (a) Radial network, (b) Meshed network

The studied network topologies radial and meshed networks are illustrated in Figure 1-6 [14]. The highly meshed network is another challenging research to be investigated by the researchers in future. As the conventional radial distribution systems are also shifting towards meshed distribution systems, the system flexibility increases for power generation. In contrast, power flow control becomes more complex. Ref. [15] points out that weakly meshed networks can accommodate more distributed generation than radial feeders by creating more uniform power flows. However, further research for meshed network systems is needed for future grid studies. Also methods to reduce meshed networks' computational complexity should be investigated [16]. This is explored in greater detail in Chapter 5 of this thesis, where simulation studies are performed in radial and meshed ADNs.

1.3. Challenges of High Penetration of PVs in Active Distribution Networks

With the continuing growth of the Distributed Energy Resource (DER) capacity in power systems with inverter based connection, the new electrical grid tends to be more interactive, distributed and flexible. Nevertheless, with the increasing proportion of PVs in the ADNs, some technical challenges occur in voltage regulation. The high penetration of PV systems leads to new problems such as, overvoltage, overloading of transformers and lines and voltage unbalances.

In ADNs, meanwhile, the PV generation is high during peak times of the day, the excessive generation is surpassing consumers' need. Thus, the excess power will be transferred to the upstream network, creating some possible voltage problems [17]. These problems mainly occur at periods of maximum generation and minimum demand, resulting in reverse power flows. Therefore, the reactive power and voltage alteration cannot be ignored for the operational behaviour of ADNs in terms of the reliable and secure operation of power systems.

The challenges of the future grid raise the need to revise the current technical policies and regulatory changes in the power system. The technical authorities should also discuss further standardization of PVs integration to the grid where both consumers and transmission/distribution level participant should participate in the alteration of power systems. Most of the grid codes still need to update their guidelines for support schemes for solar PV and governing grid connections. Detailed information about grid code requirements will also be available in Chapter 2.

1.3.1. Technical Challenges

The technical challenges of utility power system both on PV and grid side are the ones considered for the safe operation of PV and to maintain the reliability of the grid. The technical

challenges arisen with the high penetration of PVs are power quality, voltage regulation, protection and stability issues [18].

1) Power Quality: Relative to the integration of PVs to the system, the power quality can be affected. A weak distribution grid is highly prone to be affected by the inverter-based generation. Loads connected closer to the PVs are supplied by these PVs, causing less power to flow from distribution substation. The power loss from the substation to the consumer may be reduced. Transient voltage variation and harmonic distortion of the network voltage are the other problems in the power system.

2) Stability: Stability of the system is a significant issue in the distribution network. The PV integration into ADNs can be discussed through the voltage level, demand and penetration levels. Even if the voltage control techniques don't promise very fast voltage regulation, the system stability should be kept within its permissible limits in a large system [19].

3) Voltage Regulation: The voltage produced by the PVs after the generation, needs to be controlled in an effective way to enhance the capability of the power system with high penetration of PVs. The control strategies consider the voltage regulation and loss reduction in distribution feeders.

In the transmission grid, reactive power change is mainly dependent on the load types in the system. If the grid has an increase in inductive loads, this will lead to a voltage drop at the consumption side, also affecting other bus bars in the distribution network. In this case, the conventional voltage regulation strategies will try to compensate this voltage drop by possible ways to control the voltage (mainly controlled by the OLTC (on-load tap changer). In case of a decrease in inductive loads, overvoltage would occur due to reactive power increase in the grid. After the occurrence of a disturbance in the system, load demand change or loss of

generators, the voltages at all buses should be stabilized according to the grid code requirements [20].

The most significant reason requiring voltage regulation in ADNs is that, the generation does not meet the power demand. The voltage needs to be regulated if the reactive power in a bus is increasing, although the bus voltage magnitude is decreasing. Overvoltage occurs when capacitive current flows through an inductive reactance. When the lines are inductive, in case a capacitor installed at the end of the line, a voltage rise will occur due to the capacitive flow over lines, especially when the load is low rated. In modern networks with high penetration of PVs connected to the same distribution feeder, the voltage at the end of the feeder will increase as well [21]. Further mathematical explanations are also presented in Chapter 2.

Another issue occurs if the reactive power flow from the distribution grid to the upstream grid is not managed correctly, the excessive reactive power released into the transmission network can cause high voltage issues. All the above mentioned problems discussed to suggest the reactive power should be consumed within the same generation units. The local voltage control strategies will be represented in detail in the following chapter with the introduction of reactive power control strategies.

1.3.2. Economic, Policy and Regulatory Challenges

The distribution system allows connecting almost any generation plants when the connection requirements are satisfied. The PV systems have experienced the fastest adaptation in distribution networks, also helped by a continuous cost decrease in the technology itself. PV systems can be implemented simply as rooftop installations, enabling access to the customers (including residential, commercial and industrial types). On the other hand, the policies and regulations considering the conventional generation should be redesigned [22]. In this study,

the current grid code requirements and other regulatory challenges will be taken into consideration.

1.4. Contributions of the Thesis

The research presented in this thesis has been performed to tackle the overvoltage issues in ADNs with high penetration of PV units. The work aims to develop a novel voltage controller to act in a decentralized local control strategy to regulate voltage. When carrying out the research, several aspects, such as configuration of the test systems given in Appendix A, and the uncertainties introduced by PVs and loads in the network will be evaluated. Therefore, the hosting capacity of ADNs is aimed to be improved without violating the system limits. The research gaps will firstly discuss about the drawbacks of the current literature studies. Secondly, the contributions section will highlight the work completed in this thesis to tackle the problems faced in the previous studies.

1.4.1. Identified Existing Research gaps:

The research presented in this thesis is performed to tackle the overvoltage issues in ADNs with high penetration of PV units. Before carrying on to the state of art of voltage control, the research gaps addressed in this thesis are listed as below:

1. The PV inverters have limitations to absorb/inject reactive power to the system subject of their inverter capabilities. With the increased PV penetration in ADNs, the reactive power strategies used in literature, are not practical enough to prevent the overvoltage issues, especially in peak PV generation times. The modified control strategies which can help to improve the hosting capacity with the integration of the PVs into the system are desired to comply with the allowable limits of grid code requirements.

2. The literature studies, do not consider the impacts of absorbing the reactive power on the system components. Most of the studies are focused on managing voltage issues with reactive power absorption. However, the PVs reactive power absorption leads to an increase in feeder transformer and line loading. Integrated, practical control is essential, aiming to respond systems need simultaneously. Absorbing the reactive power may drop the voltage, but the other critical overloading situations of the transformers and cable should also be taken into consideration.

3. Most of the centralized controller strategies require a higher level of supervisory control with communication infrastructure, which are not matching with the structure of future ADNs. The power system turns out to have some computational problems like timing and optimization difficulty. It will cause more troubles when the penetration level of PVs increase in a decentralized manner, in the system. All these reasons lead to design decentralized controller strategies for the ADNs in a practical, reliable and resilient way. In the proposed approach, all the controllers are implemented locally, and the communication devices are eliminated, mitigating the investment cost significantly.

4. The conventional radial distribution systems are also altering towards meshed distribution systems. However, there are limited studies for solving complex meshed systems containing high PV penetration levels, with current power flow algorithms in the literature. This work considers the implementation of the proposed controller on the meshed topology besides the radial ones in the distribution level. Moreover, the work ensures easy reconfiguration between radial and meshed topologies, by modifications on the studied test benchmarks.

5. There are limited examples in the literature investigating the stochastic characteristic of PV power output and load demand in ADNs. A detailed stochastic analysis will enable distribution system operators to consider certainty in their decisions when assuming voltage control by inverters. The development of a methodology to probabilistically test the system will also help identifying standards in the grid codes, suitable for higher PV penetration levels.

1.4.2. Thesis Contributions

Hosting Capacity Enhancement

This work uses analytical techniques to assess feeder hosting capacity with high penetration of PVs in ADNs. The hosting capacity in this thesis stands for the maximum PV generation that can be integrated into the network without violating standard limits for voltage, protection and power quality and with no feeder upgrades. The PVs outgrowth in the distribution system has also introduced the use of their capabilities to enhance the hosting capacity. That means that the PV systems reactive power capability can provide voltage support to rise the feeder's hosting capacity alternatively. The studies will allow to inspect the ways to increase the PV penetration where performance criteria for developing the feeder's hosting capacity are defined in terms of the network losses and the transformer/branches loading.

The work highlighting this contribution was published in the following journal; M. Selcen Ayaz, M. Malekpour, R. Azizipanah-Abarghooee and V. Terzija, "Local photovoltaic reactive power controller for increasing active distribution networks hosting capacity," in IET Generation, Transmission & Distribution, vol. 14, no. 22, pp. 5152-5162, 13 11 2020, doi: 10.1049/iet-gtd.2020.0649.

Decentralised control

In this work, implementation of a comprehensive decentralised voltage control approach proposes exclusively local management to increase the feeder hosting capacity. The study primarily focuses on managing the power flow within the PV units locally. The system complexity tends to grow with the highly decentralised fashion of PVs in the future distribution network and possible meshed structures. Therefore, the research on decentralized control methods has gained more attention with the abovementioned concerns. Besides its necessity in

future distribution systems, another essential gain from the decentralised approach is no need of communication infrastructure. The proposed method confirm its ability to reduce the stress over the system components. Furthermore, it will contribute to the voltage regulation capability of the network through the PV inverters.

The work highlighting this contribution was published in the following journal; M. Selcen Ayaz, M. Malekpour, R. Azizipanah-Abarghooee and V. Terzija, "Local photovoltaic reactive power controller for increasing active distribution networks hosting capacity," in *IET Generation, Transmission & Distribution*, vol. 14, no. 22, pp. 5152-5162, 13 11 2020, doi: 10.1049/iet-gtd.2020.0649.

Zonal voltage control management

According to the straightforward, practical and decentralised manner of the control, this study proposes to control the voltage by partitioning the distribution network into several zones. Zonal voltage control divides the whole system into zones according to the partition index determined within the problem. Therefore, the zonal management becomes prominent, and each zone is managed independently, giving a chance for local voltage control without affecting other zones in the system. The studies are conducted over 24 hours, in 15 minutes time interval.

The work highlighting this contribution was published in the following journal; M. Selcen Ayaz, M. Malekpour, R. Azizipanah-Abarghooee and V. Terzija, "Local photovoltaic reactive power controller for increasing active distribution networks hosting capacity," in IET Generation, Transmission & Distribution, vol. 14, no. 22, pp. 5152-5162, 13 11 2020, doi: 10.1049/iet-gtd.2020.0649.

Probabilistic approach

The design of a decentralized controller should be capable of dealing with the uncertainties brought by PVs and loads. Probabilistic assessment is an alternative to solve the stochastic behaviour of future energy systems where the outcome of energy is uncertain. A rigorous

probabilistic approach is based on probabilistic data input and produces a set of results. In other words, instead of a mean value over time, there would be a distribution function representing occurrence probabilities of different quantities over the same time scale, which results in further accuracy.

1. *The work highlighting this contribution is currently under a journal preparation;* M. Selcen Ayaz, M. Malekpour, R. Azizipanah-Abarghooee and V. Terzija, " Probabilistic PV power output and load demand uncertainty modelling for Increasing Active Distribution Networks Hosting Capacity" (to be submitted).

1.4.3. List of Publications

Journal Papers:

1. **M. Selcen Ayaz**, M. Malekpour, R. Azizipanah-Abarghooee and V. Terzija, "Local photovoltaic reactive power controller for increasing active distribution networks hosting capacity," in *IET Generation, Transmission & Distribution*, vol. 14, no. 22, pp. 5152-5162, 13 11 2020, doi: 10.1049/iet-gtd.2020.0649, *(Published)*.
2. **M. Selcen Ayaz**, M. Malekpour, R. Azizipanah-Abarghooee and V. Terzija, " Probabilistic PV power output and load demand uncertainty modelling for Increasing Active Distribution Networks Hosting Capacity" *(to be submitted)*.

Conference Papers

1. **M. Selcen Ayaz,** R. Azizipanah-Abarghooee and V. Terzija, "European LV microgrid benchmark network: Development and frequency response analysis" 2018 IEEE International Energy Conference (ENERGYCON), Limassol, 2018, pp.1-6, doi: 10.1109/ENERGYCON.2018.8398759.

2. R. Azizipanah-Abarghooee, M. Malekpour, **M. Selcen Ayaz,** M. Karimi and V. Terzija, "Small Signal Based Frequency Response Analysis for Power Systems," 2018 IEEE PES Innovative Smart Grid Technologies Conference Europe (ISGT-Europe), Sarajevo, 2018, pp. 1-6, doi: 10.1109/ISGTEurope.2018.8571556.

Poster Presentations

1. **M. Selcen Ayaz**, R Azizipanah-Abarghooee, V Terzija, Development and Frequency Application of a European Low Voltage Microgrid Network, 2018 IEEE PES General Meeting Student Poster Competition.

1.5. Thesis Structure

The Thesis has 6 logically connected Chapters, each briefly described below.

Chapter 2 firstly introduces a critical literature review of voltage regulation strategies with the increased penetration of PVs in ADNs; by understanding the impacts of high penetration of PV integration on the distribution level. Firstly, a detailed overview of the distribution systems is presented. Conventional and advanced voltage control applications are summarized. Secondly, the local reactive power control strategies are introduced in the sake of future network scenarios with voltage regulation. Voltage variation problems in the distribution networks due to PVs are presented, and voltage regulation strategies are discussed. The voltage control methods in a PV integrated system can be generally divided into four categories [4]: i) centralized control, ii) distributed control and iii) decentralized control. The local voltage control method uses local measurements from the buses, where the voltage is regulated accordingly. The approach helps to reduce the losses without using costly and slow responding control resources such as, OLTC, static voltage regulator (SVR), and capacitor banks. Local reactive power control strategies are reviewed, by stating their need in future ADNs.

Chapter 3 presents a simple, practical and decentralised novel local voltage controller proposed with the zonal network partition method. Zonal voltage control divides the whole network into zones where each zone is managed independently, giving a chance for decentralised management without affecting other zones in the system. Within the zones, the PVs close to ending of the feeder uses local standard reactive power voltage controller where PVs close to the transformer act as reactive power sources. Meantime, a fully local controller is performed within the PV inverters, which only requires local and neighbouring PVs

information. The regional management fulfils the method to achieve the goal without centralised control applied on active distribution networks, with no need for communication infrastructure. In this way, the PV inverters can enhance the performance of voltage regulation ability of the system. Specific scenarios are implemented to monitor the voltage controller performance and enhancement for voltage regulation. Hosting capacity definition and performance measures for developing the feeder hosting capacity are defined in terms of the network losses, the transformer/branches loading.

Chapter 4 extends the decentralized voltage control approach to a stochastic assessment of input parameters to enhance the accuracy of the simulation results with the high penetration of PVs in distribution networks. A vital evaluation should also be considered from the stochastic nature introduced by PVs and loads in the future power systems. A brief understanding of the applicability of the stochastic approach of Monte Carlo simulations on the current work is presented. The main aim is to model the uncertainty in the ADNs with the probabilistic variables of solar PV generation and load demand. To this end, a scenario-based technique has been proposed to represent the method. Roulette Wheel Mechanism (RWM) and Monte Carlo Simulation (MCS) strategies are used to enhance the preciseness in representing Probability Density Function (PDF) s of PV generation and load demand random variables.

Chapter 5 presents the proposed method's effectiveness through comprehensive simulation results on the 33 and 69 node test systems. More importantly, each node is equipped with PV units on these test systems. The studies are performed through DIgSILENT Power Factory 2020 software with the Quasi Dynamic simulation studies. Findings depict the hosting capacity improvement with the proposed approach considering a 15-minute resolution of PV and demand profiles. The novel method offers a fully local voltage control for PVs using the quasi-

dynamic approach over 24 hours. The results are represented in terms of grid losses, transformer loading and upstream network support. Also, with the proposed strategy, the use of tap operations over 24 hours is reduced. Consequently, the feeder hosting capacity is increased. The controller reduces the reactive power burden on the feeder transformer without the need of communication interface whereas decreasing the active power losses. Afterwards, the performance of the proposed local voltage control approach also implemented to the meshed 69 node test system. Findings reveal that the new method can increase the distribution network hosting capacity almost to 125% of the feeder transformer nominal power, regardless of the studied network. As a further consideration, the stochastic assessment results are executed on 33 node test system. Hosting capacity expected value observations show that the proposed approach increases the hosting capacity by 20% in comparison to Q-voltage (Voltage Dependent Reactive Power Control) case.

Chapter 6 presents the conclusions drawn from the entire research. The work is concluded with comments of enhanced reactive power control for inverters connected to distribution networks. As a conclusion, the importance of enhancing the feeder hosting capacity is highlighted. The proposed methodology is proven its practicality with advanced simulation results. The results prove that the developed controller can increase the system hosting capacity by about 20% of the systems base power. Furthermore, the network active power loss is considerably decreased by 30% concerning existing methods. Moreover, the transformer tap changer experiences fewer tap operations over a day. Thus, the feeder hosting capacity can allocate more PVs in the ADN. In the proposed approach, all the controllers are implemented locally, and the communication devices are eliminated, mitigating the investment cost significantly.

1.6. Chapter Summary

This chapter gives an overall background of the challenges brought by the high penetration of PVs for voltage control in Active Distribution Networks (ADNs). With the integration of increased amount of PV power plants over time, voltage control is one of the critical aspects to be considered in the distribution network. Due to the variable and uncertain characteristic of PVs, over-voltage problems arise at distribution systems, primarily when the peak PV generation occurs. It leads to overloading of system components such as, lines, transformers, whereas also limits the further integration of PVs into the ADNs. This thesis proposes a novel fully local voltage controller to regulate the voltage with the high integration of PVs. To achieve a computationally efficient and practical control, this study proposes to control the voltage by partitioning the distribution network into several zones.

Another crucial challenge faced in the ADNs caused by the overvoltage at peak PV generation hours is the limitations on feeder hosting capacity. Remarkably, the use of this novel controller will allow further integration of PVs to the system by enhancing the hosting capacity of the feeder without using communication infrastructure. Finally, a stochastic approach has also been proposed in order to obtain more accurate results to enhance the feeder hosting capacity.

2. STATE–OF-THE-ART OF VOLTAGE CONTROL IN DISTRIBUTION NETWORKS

2.1. Introduction

Through the ever-fast growth and integration of PV systems into the ADNs, the stable grid operation is facing many challenges like voltage violation. Overvoltage issues rise when the maximum generation of PVs occur at noon, which restricts the DNs' PV hosting capacity. However, this timescale does not coincide with the peak demand time of the loads in ADNs. Recently the research into overvoltage problems in the ADNs has gained pace. As an outcome, several methodologies are presented in the literature to tackle voltage related problems and to increase the DN hosting capacity. To increase DN hosting capacities; feeder reinforcement, PV active power curtailment and PV reactive power control strategies are presented [23]. However, the equipment upgrades, and PV power reduction are not cost-effective for system operators and customers. Alternatively, the PV systems reactive power capability can provide voltage support to rise hosting capacity[24].

This chapter outlines a critical literature review of voltage regulation strategies with the increased penetration of PVs in ADNs, by the current state-of-the-art regarding the impacts of high penetration of PV integration on the distribution level. First, a detailed overview of voltage control is presented. Conventional and advanced voltage control applications are summarized. Secondly, the local reactive power control strategies are introduced in the context of future network scenarios with voltage regulation. In these future scenarios, power systems are expected to become more decentralised, proving that local management of the voltage is

becoming more reliable in terms of reducing complexity levels. More importantly, local control strategies are discussed in detail to reflect their importance in the context of this work. Thirdly, to illustrate overvoltage problems in ADNs, the mathematical formulation of a simple test system is represented. The voltage alteration in the system when a PV is connected is emphasized. Afterwards, the impacts of high PV penetration in ADNs are highlighted. The grid code requirements are also discussed and evaluated in terms of the PV inverter contribution to the grid.

2.2. Voltage Control in Active Distribution Networks

Voltage control is required to ensure the safe, economic and efficient dispatch of power, considering statutory voltage limits. The future power system is continuing rapid growth in CIG, dominated by solar PVs. Overvoltage issues are become gradually related to be addressed, when consumption is low and generation is high, with the increased integration of PV generation units [25]. By improving the existing voltage control methods, the greater integration of PV generation can be allowed without requirement of costly and time consuming network upgrades. Therefore, the inspection of voltage control strategies for ADNs with high penetration of PVs is essential to be able to understand the future networks. Figure 2-1 categorises the conventional voltage control techniques used in ADNs.

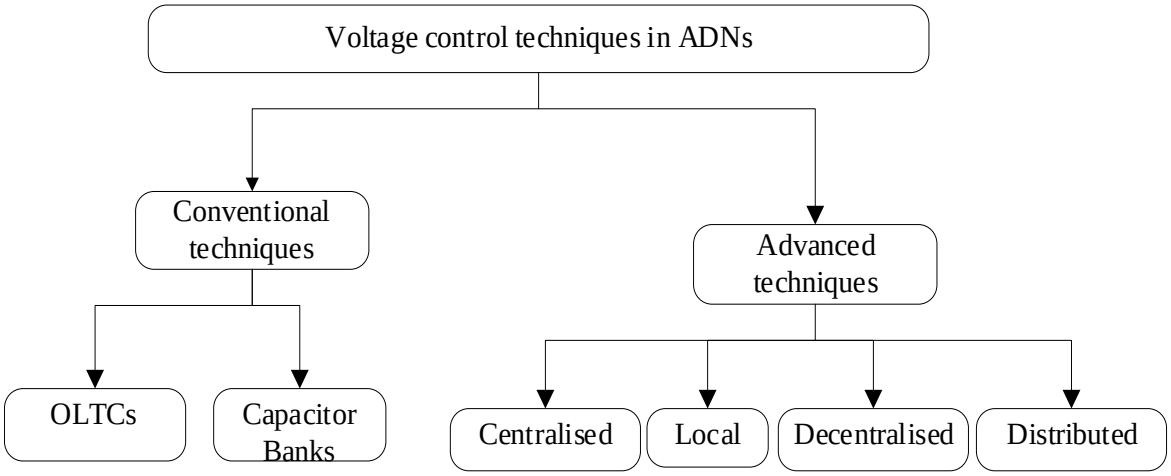

Figure 2-1. Voltage control techniques in ADNs

The voltage problems in distribution networks are under-voltage & overvoltage at any node and within the network and the nodes of the point of common coupling (PCC), leading to overloading of system components (transformers and lines) and other voltage related issues like unbalances, voltage sags. Under-voltage problems arise when high demand conditions coincide with low production of CIGs (i.e. at night there is no PV generation). In contrast, overvoltage problems generally occur when low demand conditions coincide with high CIG output (i.e. peak times of PV generation). The increased PV penetration may increase grid losses significantly if local generation exceeds all local demand resulting in excessive power flows PV towards the upstream network [26]. This work aims to tackle the overvoltage issues, which might lead to exceed the thermal limits of the system components (transformers and branch lines).

Several mathematical representations have been proposed to describe the PVs impact on the voltage profile of ADNs [22]– [24]. Intensive studies have been performed on the conventional techniques to regulate the voltage, e.g., on-load tap changers and capacitor banks [22], [30]. Although these traditional techniques are effective, the drawback of using static devices such as inductors, capacitors and OLTCs for voltage control, is the response speed is relatively slow

compared to the dynamic voltage control devices, which are continuously variable and can respond much faster. Other disadvantages for the conventional techniques include the high technical expenses, such as maintenance costs. Moreover, the traditional controllers are centralised and they need a central controller to regulate each unit in the system. The use of centralised controllers is less effective and can become infeasible if applied to manage the increasing number of PV systems at the electricity distribution level [31]. The majority of centralised control methods proposed in the literature, use high computational optimisation techniques that require investments in network monitoring (not common in DNs) and communication infrastructure. The centralised control is prone to network failures and communication issues, where it becomes less cost-effective and less robust.

Examples of coordinated voltage control architectures can be found in [32]–[36], where a few coordinated control strategy uses multi-agent systems to communicate within the DERs. The method provides a real time control with the help of optimization tools, by controlling the voltage based according to upper and lower voltage limits [37]. Genetic Algorithms [38], [39] and Particle swarm optimisation [40] techniques are used to control the voltage in literature. Nevertheless, once again, communication between network components are needed in the abovementioned techniques.

To overcome the drawbacks of centralised control, emerging techniques such as local voltage control by using reactive power capabilities of the PV inverters [9], [13], [33], [41] and storage system solutions [42]–[44] are progressively investigated. Local voltage control is based on local PCC measurement, each distributed generator (DG) works separately and uncoordinated with other devices, only with measurable local variables as the active power and terminal voltage. Various control strategies have been implemented and discussed by relative comparisons of the local control method performances [41], [45]–[47]. Furthermore, numerous papers are focused on the voltage regulation in microgrid applications [27], [48], [49] and

increasing the grid hosting capacity for the PV systems [11], [17]. When it comes to the local control, in the standard control techniques, redundant consumption of reactive power of the PVs may cause the line losses to increase and eventually instability to the system [50]. Alternatively, implementing battery energy solutions can enhance the benefits from the integration of distributed energy sources, aid power quality management, and reduce distribution network expansion costs [51]. However, to increase the distribution network's hosting capacity, battery energy storage systems (BESS) may not be economically viable solutions [52].

Other ways of controlling voltage have been proposed as the active power curtailment (APC) [53], reactive power compensation (RPC) [54] and optimal inverter dispatch (OID) [55]. Nonetheless, these methods lead the power to be curtailed and require additional compensation units. Following sections will discuss the conventional and advanced techniques for voltage control.

2.2.1. Conventional Voltage Control Approaches

In the conventional transmission grid, there are two types of voltage control devices, namely static and dynamic voltage control devices. The static voltage control devices are shunt reactors, fixed capacitors (FC) which have a fixed reactive power set value. On the contrary, dynamic voltage control devices can adapt the amount of reactive power injection/consumption according to the voltage level. These devices can be mentioned as FACTS devices; static synchronous compensators (STATCOMs) and static VAR compensators (SVCs). According to a cost-benefit analysis presented in [56], , STATCOM and voltage regulator solutions are both complex and costly. The voltage control mode is a less expensive solution, but this solution needs to be further resolved with coordinated operation. The voltage support equipment which are used in transmission systems are briefly introduced in Table 2-1.

Table 2-1. Characteristics comparison of transmission system voltage support equipment

Equipment	Equipment type	Response speed	Voltage support	Operating cost
FC	Static compensator	Slow	Poor, changes with V^2	Very low
Static Synchronous Series Compensator (SSSC)	Static compensator	Slow	Poor, changes with V^2	Low
SVC	Dynamic compensator	Fast	Poor, changes with V^2	Moderate
STATCOM	Dynamic compensator	Fast	Good, changes with V	High
Unified Power Flow Controller (UPFC)	Combination of SSSC and STATCOM	Fast	Good load flow control	High

In the distribution grid, consumer demand can also participate in generation or absorption of reactive power. If the grid has an increase in inductive loads, this will lead to a voltage drop at the consumer loads, also affecting other bus bars in the distribution network. In this case, conventional voltage regulation strategies will try to compensate this voltage drop by possible ways to control the voltage. In case of a decrease in inductive loads, overvoltage would occur due to reactive power increase in the grid. In the following, conventional voltage control techniques are explained in detail.

OLTCs: In the conventional methods, the voltage regulation provided by on-load tap changers (OLTCs), capacitor banks and step voltage regulators. However, OLTCs are not common at the LV levels. OLTC logic aims to manage opposing issues of voltage rise (due to the presence of generation) and drop (due to loads) as an autotransformer. The automatic versions are mostly used in distribution networks to provide voltage regulation besides load consumption. The main drawback of OLTC is the long operation time (range of 100ms to several seconds) compared

to system events like fault and generation loss. Some other disadvantages include high maintenance and service cost, and high failure rates of tap-changers during operation.

Capacitor Banks: Capacitor banks can provide the reactive power demand of the loads in the distribution network. The benefit of providing reactive power by capacitor banks is the reduction of the total current flowing through the feeder. This reduction of current reduces the feeder voltage drop and improves the voltage at the PCC.

Individually, the load consumption model of LV distribution networks and the PV power output are inconstant variables. Also, the reactive power amount to be supplied is varying, out of the discrete steps of the capacitor bank. Therefore, fixed compensation of reactive power is not a practical solution for voltage regulation.

To summarize traditional voltage control methods, which were designed to regulate the voltage for passive systems, are not able to sufficiently tackle the voltage issues caused by the high penetration of PVs in the system. Therefore, advanced control approaches are presented to explain what the future distribution networks will face in near future and how to overcome these issues.

2.2.2. Advanced Voltage Control Approaches

The future power networks are evolving in a way that conventional voltage control techniques are becoming costly and are not enough overcome the voltage issues, so that, advance control approaches are needed. The voltage control methods in PV integrated networks can be generally divided into four categories as follows [57], [58]: a) local control, b) centralized control, iii) distributed control and iv) decentralized control. Figure 2-2, represents the control schemes classification with high penetration of PVs. The advanced control techniques can be classified as centralised, distributed and decentralised control, based on communication. The local voltage control strategy doesn’t use communication, where it only uses local

measurements at the bus bars to regulate the voltage. This control technique will be investigated separately through Section 2.3. Local Voltage Control in ADNs

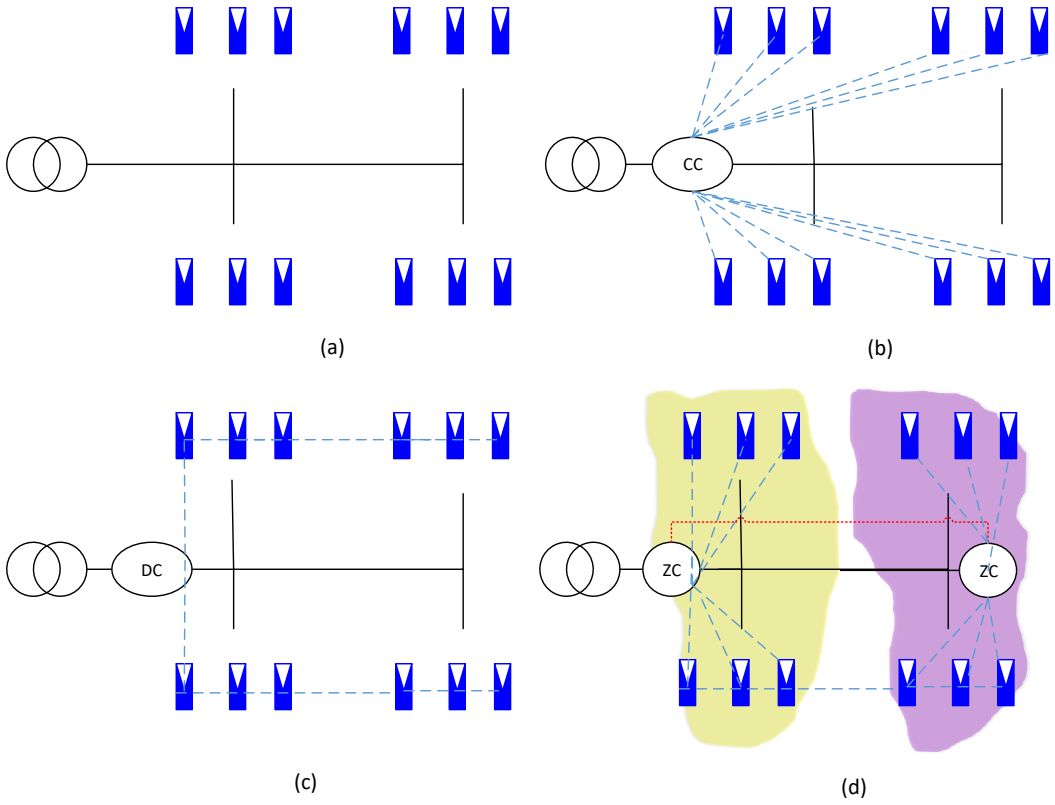

Figure 2-2. Voltage Control schemes based on communication (a) Local Control (no communication) (b) centralized control CC: central coordinator, (c) Distributed control DC: Distributed coordinator (d) decentralized control ZC: zonal coordinator [58]

2.2.2.1. Centralized Voltage Control:

In the centralized control strategy, the control actions are managed by a central controller and provided by communication channels. The management system analyses the data and the coordinator sends the information to the relevant component.

For the voltage regulation in distribution networks, the central controller needs to obtain the information of each bus on the feeder. In transmission level, this is provided by Supervisory Control and Data Acquisition (SCADA) systems. Nevertheless, the distribution grid mostly

has this information only at the primary side. From this point, the state estimation algorithms provide prediction data instead of the missing real-time data [26].

The centralized control approaches have some drawback as they have high costs in communication assets and sensors and are not feasible. The central controller needs to control many different small sized PVs also having variability, which increases the computational complexity. The power flow solution at each time step needs to be calculated, and this brings high computational burden for the system [59]. Feeder control and protection are more multi-layered in centralised control, compared to decentralized control systems. The issues about centralized control, i.e. the need extensive monitoring and communication create further challenges for the ADNs.

2.2.2.2. Distributed Voltage Control:

The distributed control structures improve the voltage regulation and mitigate the capital cost through the coordination between nodes, when compared to decentralised control [60]. The inverters are controlled in a coordinated manner, and the generated power information is shared within the nodes. When it is compared to centralised control, it requires less level of communication and less computational efforts. However, these methods have limited functionality in comparison with the centralized ones.

2.2.2.3. Decentralized Voltage Control:

In decentralized control, the controllers receive information on their local network status. Then, according to the appropriate control strategy, voltage control will be applied to the system. Therefore, decentralized controllers can respond to the load fluctuations flexibly with only having local measurements of the system [26]. But the implementation of the control strategy can increase the power loss in the system. Different units of local control strategies

can coincide with the other ones, so this can affect their operations. Some researches highlighted that the thermal overloading of resources (i.e., transformer and feeders) might arise instantaneously with voltage rise issues. As a result, when injecting reactive power to the grid for voltage regulation, the overloading of the system components should also be taken into consideration and planned within the power flow.

Decentralized coordinated control strategy is highly investigated among researchers recently due to its coordination capability over control devices to achieve the most efficient way of control with high penetration of PVs in ADNs [61]. Most of the decentralized control studies are applied for radial topologies [62]. Decentralized control method can be applied by dividing the whole grid into clusters to manage the system and by using voltage droop control methods, the system can be controlled locally. This zonal structure would decrease the computational burden by dividing the distribution network into zones, allowing practicality for future integration of PV units to the ADNs [63]. More information of partition based zonal networks will be given in Chapter 3.

A brief summary for the advanced control techniques based on exchanging the information between the participating entities can be given as: i) centralized, ii) distributed, and iii) decentralised. In centralised control, there is one central controller to receive all measurements. In the distributed control, the PVs communicate with neighbouring nodes to give a co-operative decision set by the distributed controller. Decentralised control can be stated between centralised and distributed control, taking advantages of both techniques. The next section will introduce the local voltage control as a part of decentralised method, where all the local controllers adjust the voltage at the monitored bus, by only processing local data.

2.3. Local Voltage Control in ADNs

Local voltage control can be categorised under decentralised control, where it uses local information to regulate the voltage. The local voltage control terminology is a commonly used in literature [64]–[66]. For the sake of simplicity, local control definition will be used to reflect the work in this thesis.

With the increased PV generation especially in ADNs, the local voltage control strategies are increasingly used for voltage related problems [67]. The overvoltage problem is mostly related to high real power injection the feeder. Ref. [68] suggests the reactive power-based PV inverter mitigate this problem by providing sufficient reactive power as well as voltage regulation. To control the reactive power locally by different voltage droop control strategies is a regular solution for voltage regulation in ADNs [32], [66], [69], [70].

PV inverters have limited capability to produce or absorb the required reactive power on the subject of their inverter capabilities [65] . In the case of high-power outputs like when the solar radiation is high, the available reactive power headroom also alters throughout the day depending on the weather conditions. However, the PVs reactive power absorption increases feeder transformer and lines loading, and this method requires a communication infrastructure [71]. To apprehend the facts about voltage and reactive power, Appendix B1, further explains the relation between these two indicators. In the following section, the local reactive power methods by different droop control strategies for voltage regulation in ADNs are discussed further.

2.3.1. Local Reactive Power Control Strategies for Active Distribution Networks

Reactive power control can be provided through several methods namely, fixed power factor method, active power-dependent reactive power regulation method (Q-active power) and voltage-dependent reactive power regulation method (Q-voltage) [47]. Q-active power control

is not mentioned in this work, hence, this method cannot address voltage limits [72]. The PF-power (Active Power Dependent Power Factor Control) strategy supports the feeder voltage indirectly using only PV system active power generation. The voltage regulation capability of the PF-power method is strong. However, when the generation by PVs and load demand are at a high level, the method tends to increase grid losses[73]. Also, the power factor based methods does not guarantee the equal share of reactive power by the PV inverters. Alternatively, the Q-voltage approach controls the PV reactive power directly deploying the PV local voltage V_{pv} [47]. Therefore, the grid loss is small, whereas, the voltage regulation capability might be weaker. The advantages and disadvantages of the local control strategies will be compared at the end of this section.

2.3.1.1. Fixed power factor

This method provides a constant amount of reactive power relative to active power. The drawback of this system is additional grid losses caused by unnecessary power consumption while the production is low. Figure 2-3 represents the characteristics of fixed power factor method where P_{PV} is the active power and PF_{PV} is the power factor of the PV unit.

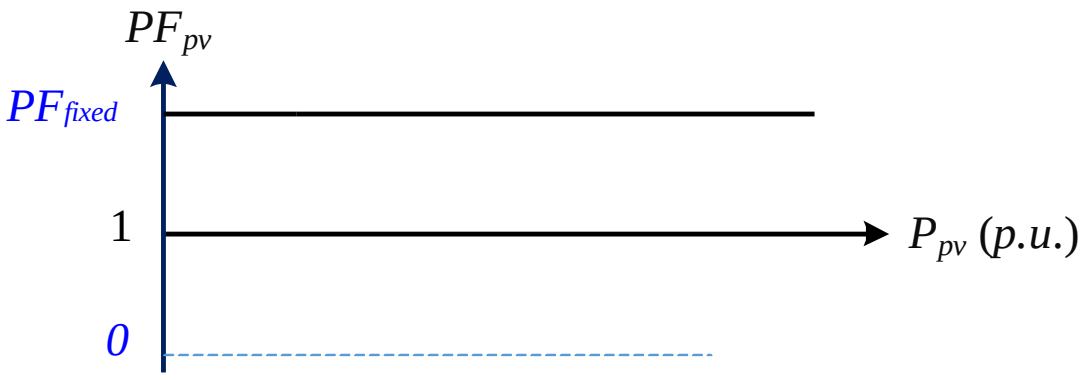

Figure 2-3. The characteristics for PV reactive power controls with fixed PF control strategy

2.3.1.2. Q-Voltage control strategy

In this strategy, the reactive power follows the PCC voltage change. The reactive power limits are defined according to the grid codes. Q-voltage control is a nonlinear P-controller, with a gain within its controller configuration. Voltage regulation is not only used for the voltage rise or drop but also a reserve to enhance the power grid accordingly different assumptions, such as, total grid losses reduction or power factor control. The reactive power over limit (Q_{over}) limits reactive power capabilities.

In this method, the voltage at the PV connection point is considered as a reference for the droop control, and the PV inverter absorbs the reactive power when the terminal voltage is higher than a specific value as given in Equation (2.1):

$$Q_{pvn} = S_{pvn}\sqrt{(1 - PF_{pvn}{}^2)} \tag{2.1}$$

Where S_{pvn}, Q_{pvn} and PF_{pvn} are the PV system nominal apparent power, reactive power and power factor, respectively. On the other hand, when the PV active power generation decreases from its nominal, the PV reactive power is limited to the following reactive power value given in Equation (2.2):

$$Q_{\text{lim}} = \sqrt{S_{pvn}^2 - P_{pv}^2} \tag{2.2}$$

Figure 2-4 portrays the character of this strategy. The reference voltage V_{ref}, can be selected according to the lower (V_{min}) and upper limits (V_{max}) of the bus voltage magnitude, with the slope "-R_v" Here, R_v represents PV voltage droop gain. The reactive power of the PV unit (Q_{pv}), alters between Q_{over} and Q_{under} values depending on the voltage.

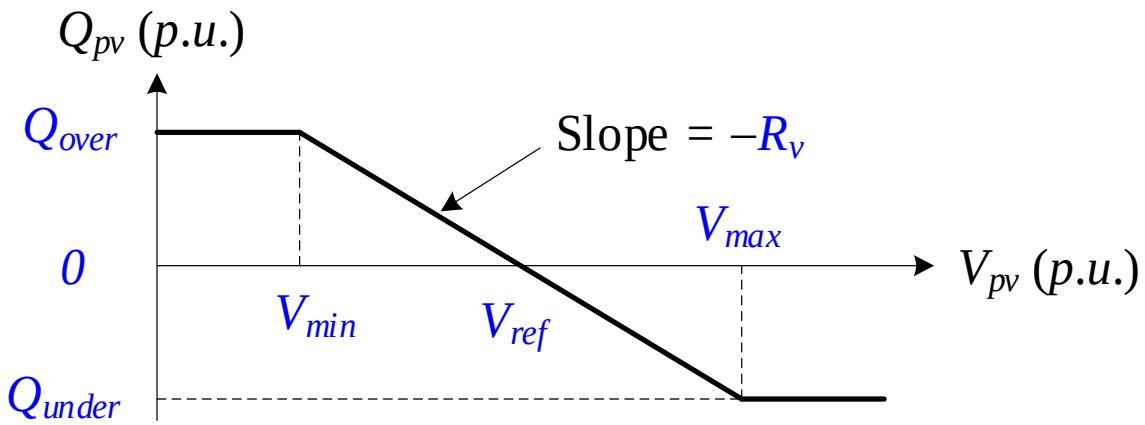

Figure 2-4. The characteristics for PV reactive power controls with Q-voltage method

2.3.1.3. The PF-power method

This strategy is called the power factor (PF)-power in this study. In this method, the reactive power is a function of the produced active power, and power factor changes between PF_{over} and PF_{under} represented in Figure 2-5. The generating units work in under-excited mode when the active power reaches to the threshold of PF_{over}. The reactive power starts to be absorbed by the inverter after this threshold. The active power-dependent power factor method was presented in Ref. [74], to control the PV system reactive power.

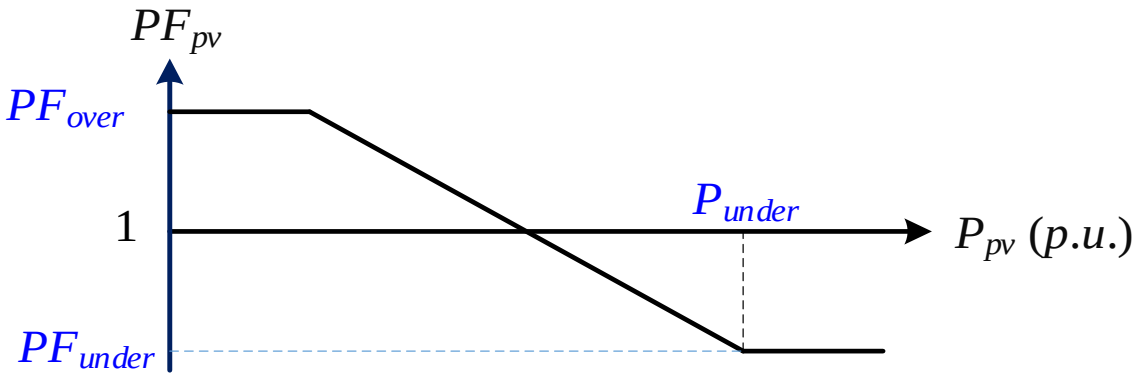

Figure 2-5. The characteristics for PV reactive power controls with PF-power method

2.3.1.4. Combined local reactive power control strategies

Combined versions of the Q-voltage and PF-power strategies are also implemented in the literature [41]. This combined strategy offers the advantages of both strategies. While Q-voltage approach controls the voltage limits, PF-Power control strategy regulates the power factor according to the active power output. That means that, when the voltage limits are within the operational limits of Q-voltage approach (i.e. 0.93<U<1.07 according to [41]), the system will operate according to this control strategy. If the voltage is not within these limits, the control method will change to the PF-Power control strategy and can improve the voltage regulation ability. Figure 2-6 illustrates the different curves for the combination of two voltage control strategies.

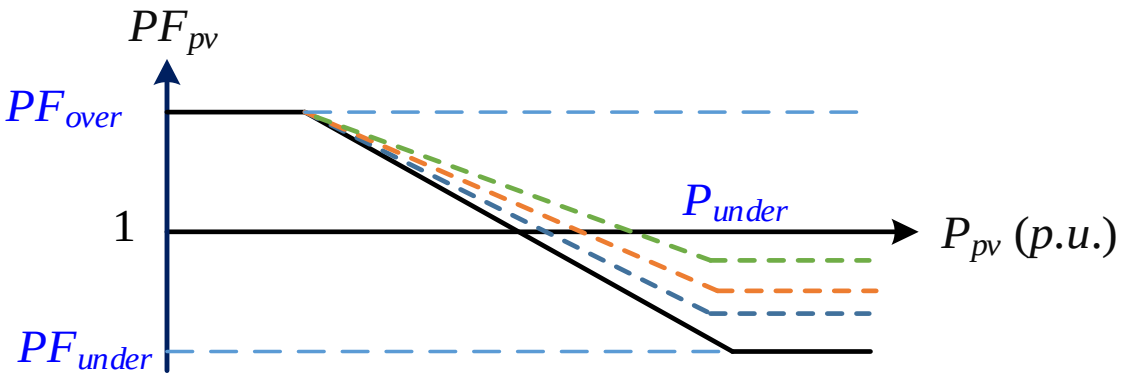

Figure 2-6. Combined Power Factor-P and Q-voltage strategy

.

Table 2-2., highlights the strong and weak points of standard reactive power strategies which are already imposed by specific grid codes of the future active power networks. In Q-voltage control, the PV reactive power is directly controlled with PV local voltage. Q-voltage control maintains the voltage at the terminal of the PV system within predefined voltage limits. The drawback of the control is the voltage regulation ability of the whole PV system is weak. PV contribution near the beginning of the feeder will be at a low level compared to the end of the feeder [73].

Table 2-2. Reactive power control strategies comparison

Control strategy	Explanation	Advantages	Disadvantages	Voltage regulation	Grid Loss
Fixed Q	Q_{ref} is determined by PV output & load consumption	When PV generation is high, control is good	Data of load & PV power is required	Weak	High (when PV generation is low)
Fixed Power Factor	Generated "Q" is proportional to "P"	When PV generation is low, voltage is not over-limit.	When power production is low, control increases loss	Strong	High
Q-voltage	collects PCC voltage to determine the Q_{ref} value	the grid loss is small	Not suitable for LV string lines	Weak	Low
Power Factor-P	Sets power factor based on the P output of PV systems.	the voltage regulation ability is strong	Excessive Q generation in some cases	Very Strong	High
Combined Power Factor-P and Q-voltage	based on PCC voltage and the P_{PV}	grid loss is less compared to previous techniques	Requires larger Q_{demand} than Q-voltage control.	Strong	Low

Power factor-P control sets the power factor based on the active power output of PV systems where it provides adequate voltage support. The grid losses and transformer loading can be high when this voltage control method is used because reactive power output continues increase if the generation is high. The combined process improves the control ability by combining two techniques. However, with the increased penetration of PVs, a more comprehensive solution is needed for regulating the voltage. Therefore, in the literature, the local voltage control strategies are missing some competencies, and this study is aimed to bring further innovative contributions, like evaluating the grid losses and transformer and line loadings in the ADNs when determining the hosting capacity.

2.4. Distribution network modeling representation

In this section, the distribution network models will be mathematically represented to illustrate the PV system effect, and the voltage will be monitored. The distribution grid shows a

difference from the transmission system from several aspects. For the distribution grid, the most significant issue is the best way to serve the end-users by delivering power. In the conventional distribution grids, the existing network was designed according to the worst-case load conditions without consideration of PV systems.

With retaining the increased PV integration to the grid, most noticeable among the DN topologies is the radial topology (reconfiguration) of the DN, also known as active radial distribution network (ARDN) [75]. For the sake of simplicity and following the practical examples, the study is firstly based on the ARDN topology. Correspondingly, the ARDN strategy is expected to be more flexible under emergency conditions such as, cyberattacks, where relying on less communication infrastructure. There are limited studies for solving complex meshed systems with current power flow algorithms with high penetration of PVs considered [76]. Nevertheless, the proposed scheme is inherent from the system topology, whereas it enables the creation and experimental approval of new topologies, control applications, communication and security.

2.4.1. Simplified Distribution network model

To further explain the context of the distribution network, a simplified LV distribution feeder is represented in Figure 2-7. The system contains the external grid, a load with P_{ld} and Q_{ld} active and reactive powers respectively, the line with $R_l \; and \; X_l$ resistance and reactance, respectively.

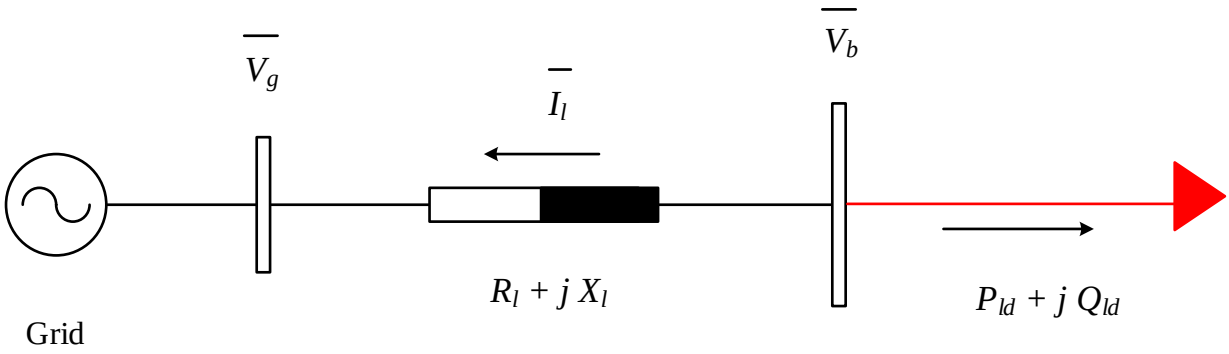

Figure 2-7. Simplified LV distribution feeder

For the sake of simplicity, let us consider the grid voltage phasor at the start of the feeder as Equation (2.3):

$$\overline{V}_g = V_g \angle 0 = 1 \angle 0 \tag{2.3}$$

Then, the bus voltage vector may be represented as follows in Equation (2.4):

$$\overline{V}_b = V_b \angle \delta \tag{2.4}$$

This voltage phasor can be rewritten in terms of the line current in Equation (2.5):

$$\overline{V}_b = \overline{V}_g + \left(R_l + jX_l\right)\overline{I}_l \tag{2.5}$$

Also, from the power equations Equation (2.6) is derived as:

$$P_{ld} + jQ_{ld} = V_b * I^* \tag{2.6}$$

where the current is rewritten in Equation (2.7)

$$I = \frac{P_{ld} - jQ_{ld}}{V_b} \tag{2.7}$$

In other words, the voltage deviation at the beginning of the feeder can be calculated in Equation (2.8):

$$V_g = V_b + \frac{P_{ld} - jQ_{ld}}{V_b} * (R_l + jX_l) \tag{2.8}$$

If the formula is distributed evenly the voltage can be written as in Equation (2.9):

$$V_g = V_b + \frac{R_l P_{ld} + X_l Q_{ld}}{V_b} + j\frac{X_l P_{ld} - R_l Q_{ld}}{V_b} \tag{2.9}$$

Here, since $RQ \approx XP$ is almost equal so the imaginary part is neglected [77].

$$\Delta V \approx \frac{R_l P_{ld} + X_l Q_{ld}}{V_b} \tag{2.10}$$

From Equation (2.10), it is evident that the voltage drop of the distribution feeder depends on the power factor of the connected load and the impedance of the distribution feeder. Therefore, the voltage drop can be prevented by injecting reactive power to the system opposing active power [78]. Let us assume that all parameter and variables in Equation (2.10) are in per unit value except the line current angle. Then, the bus voltage deviation may be rewritten in terms of the line active power and resistance as follow in Equation (2.11):

$$\Delta V = R_l P_{ld} + R_l P \tag{2.11}$$

Figure 2-8 represents the phasor diagram of the feeder without PV is inserted to the system. The voltage drop ΔV_b where the bus voltage angle (δ) and line current angle (φ) is illustrated in the phasor diagram. The next session will investigate the changes with including the PV into the ADN.

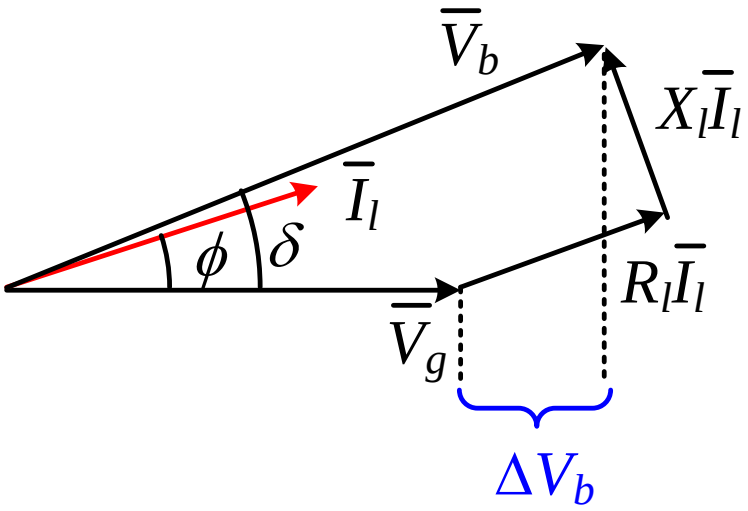

Figure 2-8. Phasor diagram of the feeder illustrated without PV reactive power absorption

2.4.2. PV integrated Distribution Network model

For the planning and stable operation of future distribution structure, it is necessary to analyse the relationship between the integration of PVs and the present distribution network's behaviour. To see how the PVs will affect the dynamics on the test system, different a simplified PV is integrated into the distribution feeder.

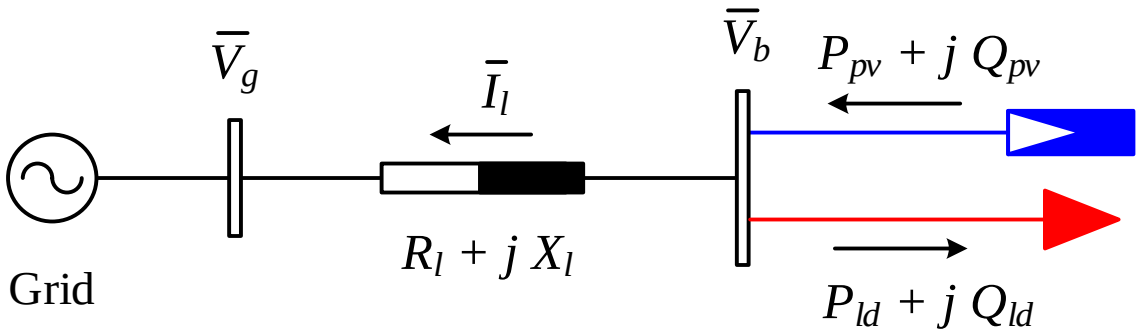

Figure 2-9. Simplified PV integrated distribution feeder

The feeder supplies a load through a line with resistance R_l and reactanceX_l, in per unit. Additionally, a PV system injects active power P_{pv} and reactive power Q_{pv} at the end of the feeder. It is assumed that the PV capacitive reactive power and the load inductive reactive power are positive in their shown direction in Figure 2-9. The process will be added the PV active and reactive powers as well. Let's accept the equations (2.3)to (2.7) as the same for the PV integrated distribution feeder.

One of the constraints that limit the penetration level of the PV power production in distribution feeders is voltage boundaries. The steady-state voltage amplitude at all the feeder buses must be kept within the prescribed limits as the Equation (2.12) [79]:

$$V_{\min} \le \left|\bar{V}_b\right| \le V_{\max} \qquad (2.12)$$

At midday, when the PV generates its maximum active power, the bus voltage may exceed its upper limit. The phasor diagram of this situation is shown in Figure 2-10, where the PV system operates with unity power factor. Since the line resistance is more extensive than its reactance in the low voltage networks [12], the angle δ will be small. Therefore, the bus voltage deviation can be approximated as follows in Equation (2.13):

$$\Delta V_b = R_l I_l \cos(\varphi) + X_l I_l \sin(\varphi) \tag{2.13}$$

Let us assume that all parameter and variables in the (2.13) are in per unit except the line current angle. Then, the bus voltage deviation may be rewritten in terms of the line active and reactive powers as follows in Equation (2.14):

$$\Delta V_b = R_l P_l + X_l Q_l \tag{2.14}$$

where the active and reactive power of the lines are given in Equation (2.15)

$$\begin{aligned} P_l &= P_{pv} - P_{ld} \\ Q_l &= Q_{pv} - Q_{ld} \end{aligned} \tag{2.15}$$

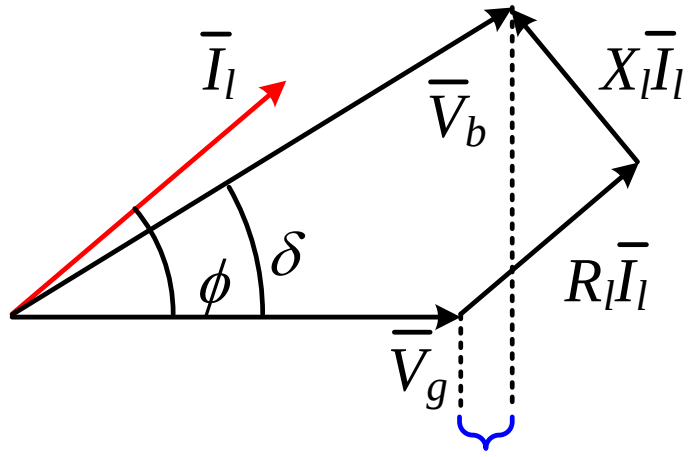

Figure 2-10. Phasor diagram of the feeder illustrated in simplified feeder with PV reactive power absorption

Note that both P_l and Q_l are positive in the direction of the line current in Figure 2-10,where the vector diagram of the simplified feeder is given and the PV system operates with a lagging power factor.

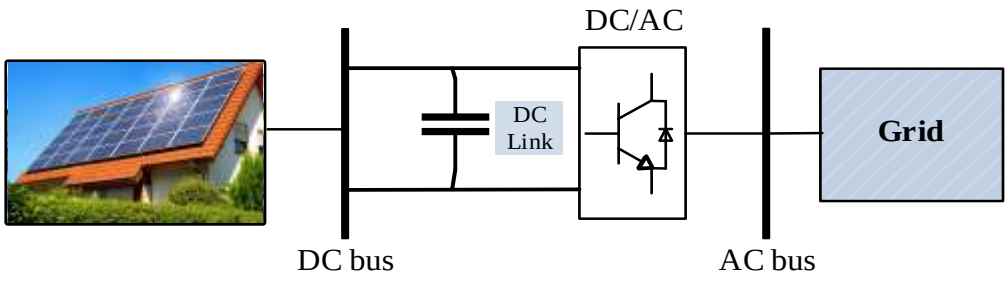

Figure 2-11. PV system connection diagram

Figure 2-11 represents the connection of the PV systems into the primary grid. As discussed in Section 2.2. , in the conventional techniques, the voltage level was controlled by the reactive power flow. A solar panel is modeled as a DC generator, which is not a reactive power source. However, the power converter connected to the PV system (DC/AC) is a source of reactive power. By using the inverter, the reactive power can be exchanged to and from the grid by controlling the inverter voltage. When several small generators (e.g. DERs) connected to the same LV level, the voltage will rise accordingly (See from above mathematical (2.10)). In modern networks with high PV penetration connected to the same LV distribution feeder, this case may also raise the voltage at the end of the feeder [80]. So that, a further attention should be emphasized at the end of the feeders of ADNs.

2.5. Impacts of the high PV penetration on the ADN

Previous sections have declared the significant impacts from high penetration of PV systems can be stated as voltage variations, voltage unbalance and stress on distribution system components. The voltage rise issue on the peak generation times is one of the main challenges brought by the connection of PVs to ADNs.

In the UK, the regulations ensure the Distribution Network Operator (DNO)s to guarantee a supply voltage within ±6% of the nominal for voltage levels above 0.4 kV and between +10% and -6% in LV under 1 kV [77]. The UK standard BS EN 50160 [78] states the 10 min average

voltage level to be between 0.94 and 1.1 p.u. (216 and 253 V) for at least 95% of the time (assessed weekly) and never below 0.85 or above 1.1 p.u. DNOs consider the worst-case scenario to ensure no voltage rise issues for the distribution network. At high voltages, (e.g. 400 kV), unless abnormal conditions, the limits are defined with a variation of±5%. However, up to 15 minutes voltage variations are allowed up to ±10% [81].. At 132 kV and 275 kV voltage levels, variations of ±10% are allowed [79]. The UK standard BS EN 50160 [82] states the 10 min average voltage level to be between 0.94 and 1.1 p.u. (216 and 253 V) for at least 95% of the time (assessed weekly) and never below 0.85 or above 1.1 p.u. Table 2-3, shows the voltage limits within the voltage level categories.

Table 2-3. Voltage statutory limits of different voltage levels [83]

Voltage Levels	Voltage Range	Voltage Limits
HV	≥ 132 kV	±5%, ±10%
MV	1 kV ~ 132 kV	±6%
LV	< 1 kV	+10% ~ - 6%

To resolve the problem, as mentioned in Section 2.2.1., DNOs use a variety of devices (OLTC and capacitors banks) to constantly regulate voltages within desired limits. Even so, when it comes to distribution level voltage control with high PV penetration levels, some impacts cannot be ignored. To solve the overvoltage issue, either reinforcing the existing system components (e.g., transmission lines, transformers) or curtailing the maximum PV capacity can be an option. However, the former solution implies huge costs, and the latter solution leads to profit loss for the PV owner. Therefore, a more local control of the distribution network to ensure more PV penetration is greatly desired.

Figure 2-12 illustrates a typical load and PV profile during a typical summer day. As seen from the figure, the PV generation is high during the day where the load demand is low. As the PV generation reduces in the afternoon, the load demand starts to climb to its peak value. This situation is introduced as a duck curve by the California Independent System Operator (CAISO) in 2012 [84].

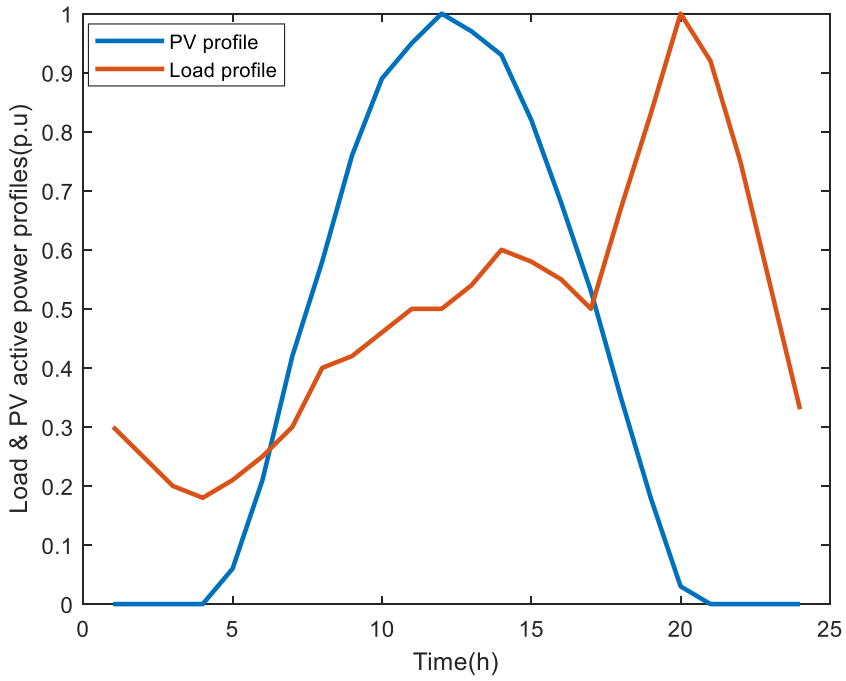

Figure 2-12. Typical PV generation and load daily demand profile during summer days

Despite this mismatch between generation and demand, the PV reactive power capability can be used to regulate the system voltage for the grid support. Accordingly, the current grid code requirements for voltage control and the reactive power control of PV inverters will be discussed in the following sections.

2.5.1. Grid code requirements for PV integration

The future grid also brings challenges with the need to revise the current technical policies and regulatory changes in the power systems. In the UK, the distribution system operator (DSO) is responsible for taking action towards the problems to regulate the power flow in the distribution

network [32]. The requirements of reactive power management for grid-connected PV plants are based on Grid code requirements of the country and location of metering. For example, ANSI C84.1 standard requires the voltage variation up to ± 5% of the nominal voltage in the system [85].

The reactive power is crucial at PV integration stage for steady-state network voltage and voltage recovery where the need for dynamic and static grid codes arise. Grid codes are already defined for wind turbines in several countries [86]–[88]. IEEE 1547-2003 standard aiming the development of distributed energy resource (DER) interconnection to power systems [79], but does not allow inverters to actively regulate the voltage at the connection point, with different kind of PVs (residential rooftop and commercial). Similarly, PV inverters are not actively allowed to participate in the voltage regulation in some other standards UL 1741 and AS 4777 [89] to avoid decentralized voltage regulation. On the other hand, German grid codes (GCCs) call for reactive power contribution [90], [91].

Even though the PV systems are not entirely allowed to participate in the voltage regulation yet, the control ability of the PV inverter over the active and reactive power is turning into an essential [78]. Recently, another discussion is about the feeders with high penetration of PV integration to exhibit voltage oscillations. Extensive solar PV power production causes feeder voltages to rise, eventually exceeding the inverter over-voltage protection of solar PV inverters, leading the PV units to be disconnected based on current grid connection standards. Thus, the grid experiences a voltage drop, where after a delay, the PV inverters return to service. But then again the voltages rise to an unacceptable level and the inverters trip. The oscillating voltages do not satisfy the requirement of "statuary voltage limit" required for voltage regulation. However, as voltage regulating PVs are added, which is the expected with the modified grid codes, these would keep end-of-feeder voltages within statutory limits [92].

The standards hold a significant place to maintain the stability, security and resiliency of the system with increased PV penetration limits. Therefore, it is essential when standards describe the reactive power support criteria, the required level of the system resilience should be maintained. The technical authorities should also discuss further standardization of PVs integration to the grid, and both consumers and transmission/distribution level participant should participate in the alteration of power systems [93].

2.5.2. Reactive power control of PV inverters

The PV systems are not generally expected to support the grid voltage. However, some commercial inverters have incorporated reactive power capacity [94]. PV inverters may provide reactive power service, either by injecting or consuming reactive power to maintain the system voltages within desired limits during continuous and contingent conditions. For instance, standard VDE-AR-N 4105 grid code states that the grid-connected distributed generation (DG)s at the LV grids should participate in voltage regulation depending on their capacity [95]. In particular, a power factor between 0.95 leading and 0.95 lagging is required to be considered for units smaller than 13.8 kVA. Furthermore, a power factor within 0.9 leading and 0.9 lagging is essential for the larger units [96]. The reactive power flow in the distribution feeder should be kept small to reduce system losses.

In distribution feeders, at low PV penetration levels (below 10%), inverters tend to have low impact on the feeder's voltage regulation during peak load condition. With medium PV penetration level (up to 25%), inverter voltage support can decrease the size of the conventional units by nearly 40%. At higher PV penetration levels (30–50%), PV inverters will take a more active role to contribute to voltage regulation [97]. These statements were considered for radial test systems, however, the findings should be case specific for different applications. In this work, the penetration levels will be in the very high level.

Figure 2-13 illustrates the reactive capability curve for a PV inverter power factor operation represented by the red line, and how it coincides with the reactive power requirement that is commonly specified for transmission interconnection. If the PV power plant doesn't meet the grid code requirements at full output without additional inverter capacity, other solutions may be de-rating the plant, or to install external reactive power support devices which can cause higher costs. Inverters would be capable of producing/absorbing reactive power when they operate at a lower power level than Prated**.** PV power plants are also achieving a stage to provide reactive capability at full output as they are also technically capable like WTs [98].

During high generation, the inverters' reactive power capability is limited by the inverter's rating [21]. Oversizing is one possible solution for the inverter to access more capacity to absorb or inject reactive power. In Figure 2-13, the inverter operates in the capacitive mode on the right side of the triangle when the overvoltage occurs. On the other hand, the inverter switches to the inductive mode on the left side of the triangle when under-voltage occurs.

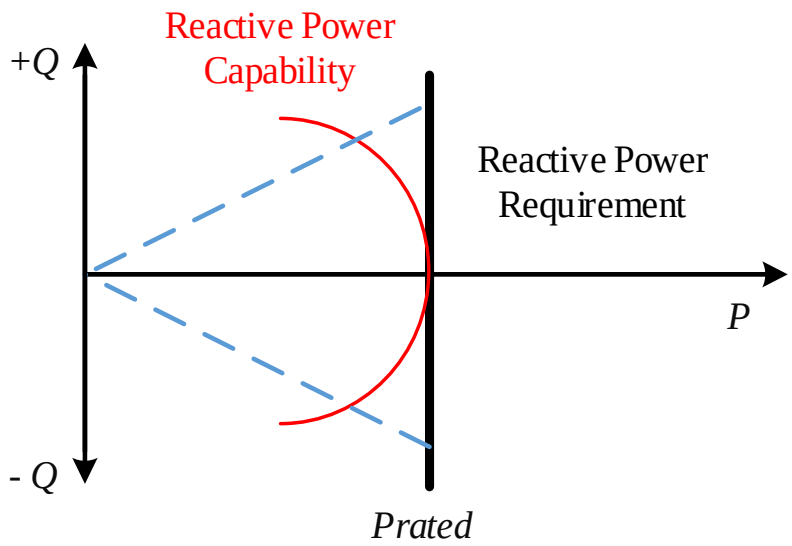

Figure 2-13. Inverter reactive power capability curve

The maximum reactive power from the PV is determined based on the PV inverter capability. The grid codes define the upper- and lower-voltage limits and the dead zone. If the voltage surpasses the considered limits, the PV inverter injects/absorbs the reactive power to control the voltage locally. It can also be highlighted that the PV reactive power consumption decreases the bus voltage deviation (See Figure 2-10). Note that when the PV active power is low, the potential risk of the overvoltage becomes smaller as well. That is since all generated PV power may be consumed locally.

The reactive power services can be used to provide ancillary service to the grid. Ancillary services can be named as reserves, regulation and load following, reactive power and voltage control, loss compensation, and system protection. Ancillary services from wind turbine includes frequency & voltage control, inertia support where PVs can also offer grid stabilisation features (voltage regulation/reactive power support). Role of these services in large-scale integration of PVs should be carefully examined, while appraising the impact of the massive use of PVs on the stability, security, and reliability of power systems. For the ancillary services supplied by PVs, more efforts have been still needed to fill the knowledge gap and to develop improved methods and solutions regarding available power estimation, faster and reliable communication and control within the plants and improved strategies. According to Ref. [99], technically, using the PVs for supplying reactive power support is feasible. As a drawback, economically, there is not enough proof for the practicality. At the moment, pilot projects are exploring this potential, but very limited real market-based applications are present.

2.6. Chapter Summary

This chapter has presented a critical literature review of voltage regulation strategies with the increased penetration of PVs in ADNs. There are technical & economical, policy and

regulatory challenges such as, managing variability and uncertainty of renewables, in the system. Solutions to technical problems can be improved by including stochastic characteristics of loads and renewables into problem solving, smart inverter adjustments and real-time system awareness.

The high penetration of PVs in radial distribution grids increase the voltage level at critical nodes, especially at the end of the feeder. The grid losses are high with the conventional voltage control techniques. The low load demand and high PV generation may result in reverse power flow, thus giving rise to the voltage in the upstream networks, also overloading the system components within the distribution network.

The voltage control methods in PV integrated networks can be generally divided into four categories as follows: i) centralized control, ii) distributed control and iii) decentralized control. The centralized approaches aim to globally optimise the network losses, voltage deviation, PVs active\reactive powers and or to contain the total number of tap operations of OLTCs. The main disadvantage of these frameworks is their massive communication infrastructures with high investment costs. The distributed control structures improve the voltage regulation and mitigate the capital cost through the coordination between nodes. However, these methods have limited optimization impact in comparison with the centralized ones. On the other hand, decentralized control provides several advantages like high efficiency, network losses reduction, local power grid support and the voltage profile enhancement. The decentralized strategies combine the benefits of centralized and distributed methods through zonal control and inter-zonal coordination in the portioned DNs. Moreover, communication devices are eliminated, that mitigates the investment cost significantly.

Recently, the future power systems are evolving in a more decentralised manner, proving that local management of the voltage is more reliable in terms of reducing the complexity level. In

the following chapters, to develop an enhanced voltage control strategy to cope with high penetration of PVs, the proposed local zonal voltage management approach will be presented. The proposed method is applied to 33 node (radial) and 69 node large-scale (radial and meshed) test systems will be compared with other traditional decentralized techniques. In addition, the stochastic assessment studies will be carried out to evaluate the system under high penetration of PVs.

3. METHODOLOGY OF THE PROPOSED LOCAL VOLTAGE CONTROLLER

3.1. Introduction

This chapter will provide an understanding of the methodology of the proposed local voltage controller and the zonal network partition method. Due to the increase anticipated in the growth of PVs in the following years, the centralised control will result in control complications with the highly decentralised control nodes in future distribution network [100]. Owing to the highly decentralised increment of PVs, network partition-based zonal voltage control is an appropriate and practical way to regulate the voltage in the distribution network [101]. Zonal voltage control divides the whole system into zones according to the partition index determined within the problem. Therefore, the zonal management becomes prominent, and each zone is managed independently. This gives the chance for decentralised management to operate without affecting other zones in the system. According to the straightforward, practical and decentralised manner of the control, this study proposes to control the voltage by partitioning the distribution network into several zones.

In the standard control approaches mentioned in Chapter 2, the PVs reactive power absorption leads to an increase in feeder transformer and lines loading. To be able to alleviate this burden, the previous studies suggest that PV units at the beginning of a feeder generate reactive power to be used at the PV systems located at the end of feeder [102]. However, this technique needs communication infrastructure. All of the abovementioned reasons are considered, and a novel local controller is proposed in this chapter to allow the further installation of PV units in ADNs.

The proposed network voltage support strategy deploys zonal reactive power management to regulate the voltage in the distribution network. This chapter will firstly give a brief understanding of the voltage sensitivity studies, and the technique will be applied to the 33 node and 69 node distribution test networks.

The fully local reactive power regulation strategy works in order for the PV systems to increase the feeder hosting capacity without using communication infrastructure. In the suggested framework, firstly the distribution feeder is partitioned into several zones based on the feeder's electrical bottlenecks taking into account of the line loadings. The electrical bottleneck is the congestion point where the power transfer capability of the power system is limited by the maximum allowable power transfer of the lines. Afterwards, a fully local controller is performed within the PV inverters, which only requires local and neighbouring PVs information. This enables the method to achieve the goal without centralised control. After, the distribution network is partitioned into zones according to the partition index, within the zones, each zone is divided into two groups of PVs serving different purposes. The PV units placed in the vicinity of the electrical bottlenecks are equipped with the proposed local controller to moderate burden on the corresponding bottlenecks. Other PV units support the network voltage using a conventional local voltage-dependent reactive power controller.

The zonal control methods demonstrate its efficiency and ability to overcome the technical challenges of centralized control for DN feeders. The proposed scheme has nearly the same control effect as the centralized control scheme achieves, however, zonal control is more feasible [100]. The inadequacies of existing control methods can be solved by the main contributions of the novel controller, is given as follows: 1) the aim of this work is to reduce the high computational burden of existing cluster partition methods, which most consider only the active power loss as an index. In this chapter, regarding the voltage sensitivity, the active power loss and reactive power exchange between the zones are selected as the indexes to be

monitored. More importantly, the voltage regulation capability of PVs is also investigated to increase the feeder PV hosting capacity.

2) The proposed voltage control can achieve independent reactive power exchange within each cluster by no need of communication. Besides reducing the complexity of the control and communication burden, it also improves voltage regulation speed and avoids excessive generation.

3) Compared with previous local voltage regulation methods [57], [63], [64], this technique has a simple structure and better suitability for governing high number of PV units in the ADNs. Discrete variables like transformer tap positions are also considered.

4) The proposed method is capable of being implemented on any network topology independently. To prove the practicality, simulations are performed for both radial and meshed distribution test systems.

Considering all abovementioned benefits of the proposed local controller, to be able to implement the method to the DN, the understanding of hosting capacity and definition of constraints are essential. Hosting capacity and the mathematical equations of constraints will be given first. Next, the proposed partition algorithm is represented and deployed to a simple test system. Subsequently, the voltage sensitivity studies are illustrated. Last, the summary for the chapter is given.

3.2. Hosting Capacity of the Feeder

Before defining the problem, the hosting capacity definition should be discussed. The hosting capacity (HC) is defined as the maximum PV generation that can be integrated into the network without violating standard limits for voltage, protection and power quality and with no feeder upgrades [103]. DNOs are responsible for indicating maximum available headroom in the

network to accommodate new DER integration to the system while keeping the voltage in the safe zone. In this context, several methodologies have been presented to increase ADNs hosting capacities such as, feeder reinforcement, PV active power curtailment and PV reactive power control [23]. However, the equipment upgrades and PV power reduction are not cost-effective for system operators and PV generation owners, respectively.

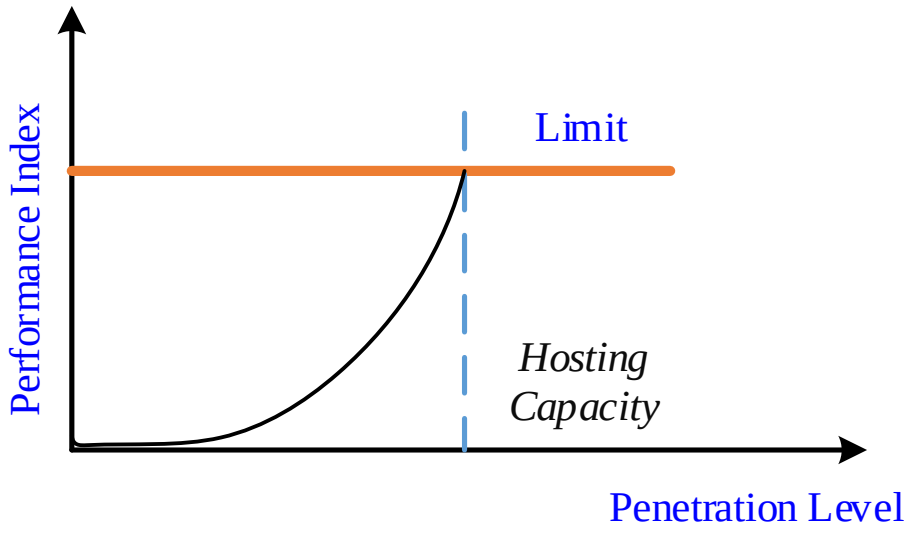

Figure 3-1. The hosting capacity according to penetration level and Performance Index

Active network management, energy storage systems and demand-side response are some of other solutions from the literature [104]. Nevertheless, these methods usually need advanced communication infrastructure as well as their high cost. Some papers also take interest to augment DG and ESS capacity together [105]. However, then the combined hosting capacity problem is very challenging. Figure 3-1 represents the effect of increased penetration level following the performance index. The limit can be defined in terms of the defined performance index.

The PVs outgrowth in the distribution system has also introduced the use of their capabilities to enhance the hosting capacity. That means that the PV systems reactive power capability can provide voltage support to rise the feeder's hosting capacity alternatively. In this case, the PV

inverter will use its reactive power capacity to contribute to the voltage regulation. Reactive power control has been proven as a useful tool to increase the HC in the feeder. Still, this should be done in a smart way to tackle the grid losses and excessive reactive power consumption in the network. According to the technical report in [106] , in twenty year time the network will be able to increase the penetration level to 100 percent due to generation and reactive power absorption without need of curtailment.

One of the critical points while defining hosting capacity is to determine the performance index limits according to power system quality parameters i.e. over/under voltage limits or others as security constraints. Hosting capacity can be directly associated with grid losses and minimisation of reactive power support [107]. Voltage and thermal limits of system components (e.g. line and transformers) are generally involved in the hosting capacity analysis. Overvoltage is a protruding factor that restricts the ADNs' feeder hosting capacity. This work will comprise of voltage limits, transformer loading and branch flow limits. Besides, fault level constraints [108] and security constraints [109] are also important factors which also can be considered in further studies.

3.2.1. Calculation of the feeder hosting capacity

This section introduces the terminology for the problem formulation and constraints for voltage control captured by the methodology proposed in this thesis. The hosting capacity is a measure of how much new production (PV in this case) or new load allowed to be connected to the network without jeopardising the consistency of the network. As mentioned earlier, the feeder hosting capacity can be considered from different perspectives namely voltage level, feeder topology, system elements, controllable elements (e.g. transformers) and voltage regulation.

The calculation of hosting capacity can be done instead by analytical methods or some programming techniques and running optimal load flow.

In this work, the main problem can be defined as increasing the PV penetration in the system without limiting the hosting capacity. To tackle the challenges of the feeder hosting capacity, some performance measures are introduced to outline the capability of the feeder. The bus voltage limits, current limits and transformer loading will be observed while high penetration of PVs is included in the ADN. Load flow analysis will be executed, and the performance indexes will be compared to the limits. The algorithm will check if the grid has a capacity allowance for more penetration. That will continue until one of the limitations are surpassed. Finally, that would determine the maximum allowable PV penetration to be allocated by the ADN.

3.2.1.1. Constraints

The network hosting capacity is considered from the perspective of three following performance indexes namely:

i. Bus voltage constraints:
ii. Transformer loading constraints
iii. Branch flow constraints:

(i) Bus voltage constraints,

Each bus voltage should meet the limits as: the maximum and minimum voltage constraints are defined as follows[79], in Equation (3.1) and (3.2):

$$\text{Maximum voltage constraint}_{t,i} = 100\left(\frac{\text{Max. voltage of buses } (p.u.) - 1}{V_{\max} - 1}\right) \quad (3.1)$$

$$\text{Minimum voltage constraint}_{t,i} = 100\left(\frac{\text{Min. voltage of buses } (p.u.) - 1}{1 - V_{\min}}\right) \quad (3.2)$$

where, the boundaries of V_{max} and V_{min} are 1.1 and 0.9 per unit *(p.u.)* in this study, respectively, for each time interval t and scenario i.

(ii) transformer loading:

The transformer loading constraint in each scenario is equal to the maximum loading of the transformer over a day [110]. Its MVA rating will limit the maximum amount of apparent power flow through the transformer, presented by Equation (3.3).

$$\text{"Transformer loading constraint"} = S_{tr,f,t,i} < S_{MVA} \quad (3.3)$$

Where $S_{tr,f,t,i}$ represents the forward apparent power flow across the transformer in each time interval t and for the scenario i, S_{MVA} is the MVA rating of the transformer. In this study, not being in the scope of the study, reverse power flow constraint is not included in the calculations.

(iii) branch flow

A branch flow constraint is also defined regarding the network lines loading. The flow of power through the distribution line should be less than its thermal capacity [111], by Equation (3.4):

$$\text{"Branch flow constraint"} = It_{t,i} < Imax \quad (3.4)$$

3.2.1.2. Index parameters

The algorithm aims to partition the distribution network into several clusters with reducing the losses in the system, also increasing the hosting capacity. For this aim, two important index parameters are selected for evaluating the performance of the network. The selected indexes are based on the network active power losses and the interchanged reactive power between

zones. Previous papers only considered the active power loss, without the consideration of exchanged reactive power between zones [111]. In the proposed work, the exchanged reactive power between zones is also considered as an additional index. The selected function will aim to avoid the generation reduction in PV generation for the DNs with high penetration of decentralised PV units.

The approach doesn't consider the centralised optimisation model, in means of the method doesn't include an optimisation algorithm, but instead minimised the network active power losses and the interchanged reactive power between zones. The strategy is arranged according to the severity of voltage increment on the adjacent buses. The next section will give the voltage sensitivity studies required for the problem formulation of the proposed network partition algorithm.

3.3. Voltage Sensitivity Studies

For a better understanding of the proposed local voltage controller and to be able to compare it with standard reactive power control strategies, this section will focus on sensitivity studies of two primary strategies from the literature namely PF-power and Q-voltage. These control strategies are compared to comprehend their effect on voltage regulation. Afterwards, the proposed local voltage controller will be investigated from the voltage sensitivity point of view.

3.3.1. Standard Reactive Power Strategies (PF-power and Q-voltage strategies)

In this section, the performance of the PF-power and Q-voltage schemes are firstly investigated by voltage sensitivity analysis. The active and reactive power flows in a radial feeder with four PV systems are shown in Figure 3-2. The PVs reactive power is controlled by the PF-power and Q-voltage characteristics.

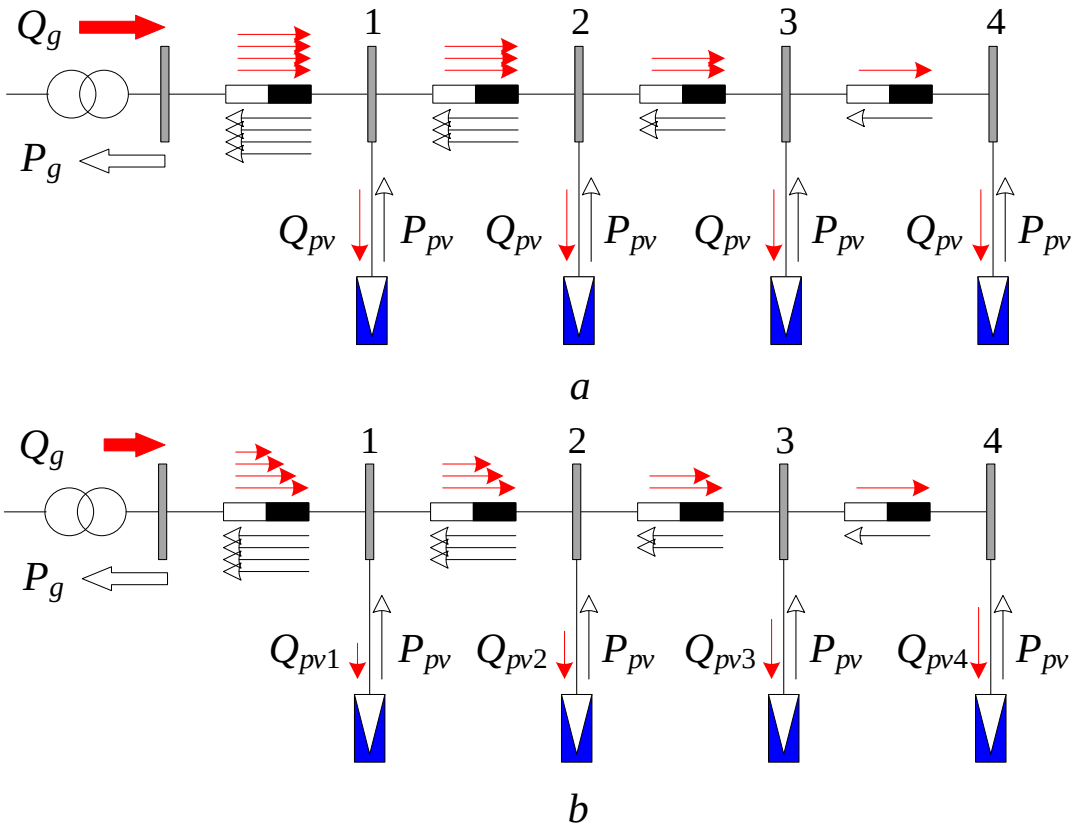

Figure 3-2. The PV systems reactive power flow (a) The PF-power scenario, (b) The Q-voltage scenario

Let us presume that the PV systems are generating their nominal active power. Also, all loads are ignored to model the worst-case scenario from the overvoltage point of view. The required data for calculating overvoltage at the end of the feeder are listed in Table 3-1. All parameters are in per unit except for the PV power factor and voltage droop gain.

Table 3-1. The parameters of the four PVs feeder

$P_{pvn}\ (pu)$	PF_{pvn}	$R_l\ (pu)$	$X_l\ (pu)$	$V_{min}\ (pu)$	$V_{max}\ (pu)$	$V_{ref}\ (pu)$
0.25	0.9	0.04	0.03	0.9	1.1	1

In case of the PF-power scenario, the voltage deviation at bus 4 can be derived using Equation (2.11) as follows in Equation (3.5) :

$$\Delta V_{b4} = \sum_{i=1}^{4} i\left(R_l P_{pv} + X_l Q_{pv}\right) \tag{3.5}$$

If PV systems operate with their unity power factor, the overvoltage becomes Equation (3.6):

$$\Delta V_{b4} = \sum_{i=1}^{4} iR_l P_{pvn} = \sum_{i=1}^{4} 0.01i = 0.1 \tag{3.6}$$

In PF-power scenario, when each PV consumes its nominal reactive power, the voltage rise rate decreases as follows in Equation (3.7):

$$\Delta V_{b4} = \sum_{i=1}^{4} i\left(0.04P_{pvn} - 0.03Q_{pvn}\right) \approx 0.06 \tag{3.7}$$

The feeder transformer apparent power is calculated as Equation (3.8):

$$S_{tr} = \sqrt{\left(4P_{pvn}\right)^2 + \left(4Q_{pvn}\right)^2} \approx 1.1 \tag{3.8}$$

In other words, the PF-power method provides 0.4% voltage reduction per 1% increment in feeder transformer capacity. In the case of the Q-voltage scenario, the voltage rises at bus 1 can be derived considering the Equation (3.9):

$$\Delta V_{b1} = 4\left(R_l P_{pvn} + X_l Q_{pv1}\right) \tag{3.9}$$

With Q_{pv1} as a function of the voltage of bus 1 which can be calculated as Equation (3.10):

$$Q_{pv1} = -R_v \Delta V_{b1} \tag{3.10}$$

With Q_{pv1} as a function of the voltage of bus 1 which can be calculated as Equation (3.11):

$$Q_{pv1} = -R_v \Delta V_{b1} \tag{3.11}$$

The voltage droop gain can be derived as follows in Equation (3.12):

$$R_v = \frac{Q_{pvn}}{V_{\max} - V_{ref}} \approx 1.2 \tag{3.12}$$

Substituting Equation (3.10) into Equation (3.9) yields:

$$\Delta V_{b1} = \frac{4R_l P_{pvn}}{1 + 4X_l R_v} \tag{3.13}$$

The voltage deviation in bus 2 may be formulated as Equation (3.14):

$$\Delta V_{b2} = \Delta V_{b1} + 3\left(R_l P_{pvn} + X_l Q_{pv2}\right) \tag{3.14}$$

Then, this voltage deviation is found by replacing ΔV_{b1} with, (3.13) in (3.14) as follows:

$$\Delta V_{b2} = \frac{3R_l P_{pvn} + \Delta V_{b1}}{1 + 3X_l R_v} \tag{3.15}$$

Following a similar procedure, it can be written as Equation (3.16):

$$\Delta V_{b3} = \frac{2R_l P_{pvn} + \Delta V_{b2}}{1 + 2X_l R_v} \tag{3.16}$$

Finally, the voltage deviation at bus 4 is as Equation (3.17):

$$\Delta V_{b4} = \frac{R_l P_{pvn} + \Delta V_{b3}}{1 + X_l R_v} = 0.081 \tag{3.17}$$

Note this is permissible. The feeder transformer apparent power in this scenario is calculated as Equation (3.18):

$$S_{tr} = \sqrt{\left(4P_{pvn}\right)^2 + \left(Q_{pv1} + Q_{pv2} + Q_{pv3} + Q_{pv4}\right)^2} \approx 1.04 \tag{3.18}$$

After all the numerical calculations, the outcome reveals that the Q-voltage method provides roughly 0.5% voltage reduction per 1% increase in the feeder transformer capacity. Therefore, the Q-voltage method is a more cost-effective solution than the PF-power strategy to mitigate the overvoltage problem. It is because the voltage sensitivity analysis determines the most efficient locations to serve reactive power for the feeder voltage support from the PV systems placed at the end of the feeder [80]. As an outcome of the sensitivity studies, it is possible to say that the PV system absorbs less reactive power under Q-voltage control strategy when compared to the Power Factor-P control strategy.

3.3.2. Proposed Local Reactive Power Control Strategy

The reactive power flow under the proposed scenario is illustrated in Figure 3-3 at midday hours with a high PV generation on the selected day. According to the voltage sensitivity analysis, this study suggests that the PV systems in Group A2 will support network voltage using the Q-voltage scheme. This suggestion potentiate the voltage regulation of the system as explained in Ref. [41] since the same amount of reactive power becomes more efficient when the PV systems are placed at the end of the feeder. In this group, the feeder voltage is locally supported by the PV units, individually. On the other hand, the reactive power of the PV systems in the group A1 is modulated through the proposed local controller.

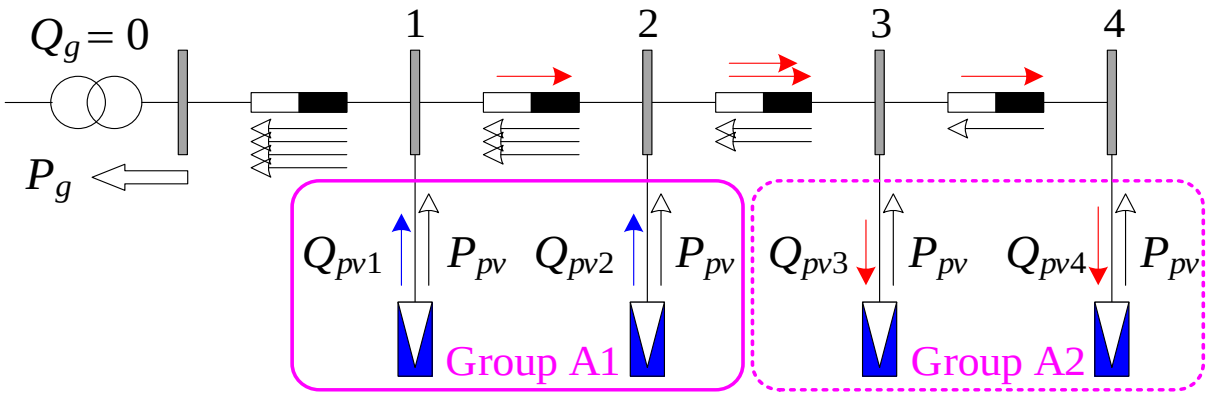

Figure 3-3. The PVs reactive power flow with the proposed method

The PVs in group A1 supply the reactive power for those of group A2. Hence, the reactive power flow in the first line will be minimized, and the bus 1 voltage deviation is given by Equation (3.19):

$$\Delta V_{b1} = 4 R_l P_{pvn} \tag{3.19}$$

For simplicity, suppose that each of these first two PV systems generates one-half of the cumulative reactive power of the other two PV units. Therefore, the voltage increment of bus 2 becomes as in Equation (3.20):

$$\Delta V_{b2} = \Delta V_{b1} + 3R_l P_{pvn} + 0.5X_l \left(Q_{pv3} + Q_{pv4}\right) \tag{3.20}$$

On the other hand, the voltage deviation at buses 3 and 4 may be expressed as Equation (3.21) and (3.22), respectively:

$$\Delta V_{b3} = \Delta V_{b2} + 2R_l P_{pvn} + X_l \left(Q_{pv3} + Q_{pv4}\right) \tag{3.21}$$

$$\Delta V_{b4} = \Delta V_{b3} + R_l P_{pvn} + X_l Q_{pv4} \tag{3.22}$$

The reactive power of the PV systems in group A2 is determined by the Q-voltage characteristics as follows in Equation (3.23) and (3.24), respectively:

$$Q_{pv3} = -R_v \Delta V_{b3} \tag{3.23}$$

$$Q_{pv4} = -R_v \Delta V_{b4} \tag{3.24}$$

ΔV_{b3} can be derived as Equation (3.25):

$$\Delta V_{b3} = \frac{R_l P_{pvn}\left(9 - 7.5R_v X_l\right)}{1 - 4R_v X_l + 1.5R_v^2 X_l^2} = 0.081 \tag{3.25}$$

Finally, the overvoltage at the end of the feeder is given by Equation (3.26):

$$\Delta V_{b4} = \frac{\Delta V_{b3} + R_l P_{pvn}}{1 - R_v X_l} = 0.088 \tag{3.26}$$

which is smaller than the allowable maximum voltage rise. This voltage increment rate is about 0.01 larger than that of the Q-voltage scenario, however, the proposed method releases the transformer capacity occupied by the PVs reactive power. In comparison with the method in Ref. [102], the suggested framework does not need any communication structure. It can be observed that this framework results in a simultaneous and significant reduction of the feeder transformer and the network lines loading. Extended sensitivity studies applied on 33 bus test system can be found in Appendix B2.

3.4. The proposed network partitioning algorithm

The network partitioning is a crucial part of the proposed reactive power control framework for active distribution feeders. In this study, a precise but straightforward practical algorithm is developed to find how the candidate PV systems will participate in the reactive power exchange in the clusters.

The fully local reactive power regulation strategy works in order for the PV systems to increase the feeder hosting capacity without using communication infrastructure. In the suggested framework, firstly the distribution feeder is partitioned into several zones based on the feeder's electrical bottlenecks from the perspective of lines loading condition. Afterwards, a fully distributed local controller is performed within the PV inverters, which only requires local and neighbouring PVs information, enables the method to achieve the goal without centralised control. After the distribution network is partitioned into zones according to the partition index, within the zones, each zone is divided into two groups of PVs serving different purposes. The PV units placed in the vicinity of the electrical bottlenecks are equipped with the proposed local controller to moderate burden on the corresponding bottlenecks. Other PV units support the network voltage using a conventional local voltage-dependent reactive power controller.

In this algorithm, the selected index parameters are considered with the horizon of 15 minutes time interval, with obtaining the monitored parameters from the network. Two parameters are considered, namely the active power loss of the network losses and the interchanged reactive power between zones.

It should be highlighted that this approach would be in use for any case of the distribution test system (meshed, radial, etc.) for practical purposes. In the following chapters, simulation results for both radial and meshed topologies are presented. Besides being suitable with each

network topology, the proposed partition method can also update and adapt itself to the generation alteration in the system for further applications.

3.4.1. Network Partition Strategy

The proposed method mainly partitions a multi-lateral distribution feeder into several zones through finding the feeder electrical bottlenecks from the perspective of the lines loading values. In each zone, the PV systems are divided into two groups. The available reactive power capability of the PV systems of the group nearby a bottleneck is deployed to decrease the reactive power flow at the bottleneck. To this end, a local measurement monitors reactive power flow at the PV terminal. Accordingly, the PV inverter injects\absorbs the measured reactive power into\from the network in a fast and flexible manner considering the inverter power limit. On the contrary, the PV units at the second group provide grid voltage support using a traditional local droop-based voltage controller. Thus, the reactive power burden on the feeder bottlenecks as well as the feeder transformer will be reduced significantly. By this technique, zones will be effectively controlled with the reduced computational burden of the control variables. Figure 3-4 illustrates the network partition algorithm strategy. The network algorithm can be divided into two sections, each section with “n” groups.

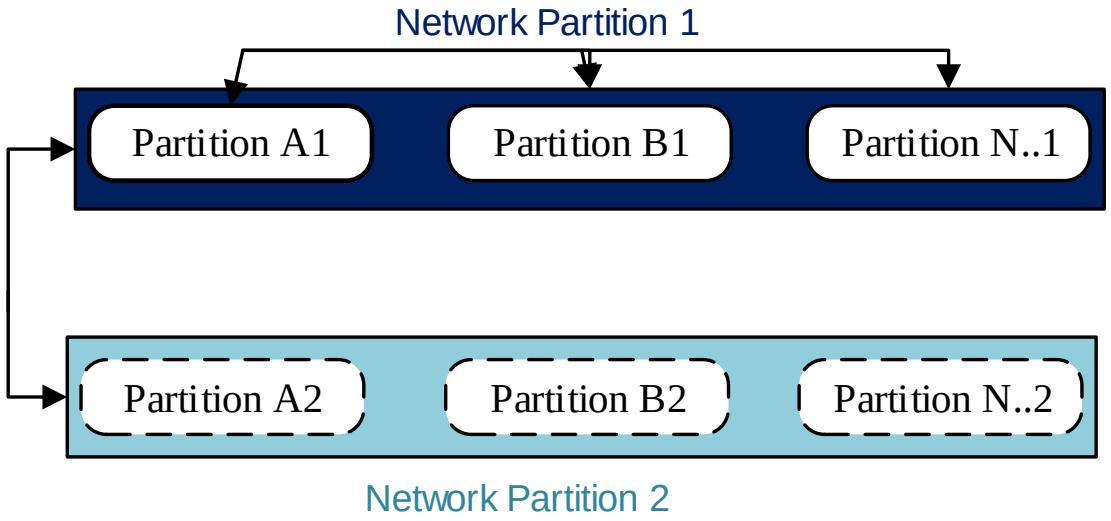

Figure 3-4. Network Partition Algorithm

In the existing zonal control algorithms, the reactive/active power of the PV systems was controlled in such a way that an objective function is minimised [112], [113]. In these studies, the network active power losses and the interchanged reactive power between zones were selected to be optimised as the fitness function. However, massive communication infrastructures are required to implement these zonal control strategies. Optimisation techniques endeavour to solve the optimization problem in a centralized manner, which requires massive communication infrastructures to implement these zonal control strategies with the large-scale integration of PVs to ADNs [112]..

In the proposed study, the heavy computational burden by centralised strategy is overtaken with a decentralised local control strategy. Therefore, the need for centralised control is eliminated by grouping the ADN into zones by using a simple technique. Detailed information will be provided in Section 3.4.3. To be able to understand the local voltage control scheme in detail, advanced sensitivity studies are presented in Appendix B2. In the proposed study, at the zones located at the end of feeder laterals, the PV systems support the grid voltage through

a standard local Q-voltage control. For the rest of the PV systems, a local controller is proposed to reduce the reactive power flow.

3.4.2. Problem Solving

The proposed network voltage support strategy deploys zonal reactive power management to control the voltage of ADNs without surpassing the voltage limits. In order to solve the problem, the PV system design will be investigated, followed by the integration of the proposed controller.

3.4.2.1. Design and control of the PV system before implementation of the controller

The PV system is demonstrated through DIgSILENT Power Factory software, represented in Figure 3-5. The PV module is interfaced with the AC grid through the PV inverter, where the inverter is represented by the Static Generator block. The inverter is controlled by the PQ controller which provides it with the reference values for *id* and *iq*. "PLL" is the device to obtain the phase degree of the output current of the PV inverter and provides the utility voltage angle for static generator [114].

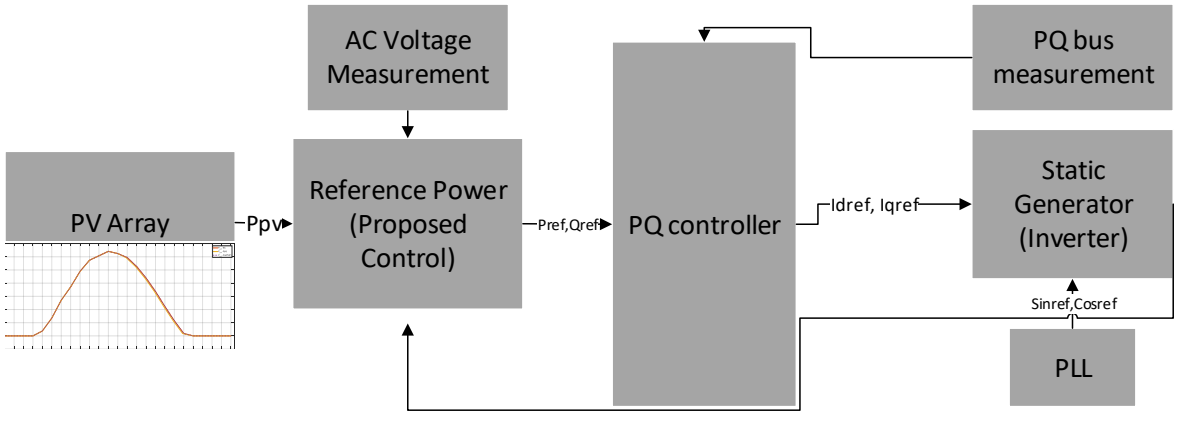

Figure 3-5. A general overview of the PV topology

The bus voltage measurement and PV array active power are inputs to the proposed controller. P_{ref} and Q_{ref} are the active and reactive power reference values calculated by the controller. Active power reference (P_{ref}) is determined by the PCC measured active power value and the PV power input (P_{PV}).

The reference power block collects the voltage and PQ measurement data. The voltage error signal is determined through measurement and reference values then reactive power control method is applied. Output of the controller gives the output signal, Q_{ref}. On the other hand, the PV system 24 hour active power data is presented by a power factor of 0.9. Hereby, the P_{ref} to be used in PQ controller, is evaluated.

PQ measurements are taken from the buses of each terminal. The PQ controller consists of two PI controllers, which compare the bus measurement of PQ data with the P_{ref} and Q_{ref}values coming from the power reference block. The PI controllers have the droop value (K =0.5) and time delay (T=0.01). Outputs of the PI controllers are id_{ref} and iq_{ref} , respectively. These two signals will be inputs for the static generator with the reference sin and cos signals obtained by the PLL. The static generator represents the PV generator in the frame. This frame doesn't consider the use of inverter and maximum power point tracking (MPPT) models, simplified to observe the different control methods more with time-varying PV system with high resolution simulation configurations.

3.4.2.2. Application of the local reactive power controller

In the proposed control scheme, the available PV inverter capacity is deployed to decrease the up-stream reactive power flow.

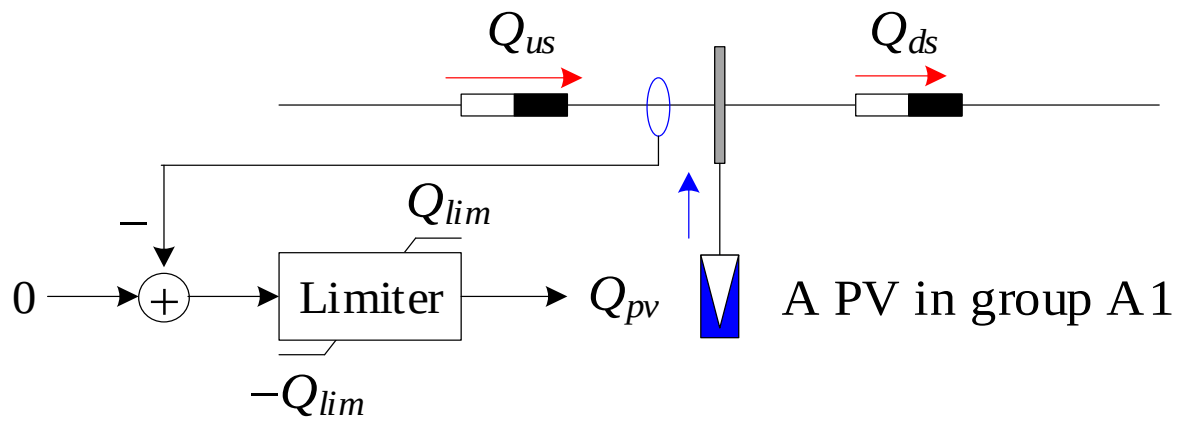

Figure 3-6. The proposed local controller for PVs reactive power

Figure 3-6 presents the proposed local controller strategy. Q_{us} And Q_{ds} denote up-stream and down-stream reactive power flow in the PV terminal, respectively. A measurement device monitors the up-stream reactive power Q_{us} at the PV terminal within every 15 minutes. After the measured value is received, the PV system tries to minimise the amount of the up-stream reactive powerQ_{us}. However, this objective function is subject to the PV reactive power limit Q_{lim} defined previously in the Equation (2.2).

To introduce the local reactive power control strategy, the four bus and four PV feeder has been partitioned into zones as previously explained in the problem formulation. As it is portrayed in Figure 3-7, the first two PV systems are clustered as Group A1 and the other two PVs as Group A2.

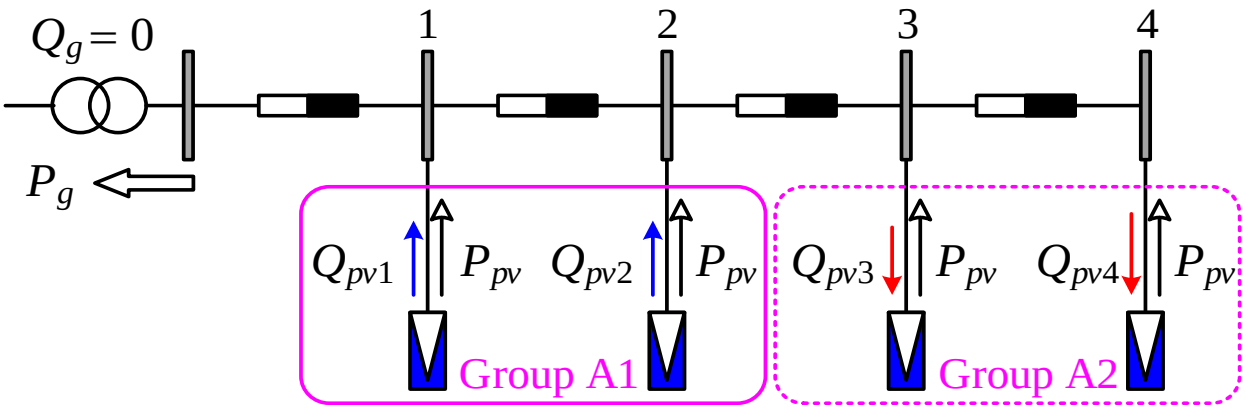

Figure 3-7. The PVs reactive power flow with the proposed method

Following the voltage sensitivity analysis, this study suggests that in Figure 3-7, the PV systems in Group A2 support network voltage using the Q-voltage scheme. In this group, the feeder voltage is locally supported by the PV units, individually. On the other hand, the reactive power of the PV systems in the group A1 is modulated through the proposed local controller (Figure 3-6). In the proposed strategy, according to the contributions stated above, the need for centralised control is eliminated by grouping the ADN into zones by using a simple technique.

According to proposed controller, the PVs allocated for the second group in each zone will work according to the Q-voltage strategy to decrease the grid losses. Network power losses can be presented as given in Equation (3.27) where *B* is set of network branches *ij*;

$$Network\ power\ loss = \sum_{(ij \in B)} P_{(ij)}^{loss} \tag{3.27}$$

Thereby, the overloading of the system components, transformers and lines, would be reduced with the proposed control technique. The hosting capacity would be increased since this set point will improve the performance of the system. The excess reactive power will be consumed within its generation unit, without reaching to the upstream network. On the other hand, if the generation is meeting the demand for other consumers connected to the other terminals, those PV systems can continue their control strategy without consuming reactive power. That would

increase the flexibility of the system and contribute to the decentralized control strategy in means of the absence of central supervisory control. The issues like computational burden and communication time delay will be avoided in this regard.

3.4.3. Deployment of the local voltage control scheme with network partitioning

It is very crucial to deploy the local voltage control strategy to solve the overvoltage issue challenges. To clarify the method, the flowchart in Figure 3-8 represents the deployment of the local voltage scheme.

The flowchart is also explained step by step:

Step 1: the network data that includes the line parameters, and the feeder transformer is loaded to the algorithm.

Step 2: to consider the worst-case scenario, all the loads are disconnected from the network.

Step 3: each PV system is connected to each node of the feeder. For initial conditions, it is assumed that all the PV systems are initially equipped with the conventional Q-voltage local controllers.

Step 4: the feeder transformer loading is monitored. If the transformer is not fully loaded, the nominal power of the PVs will be increased until the transformer reaches its full load operation.

Step 5: if the transformer is fully loaded, the algorithm will find the bottlenecks from assessing the line loadings.

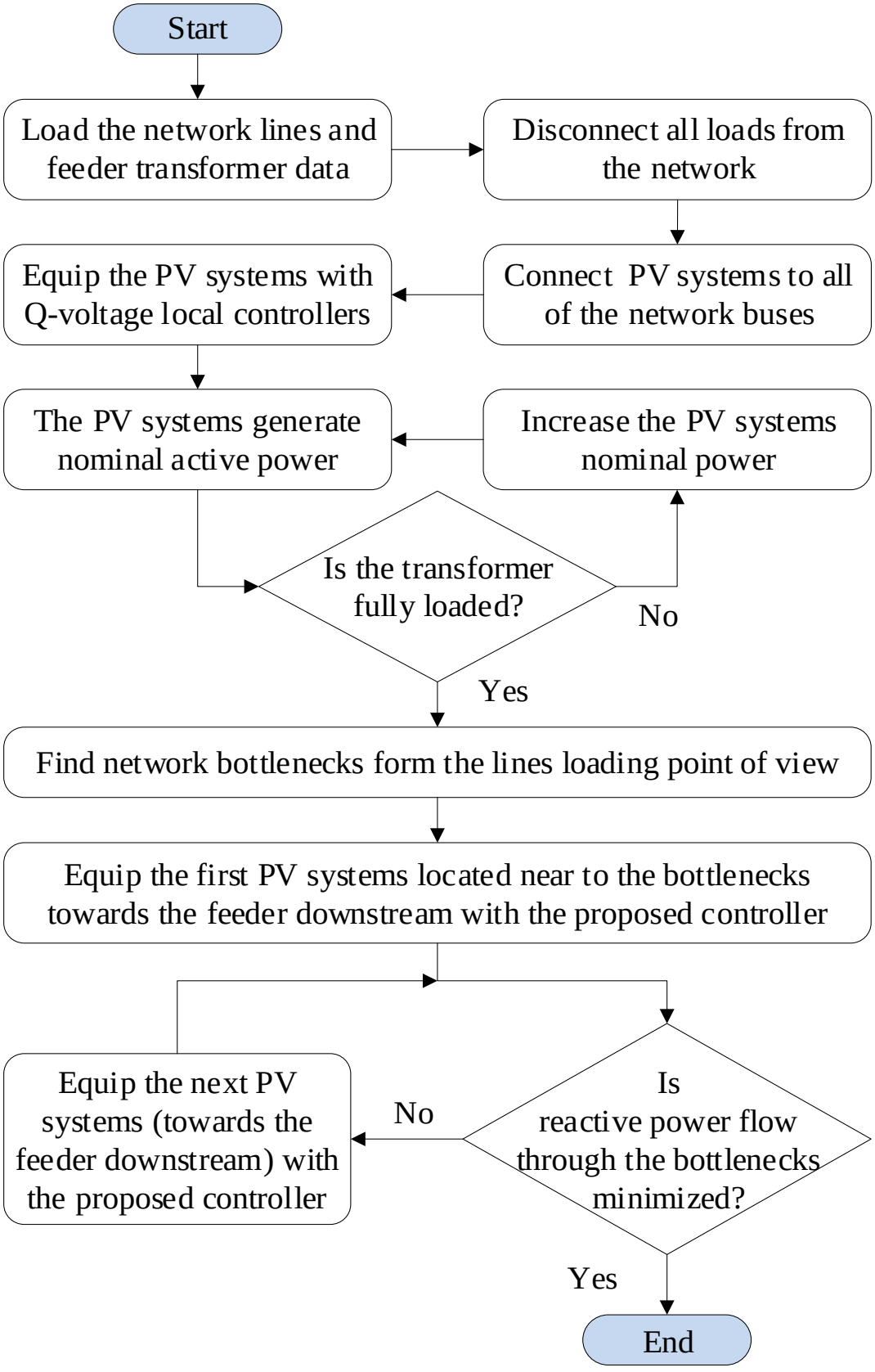

Figure 3-8. The flowchart of the network partitioning algorithm

Step 6: The PV systems near to the bottleneck of high line loading will be equipped with the proposed local reactive controller towards the downstream feeder to reduce the reactive power flow.

Step 7: if the equipped PV systems are not capable of reducing the line loading, neighbouring PV systems closer to the downstream feeder will also be equipped with the proposed controller until the loading will be reduced to permissible limits.

Subsequently, the algorithm finds the network electrical bottlenecks from the perspective of lines loading condition. Figure 3-9 represents the illustration of the bottleneck in the previously studied four bus test system. In case of the feeder laterals, the lateral's connection point to the main feeder may be defined as a bottleneck. As illustrated, the PV system presented in the rectangular shape, has the proposed local controller to reduce the flow towards the bottleneck.

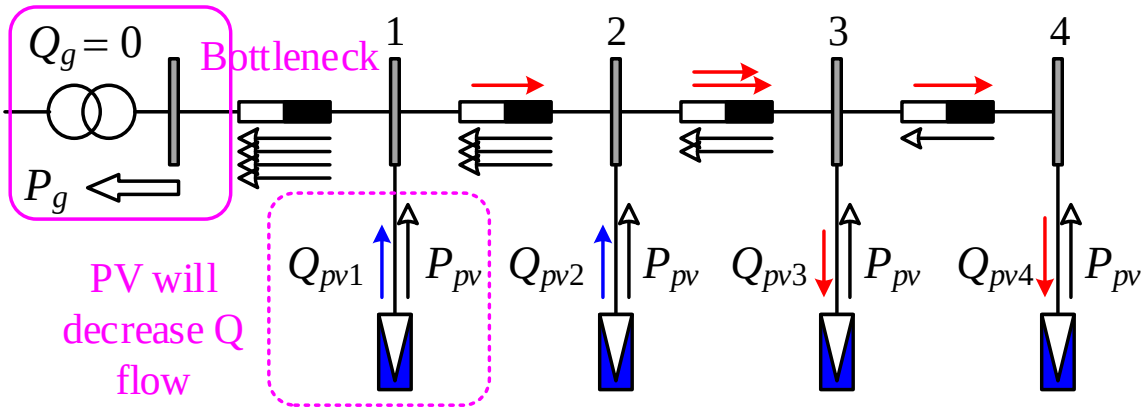

Figure 3-9. Bottleneck in the system

The following PV systems, which are in the vicinity of the bottlenecks towards the feeder downstream, will be equipped with the proposed local controller if needed. Then, the algorithm monitors the reactive power flow through the bottlenecks. If it is not minimized, the algorithm runs to equip the following PV units with the suggested controller as well. The process will be repeated toward achieving the desired results.

3.5. Chapter Summary

This Chapter introduces the methodology of the proposed local voltage control method by the hosting capacity constraints, from the main voltage control problem identified in Chapter 2. For the network management, an upfront algorithm has been developed to do network partitioning for real-world distribution multi-lateral feeders. In the first step, the algorithm finds the network bottlenecks according to the lines loading. It is worth to note that the worst-case network scenario is selected to find the bottlenecks. In the worst case, all the network loads are disconnected, and it is assumed that PVs would generate their maximum active power. Following, the sensitivity studies for the standard reactive power control strategies, this study suggests that each zone is divided into two groups. PV systems in Group 2 will support network voltage using the Q-voltage scheme, where Group 1 tries to reduce the reactive power flow towards the upstream network. This suggestion potentiates from the explanation that the voltage regulation gets more effective since the same amount of reactive power becomes more efficient when the PV systems are placed at the end of the feeder. Afterwards, PV and load profile information are given for the studied test systems.

The network partitioning is a vital part of the proposed reactive power control framework for active distribution feeders. In this study, a practical but straightforward algorithm is developed to find the candidate PV systems to be clustered. This mainly divides a multi-lateral distribution feeder into several zones to equip the PV systems located in half of these zones with the proposed local reactive power control strategy. In contrast, the other zones are regulated by Q-voltage controller. The algorithm runs to minimise selected indexes, active power network loss and interchanged reactive power between zones. The upstream reactive power is measured every 15 minutes and the PV system tries to minimise upstream reactive power flow with a limiter from PV inverter. This process will be repeated towards achieving desired outcomes.

As a result, the voltage is kept within permissible limits, and the transformer loading decreases. Therefore, it leads to a growth in the hosting capacity of the feeder, allowing more PV units to be part of the ADN.

4. METHODS BASED ON STOCHASTIC EVALUATION FOR PV DOMINATED ADNs

4.1. Introduction

This chapter presents a stochastic assessment of input parameters to enhance the accuracy of the simulation results with the high penetration of PVs in active distribution networks. In the previous chapter, the feeder hosting capacity of the distribution network challenges was addressed by three constraints as bus voltage, branch flow and transformer loading. Besides considering these constraints, a vital evaluation from the stochastic nature introduced by PVs and loads in the future power systems, is studied.

The modern power systems consist of high penetrations of DERs, considerably photovoltaic panels, wind turbines and storage devices. Several benefits will be achieved by the new smart infrastructure, e.g. PVs to be capable of injecting power to the grid and participating in the demand-side response. However, the stochastic nature of the PVs may cause critical problems for the distribution grid, such as the variability and uncertainty from PVs. Moreover, the load demand is another uncertain variable which needs to be considered when analysing the distribution network.

Sensitivity analysis is a possible solution to determine uncertainty, but it can solve one uncertain variable at once. With sensitivity analysis, the most influencing uncertain parameter can be found, but it can't select optimal design under conditional uncertainties [102]. The deterministic approaches have shortfalls to represent the current profile of the grid with

uncertain characters of PV and loads. Consequently, the stochastic analysis is an effective method to pre-manage the integration of PVs in distribution networks.

The goal of this chapter is first to present an overall hierarchical background for stochastic approaches and their applications on modern power systems. After, the chapter will give a brief understanding of the applicability of the Monte Carlo simulations (MCS), to model the uncertainty in the ADNs with the random variables of solar PV power output and load demand. To this end, a scenario-based technique has been proposed to represent the method. Roulette Wheel Mechanism (RWM) and MCS simulations are used to enhance the preciseness by representing Probability Density Function (PDF) s of PV power output and load demand random variables. This chapter will assess the hosting capacity with more accuracy in the results by using the scenario generation & reduction. The stochastic variability of fifteen minutes load demand and PV power output are represented by thousand set of scenarios for a day throughout the year. For computational efficiency, the scenario reduction is applied, resulting in ten reduced scenarios as representative of the probability distributions of initial thousand scenarios.

4.2. Overview of the Approaches for Uncertainty Modelling

The challenges of the integration of renewable energy sources and different type of loads increase the uncertainties in the power system operation [115]. Uncertainty can be the load demand or power generation offered at that particular time, alteration in weather conditions in a dynamic system.

Table 4-1 gives a brief impression over deterministic and stochastic model representations. Stochastic models have inherent random uncertainty where individual samples or empirical distributions from a set of samples are created. Usually, the stochastic models work in a discrete

time scale. The problem is decomposed into phases, and the solution is developed as a step by step approach.

Table 4-1. Deterministic and stochastic models′ comparison

Deterministic Models	**Stochastic Models**
Not always probable to solve uncertainties (multivariate uncertainty analysis problem)	Reflect real world problems with a range of possible future outcomes
The output is determined by the parameter values & initial conditions	Probability distributions govern the data known/estimated
system variables are combined to produce the system outputs, referring to all physical constraints	Possess some inherent randomness using distribution functions, subject to change with uncertainties
calculation time is limited for applications on larger systems	Calculation time is inherent from the size of the system, depends on the sample number
basic computations are enough to solve deterministic models, even without simplifying the mathematical models	Computational burden may increase in some kind of stochastic models (e.g. MCS)

A probabilistic method can accurately present the behaviour of the future power system in regards to uncertainties in the system. A probability density function is determined to observe the selected parameter to change a small-time step in a random direction. Repeating this approach several times, a frequency distribution of concentrations is being interpreted as a probability distribution. Following, based on the model, the concentration will be in range with a given probability. Neglecting the uncertainty of the PVs and loads may result in the incorrect assessment of solutions in reality. Therefore, recently important research institutes like EPRI, identify the need for probabilistic assessment to be included for defining uncertainties in future

distribution system studies [116]. Moreover, with the implementation of probabilistic analysis, the accuracy of the stochastic nature of PVs can be presented.

In the literature, there are several approaches to solve existing uncertainty problems. Figure 4-1 represents the fundamental approaches to solve uncertainties in the system depending on different techniques. They can be categorized as approximate methods, fuzzy methods, robust optimization methods, interval optimization and probabilistic approach. An extended explanation for fundamental approaches to solve uncertainties is presented in Appendix B3.

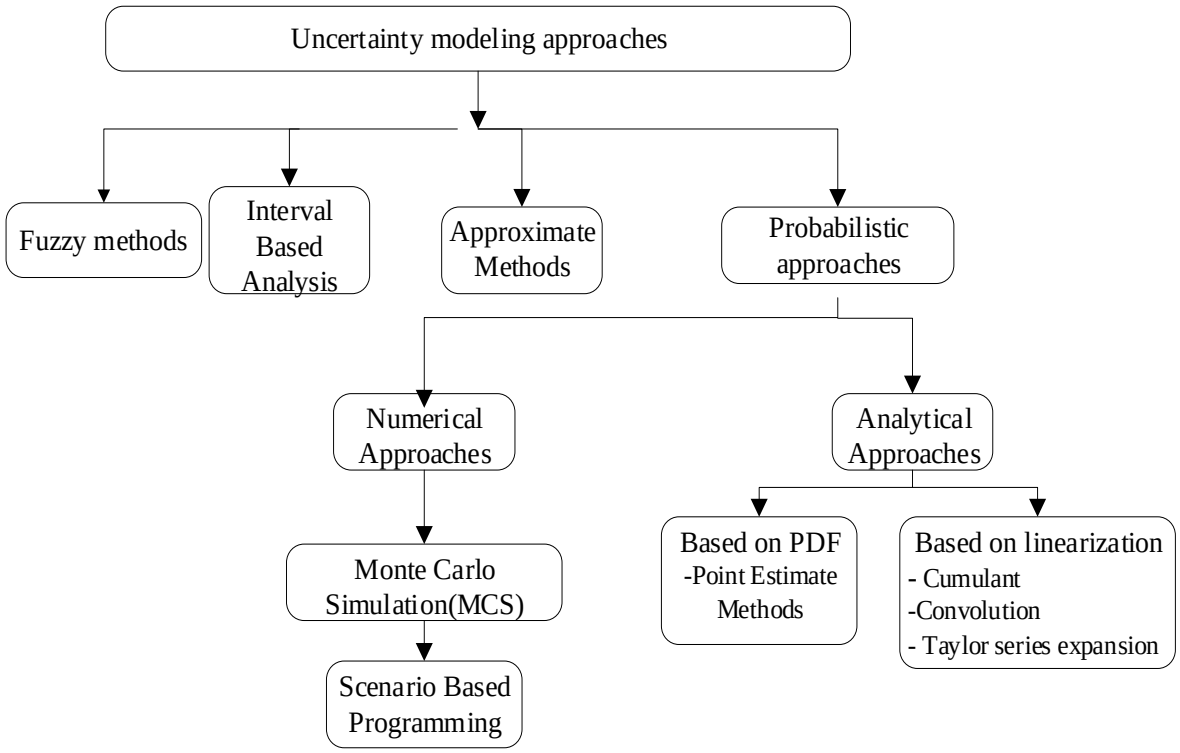

Figure 4-1 Classification of uncertainty modelling.

Stochastic approaches are presented to improve accuracy of models with the eventual aim of reducing uncertainties in terms of renewable sources and consumption units [117]. To evaluate the uncertain random variables, studies [118]–[120], ensure that the Monte Carlo simulation (MCS) technique is a widely accepted method for the stochastic analysis. MCS includes several sampling uncertainties to resolve distributions of unknown stochastic parameters. Studies [121], [122] are conducted to increase the hosting capacity of ADNs with considering the

uncertainties of renewables. An extensive formulation is proposed for the hosting capacity enhancement of distribution network by using linear stochastic model, where the Roulette Wheel mechanism (RWM) is used to generate load samples for representing load uncertainties [123]. In [124], the association between the number of PVs connected to distribution network and hosting capacity is investigated. Considering the stochastic nature of PV generation and load demand and presenting them with random forms of probabilities, voltage levels were calculated to assess the PV hosting capacity. Next section will focus on the probabilistic methods to solve PV and load uncertainties.

4.3. Probabilistic Approach to Represent PV an Load Uncertainties

Probabilistic assessment is an alternative to solve the stochastic behaviour of future energy systems where the outcome of energy is uncertain. A probabilistic approach is based on probabilistic data input and produces a set of results. That means that instead of a mean value over the time, there would be a distribution function representing occurrence probabilities of different quantities over the same time scale. After obtaining the distribution function, the quantities which are mean values and standard deviations can be derived.

4.3.1. Classification of Probabilistic Approaches

Probabilistic approaches are divided into numerical and analytical methods. Furthermore, analytical methods can be categorized as convolution and cumulant methods. The stochastic frame in probabilistic approach uses constant distribution or probabilities linked with each scenario to define the uncertain parameters. Stochastic programming (SP) is considered as an appropriate approach for managing uncertainties where it is based on convex optimization problem, solving Monte Carlo (MC) approximations with many scenarios [125]. SP considers several scenarios and optimizes both design & scheduling, where PDFs of uncertain parameters are predicted in an acceptable way. Later, SP ensures feasibility for uncertainties and optimise

for a measure of performance. Literature studies [118]–[120], ensure that the Monte Carlo simulation (MCS) technique is a widely accepted method for the probabilistic analysis. MCS includes several sampling uncertainties to resolve distributions of unknown stochastic parameters. PDFs are marginal distributions, where the performance index is assessed separately for different uncertainties of the system with MCS. Solving the deterministic model multiple times by MC samples (random inputs are defined) for the uncertain model are repeated in terms of providing more accurate results [126].

Two-stage stochastic optimization is another advanced method used widely in the literature [127], [128]. As a drawback of this solution, a large number of scenarios can cause a computational burden. This reveals the importance of scenario reduction techniques [129]. An enhanced alternative approach, multi-objective optimisation, needs the normalisation of objective functions between ideal and nadir points [130]. In this chapter, the uncertainty problem will be modelled according to a scenario generation based method, focusing on the PV output power and load demand forecast.

4.3.2. Probabilistic Modelling of PV Power Output and Load Demand

Concentrating on the uncertainties by the renewable sources, the wind and solar power generation were investigated widely in the literature [131]–[133]. Uncertainty can be defined by different distributions around the nominal value (i.e., Gaussian [134]). The uncertainty is probabilistic, and probability distributions controlling the data are whether known or predictable. A recognized continuous PDF used in many studies for wind speed, is Weibull distribution. It is used to generate scenarios for wind power forecasting. However, the Weibull distribution only provides short time scales of PDFs for the wind speed, resulting from being a static approach [132].

Predominantly due to PVs stochastic nature, it is challenging to consider the deterministic or heuristic mathematical models which are not accurate enough to redirect the capability of high integration of PVs in power systems [135]. In studies [136]–[138], the PV generation is mostly considered by the deterministic calculation of the PV power. However, deterministic model of PV power production, does not fully consider the stochastic character of the energy sources. PV systems output their maximum generation for a specific time of the day. Studies show that, an accurate PV output forecast is vitally needed to foresee and adapt the further integration of PVs into the power system [139]–[142]. In Ref. [138], PV production is represented in terms of time series. Correspondingly, in the proposed method, PV output power and load demand are the uncertain parameters. These parameters will be modelled with forecasted values, to obtain PDFs. As a result, the stochastic assessment of PV generation would provide more independent elaboration of PVs integration. A comprehensive review on probabilistic forecasting of PV power production and electricity consumption is given in Ref. [143].Likewise the PV power output, the power consumption units are also vital to the stochastic of the system to have a forthcoming perspective of load demand [144].

Computational burden and extensive time are the outcomes of modelling the stochastic nature of PVs and loads with the existing methods. To overcome this issue, efficient probabilistic methods can be applied to reduce the computational burden of calculations whereas getting accurate results [135]. MCS technique used with scenario generation and reduction strategies is an optimal way to ensure uncertainty analysis and modelling in power system studies. MCS aims to generate random numbers to reach the desired accuracy. However, not to lead to the high computational burden, scenario reduction is a possible way to prevent this outcome.

This work is focused on a Monte Carlo method by using scenario generation and reduction techniques. Scenario generation will be first step of this study and scenario reduction method will be used to reduce excessive computations. While actively controlling the voltage by

reactive power capabilities of inverters in the network, it is also very crucial to evaluate stochastic impacts of PVs and load as an alternative to worst-case assessment studies.

4.4. Methodology: Modelling uncertainties in ADNs with Monte Carlo approach

This section describes the Monte Carlo based approach to model the uncertainties in this work. Primarily in the literature, the studies mentioned and used a deterministic model of PV power production, without considering the stochastic character of the energy source. Due to PVs and loads stochastic nature, it can be challenging to evaluate the deterministic mathematical models which are usually used for PV power prediction and load demand. The uncertainty discretisation in power systems requires specific considerations. In the proposed method, the uncertain variables PV output power and load demand will be presented in forms of PDFs according to the solar power generation and load demand. Through scenario generation method, the stochastic nature of proposed problem will be decomposed into a deterministic solution. Figure 4-2 illustrates the steps followed in this uncertainty modelling.

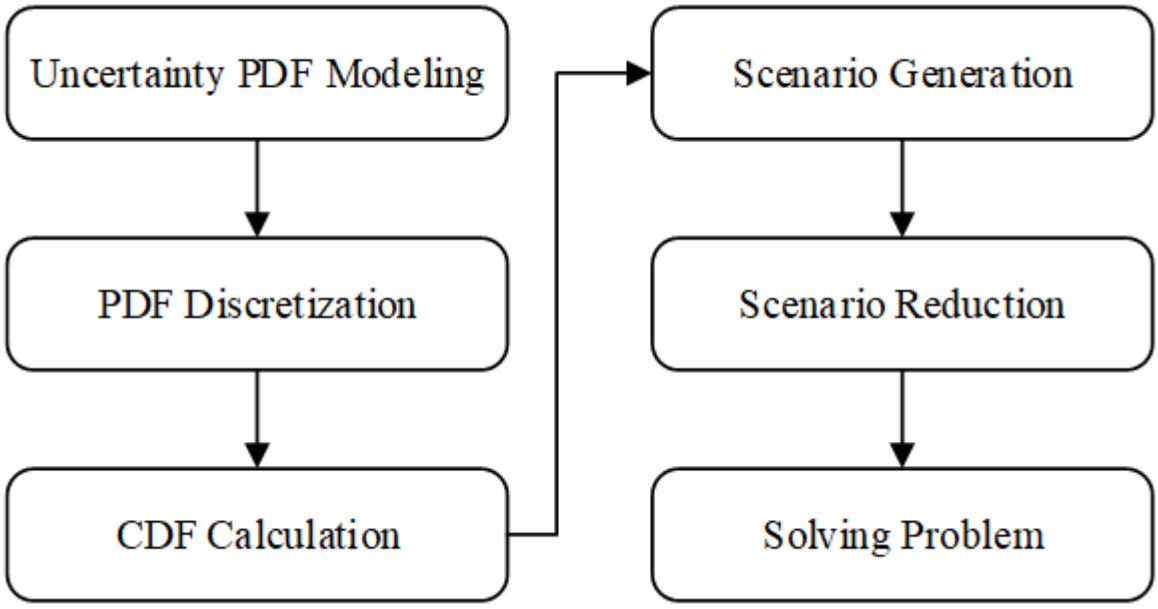

Figure 4-2. Uncertainty modelling steps for PV generation and load demand

Probabilistic assessment is related to the definition of probabilistic randomness. The probabilistic variables are transformed into linear and nonlinear programs to solve uncertainty. Though, the randomness inclines to the structure of uncertainty, which presented in the form of PDF. The computational process will gather the inputs and create their distributions to produce the desired outcomes. In the deterministic approach considerations of this study, the load flow is executed daily (24 hours), which obtains the mean values of each hour data (see detailed information in Section 5.2.1.). The input parameters to the system were assumed to be deterministically known. However, the mean value consideration doesn't fully represent the uncertainty of PVs practically due to changes in PV generations and load variations. When defining the uncertainty, the stochastic nature of the PVs and loads should be taken into account.

This section will focus on modelling the PV power output and load demand with the stochastic approach. In other words, instead of using only one mean value per each hour (constant value), a larger number of data constituted in a probability density function will be entered as an input. That would increase the accuracy, and reliability of the results which are obtained to reach to the desired preciseness [145]. It also proves that the stochastic approach is more effective at voltage regulation compared to the deterministic approach [146]. Monte Carlo Studies with the probabilistic assessment will determine probability distribution for the system stochastic variables. The results will be represented through probabilistic approach by using MATLAB and DIgSILENT software.

4.4.1. Uncertainty PDF modelling of PV power output and load demand

The real time stochastic variables, load demand and PV power output, are represented in the uncertainty modelling. These two uncertainties are modelled based on their error defined by

their PDFs. The traditional load profiles are not sufficient to reflect the more volatile load profiles is ADNs. Thus, the loads are modelled by the Gaussian distribution function since their timescale generally changes over hourly [147]. Likewise, the PV power output is modelled by the Beta distribution. The PV power output and load demand are represented as the random variables in this study and their PDF function formulas are given by the equations (4.1)- (4.3). Thus, the real time uncertainty realizations are represented by their probability distributions and a further scenario-based method is proposed for creating the scenarios.

4.4.1.1.Uncertainty modelling with PV and load variables

The load demand and PV active power will be modelled based on their error defined by the PDF. A probability of a random *x* variable, in the interval [*a*, *b*], is referred to the area under the PDF curve. In order to model the uncertainties, firstly the PV power forecast error is modelled with the Beta distribution. Beta PDF is a common approach to model the PV output power distribution [148]. For modelling the uncertainty of the PV power, random samples are generated using the Beta distribution. Beta distribution is selected due to its flexibility in terms of the shape parameters α and β. Equation (4.1) represents the PDF of Beta distribution where $B(\alpha,\beta)$ is the Beta function in Equation (4.2). Here the probability density function is denoted by, *PDF*, as $f(x)$,

$$f(x;\alpha,\beta)=\begin{cases}\dfrac{1}{B(\alpha,\beta)}x^{\alpha-1}(1-x)^{b-1} & \text{if } 0<x<1\\ 0 & \text{otherwise}\end{cases} \tag{4.1}$$

$$B(\alpha,\beta)=\int_0^1 x^{\alpha-1}(1-x)^{\beta-1}dx \tag{4.2}$$

The PV power forecast error is represented in Figure 4-3. This function specifies the insignificant change in probability for intervals of x. The area between the probability density function and the x-axis from a point a to a point b corresponds to the probability of having a

value between α and β [149]. In this study, the solar radiation parameters for Beta distribution are assumed to be α = 6.38, β = 3.43. B (α, β) is the area under the graph of the Beta PDF from 0 to 1, where the values of *x* in the range between (0, 1) have nonzero probabilities.

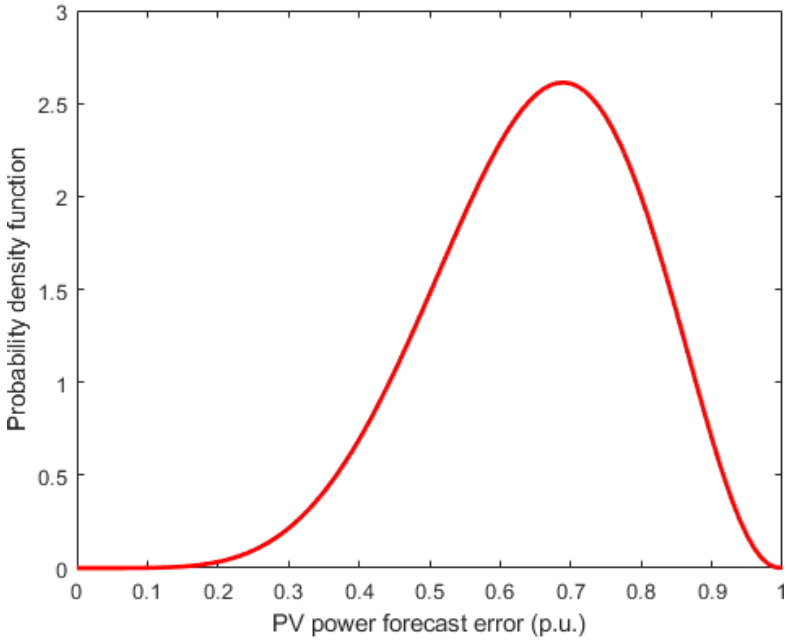

Figure 4-3. PV power generation forecast error with the PDF (Beta distribution for α = 6.38, β = 3.43)

Secondly, the load uncertainty is modelled according to Ref. [128], where Gaussian distribution is selected. Gaussian probability distribution is a proven method to represent the load uncertainty for more accuracy [147]. This distribution is represented in terms of mean (μ) and standard deviation (σ). It can be used to describe real parameter measurement errors (e.g., load demand) where the distribution is unknown.

$$f(x;\mu,\sigma) = \frac{1}{\sigma\sqrt{2\pi}} e^{-\frac{(x-\mu)^2}{(2\sigma^2)}} \tag{4.3}$$

PDF of the load demand is represented in Equation (4.3), where x is the given load demand, μ and σ are mean and standard deviation of demand, respectively. Figure 4-4 represents the PDF of a Gaussian distribution function with the mean value zero and the standard deviation σ.

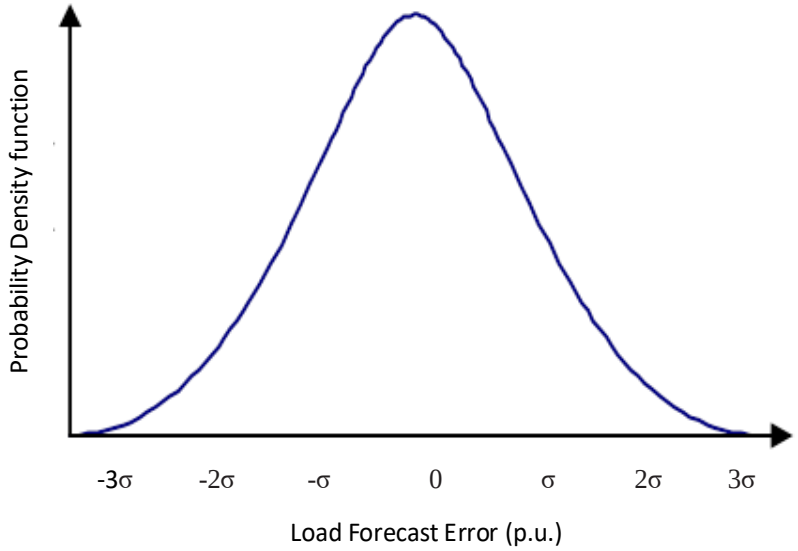

Figure 4-4. A Gaussian distribution PDF representation

4.4.1.2.Mathematical Representation of Uncertainty Scenarios

Beta and Gaussian distributions are chosen for modelling the uncertainties of solar active power generation and electric load, respectively. The uncertainty is captured by the associated randomness before evaluating the measurement error. Following, the PV powers output and load demand for each scenario can be presented as follows in Equations (4.4) and (4.5):

1) PV power output for each scenario can be defined as:

$$\begin{aligned} &P_{(PV,t,s)} = P_{(PV,t)}^{forecast} + \Delta P_{(PV,t,s)} \\ &PV = 1,\dots N_{PV} \\ &t = 1,\dots N_T \\ &s = 1\dots N_s \end{aligned} \tag{4.4}$$

2) Load demand for each scenario can be defined as:

$$\begin{aligned} &P_{(D,ld,t,s)} = P_{(D,ld,t)}^{forecast} + \Delta P_{(D,ld,,t,s)} \\ &ld = 1,\dots ND \\ &t = 1,\dots N_T \\ &s = 1\dots N_s \end{aligned} \tag{4.5}$$

Here $P_{PV,t,s}$ and $P_{D,ld,t,s}$represent the photovoltaic power output of unit *PV* (kW), ld_{th} load level (kW), respectively. $\Delta P_{PV,t,s}$ (kW), $\Delta P_{D,ld,,t,s}$ (kW) are the photovoltaic power forecasted error for unit *PV*, load demand forecasted error for load level *ld;* in the time '*t'* at scenario '*s'*. N_{pv}, *ND, T and* N_s are numbers of PV units, load levels, time intervals and the number of scenarios, respectively.

4.4.2. PDF Discretization

The probability distribution of a random variable is presented here with a set of scenarios for the load forecast error. Each scenario is related to a single realisation of the random variables selected in the overall scheme. In the beginning, the PDF is centred on the distribution mean (zero) where it's divided into seven segments shown in Figure 4-5. Each interval is owning an accumulated normalized probability. The probabilities of each interval are normalized, where the summation becomes equal to unity.

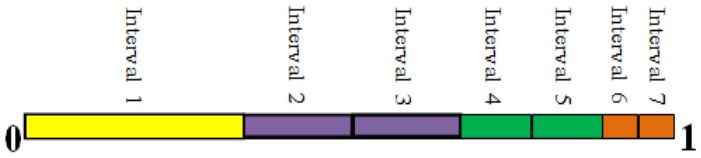

Figure 4-5. Accumulated normalized probabilities of the load forecast error intervals

Furthermore, Figure 4-6. Points out the corresponding interval representation for accumulated version of load forecast error. As shown in Figure 4-6, the highlighted segment α3 corresponds to interval 3 in accumulated version, Figure 4-5.

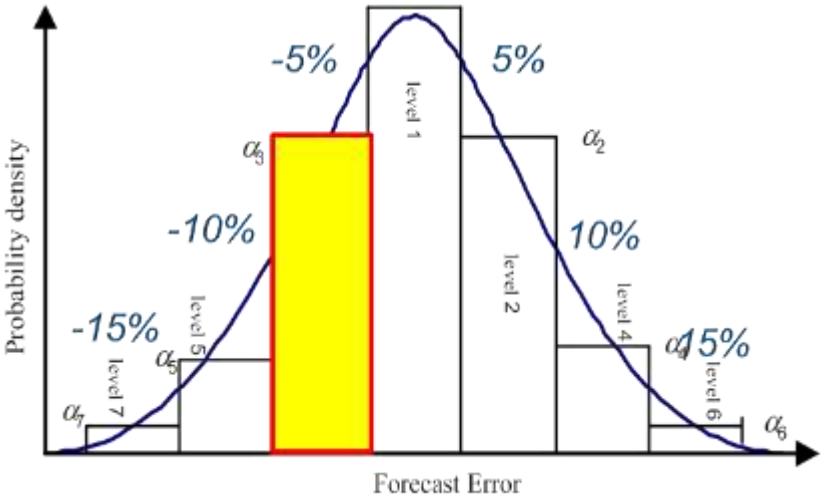

Figure 4-6. Segment representation of load level forecast error PDF

The load forecast error PDF discretization for the time period *"t"* is illustrated in Figure 4-7. Each interval corresponds to one standard deviation value (σ) between 0 and 1 as well as a probability associated with $\beta_{\ell,t}$ (ℓ=1,…, 7). The segments present the histogram of sampled values where the blue line represents the exact Gaussian distribution. The RWM method will be then used to generate the scenarios for each hour which will be explained in the scenario generation section.

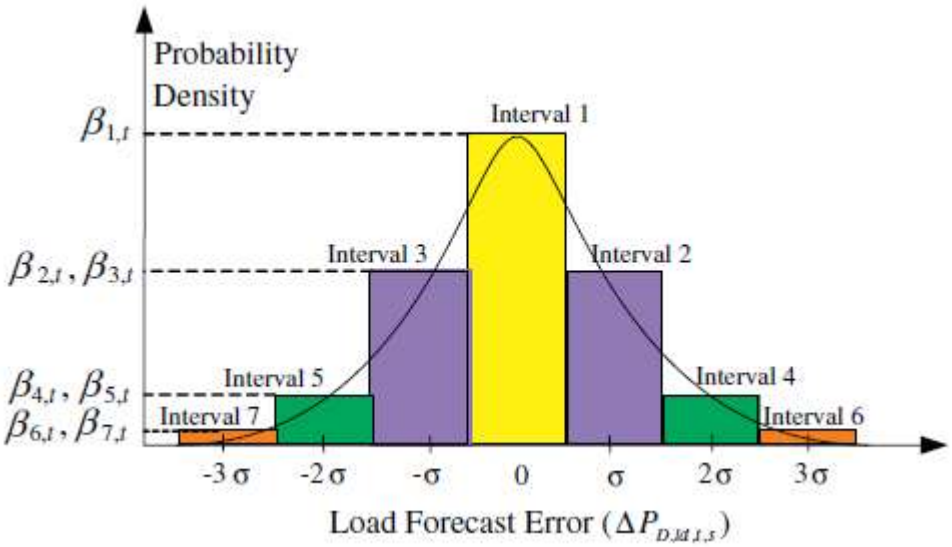

Figure 4-7. Load Forecast Error PDF Discretization

4.4.3. CDF Calculation

The definition of Cumulative Distribution Function (CDF) states that the probability is evaluated according to the random variable, being less or equal to the given *x* value. The CDF formula for a Gaussian distribution is given by *F*(*x*), provided by Equation (4.6);

$$F(x;\mu,\sigma) = \frac{1}{\sigma\sqrt{2\pi}} \int_{-\infty}^{x} e^{-\frac{(t-\mu)^2)}{(2\sigma^2)}} dt \qquad (4.6)$$

where μ is the mean or expectation of the distribution and σ is its standard deviation of a Gaussian distributed "*x*" value.

Let us assume to have a Beta distribution for the PV power generation input with the shape parameters α=2, β=4. To represent the PV generation input, all characteristic values are converted into a CDF form of random variables (between 0 and 1). The formula for the CDF of the beta distribution also called as "incomplete beta function" (denoted by I_x) is defined as Equation (4.7) [150];

$$F(x) = I_x(\alpha,\beta) = \frac{\int_0^x t^{\alpha-1}(1-t)^{\beta-1}dt}{\beta(\alpha,\beta)} \qquad 0 \le x \le 1; \quad \alpha,\beta > 0 \qquad (4.7)$$

where *B* (α, β) is the beta function. Figure 4-8 represents the CDF curve for the given PDF. For representing the distribution of PV power output with CDF, every single value (i.e. night hours will be zero generation) is indicated so that the data would be realistic. The random number "*x*" obtains values from the interval between [*0, 1*]. The PDF reaches "0" when CDF receives the final value "1". In other words, CDF is the derivative of the PDF for the value of "*x*" between [*0, x*]. Furthermore, the PDF's integral over the entire space is always equal to "1" where the probability density function is non-negative everywhere. The CDF is represented for illustrative purposes to be able to compare with PDF representation.

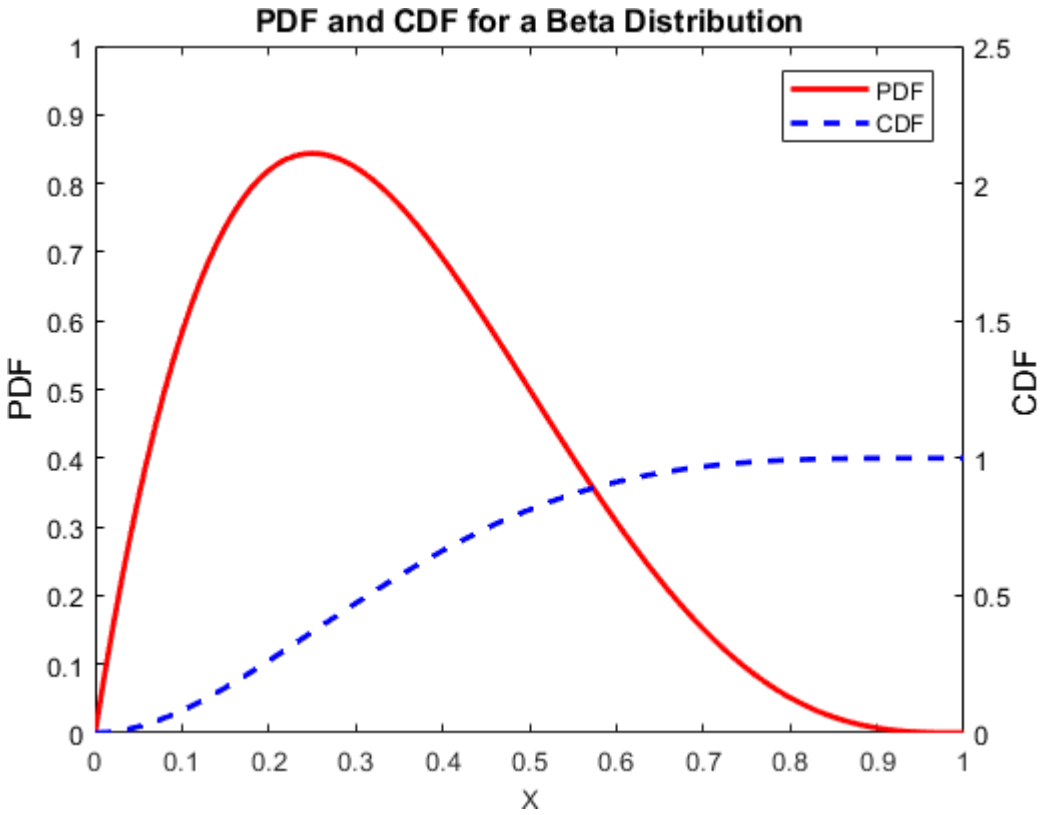

Figure 4-8. PDF and CDF for a Beta distribution (α=2, β=4)

4.4.4. Scenario Generation

The scenario generation is a crucial step distinguishing the approach from deterministic models; before creating many scenarios subsequently for the problem to be solved in the following steps. In order to generate scenarios, random variables should be created for each input random variable, corresponding to a value between 0 and 1. Then, the uncertainties are modelled based on the error obtained by the Probability Density Function. The PDFs are represented by a set of scenarios. An extensive collection of scenarios are created with the Monte Carlo simulation technique. As the approach to generate the scenarios, Roulette Wheel Mechanism (RWM) is used accordingly [144]. Random numbers are computed as follows in Equation (4.8):

$$\sum_{j=1}^{r}(\frac{k_j}{n_j}(\sum_{(i=1)}^{N} v_i) mod 1, k_j = 1,...,N,\ j = 1,...,r \tag{4.8}$$

Intended for each random variable in individual time intervals, a random number is produced between 0 and 1 according to the random number generator. In this proposed work, there are 1000 set of realisations created for each random variable in one scenario. Each scenario has a probability of occurrence represented in a numeric value. Following the random numbers and probabilities from PDFs obtained, RWM generates scenarios for each hour represented in vector form recognising load demand and PV power output with binary parameters as following Equation (4.9):

Scenarios

$$s = \left\{ W^{l}_{(1,t,s)},....,W^{l}_{(7,t,s)}, W^{pv}_{(1,t,s)},...,W^{pv}_{(7t,s)} \right\}_{(t=1,..,T)} \tag{4.9}$$

The random numbers are produced for PV power generation and load demand for each time interval. The probabilities which are equal or less than the random numbers are selected, and their binary parameter is valued as 1, whereas the parameters of the other intervals equal to 0. This process repeats until the desired number of scenarios are generated. Eventually, the normalized probability of each scenario is calculated by Equation (4.10).

$$\pi_s = \frac{\Pi^{T}_{(t=1)}(\Pi^{ND}_{(ld=1)}(\sum_{(l=1)}^{7}(W^{l}_{(l,t,s)}\beta_{(l,t)}))\Sigma^{7}_{(pv=1)}(W^{PV}_{(pv,t,s)}\beta_{(pv,t)}))}{\sum_{(s=1)}^{(N_s)}\Pi^{(N_T)}_{(t=1)}(\Pi^{ND}_{(ld=1)}(\Sigma^{7}_{(l=1)}(W^{l}_{(l,t,s)}\beta_{(l,t)}))\Sigma^{7}_{(pv=1)}(W^{PV}_{(pv,t,s)}\beta_{(pv,t)}))} \tag{4.10}$$

where ND is the total number of load levels in each hour. $\beta_{l,t}$, $\beta_{pv,t}$ are the probabilities for the lth load interval and PV_{th} photovoltaic power interval, respectively.

4.4.4.1. Computational Approach: Monte Carlo Method

The computational method for probabilistic assessment can be calculated by Monte Carlo Simulations (MCS). This technique generates random variables to establish their PDF for solving the problem of nonlinear, complex models. Steps are given to create 1000 samples of the simulation model to create a PDF.

Step.1 Firstly a random sampling model will be used

Step.2 The uncertainties will be modelled by creating a set of random inputs using their PDF

Step.3 Evaluate the model and calculate the scenarios

Step.4 Repeat steps 2 and 3 for i = 1 to N

Step.5 Analyse the results using histograms, bootstrapping, summary statistics, confidence intervals and etc.

4.4.4.2. Constraints

The same constraints used in deterministic approach are extendedly considered in stochastic approach "3.2.1.1. Constraints". Equations below are considered.

Bus voltage constraints,

Each bus voltage should meet the limits as: the maximum and minimum voltage constraints are defined as follows Equation (4.11) and (4.12), [79]:

$$\text{Maximum voltage constraint} = 100\left(\frac{1}{V_{\max}-1}\right)\sum_{s=S}\rho_s\sum_{ij\in B}[\mathrm{V}_{ij,s}^{\max}(p.u.)-1] \tag{4.11}$$

$$\text{Minimum voltage constraint} = 100\left(\frac{1}{1-V_{\min}}\right)\sum_{s=S}\rho_s\sum_{ij\in B}(\mathrm{V}_{ij,s}^{\min}(p.u.)-1) \tag{4.12}$$

where, the boundaries of V_{max} and V_{min} are 1.1 and 0.9 per unit in this study, respectively. $V_{ij,s}^{max}$ and $V_{ij,s}^{min}$ are "(*i,j*)" th elements of the scenario "s", for V_{max} and V_{min}, respectively. ρ_s is occurrence probability of scenario s The transformer loading constraint in Equation (3.3) and line loading constraints in Equation (3.4) remain same for this considered study.

4.4.5. Scenario Reduction

A large number of scenarios increase the problem dimension and requires a long-run time. Also, some of the scenarios take over similarities and correlation with previous ones. Thus, to reduce the computational burdens and remove similar scenarios, the scenario reduction method is considered to eliminate redundant scenarios. Ref. [151] follows the scenario reduction method to gain probabilities of random variables. Scenarios with very low probabilities and high similarity to other scenarios are eliminated [152].

In this work, there would be 96 samples of each input value (PV generation and load demand) over a day, where the scenarios would be generated in a 15-minute occurrence. The 15 minute interval data are obtained on all scenarios to reflect more efficient data collection routines from meters in reality. These 24-hour samples would be executed 1000 times to achieve the extensive set of realizations. Then, the 1000 set of realizations will be reduced to 20 realizations, where they are sorted descending from the higher to lower probability according to the backward method [153]. The simultaneous backward method is implemented since this procedure depends on the accuracy of the approximation.

ξs (s $= 1, \dots,$ Ns) with the N_s scenarios each having a probability π_s. Also the distance scenario pairs (*s,s'*) are represented with $DT_{s,s}{}'$. These data with the simultaneous backward method is reduced to 20 scenarios as follows:

Step 1: S are the complete set of scenarios, and DS is the scenarios to be deleted (initially zero). The distances of all scenario pairs are calculated as in Equation (4.13);

$$DTs,s' = \sqrt{\sum_{i=1}^{d}(v_i^s - v_i^{s'})^2} \quad (4.13)$$

Step 2: For each scenario k, $DT_{k,r}$ =min$DT_{k,s'}$, $k \in S$ and s'≠ k where r is the scenario index with being closest to scenario k.

Step 3: Calculate $\mathrm{PD}_{k,r} = \pi_k \times \mathrm{DT}_{k,r}$ where $k \in S$. Select d where $\mathrm{PD}_d = min\mathrm{PD}_k, k \in S$.

Step 4: $S = S - \{\mathrm{d}\}$, DS= DS+ {d},$\pi_r = \pi_r + \pi_d$.

Step 5: Repeat Step 2 – Step 4 until the desired number of scenarios are left.

Step 6: Stopping rule is applied in order to stop simulations when desired number of samples are achieved by Equation (4.14), [154].

$$cv_f = \frac{\sigma_f}{\mu_f\sqrt{N_s}} \quad (4.14)$$

where σ_f and μ_f are standard deviation and mean values of random variable "f". cv_f is monitored to stop the simulations accordingly.

The required scenario number for the desired accuracy of MCS is selected as 20 scenarios. These 20 scenarios are accordingly represented in simulation results. To represent the achieved accuracy in the simulation results, the outcomes will be represented in terms of;

1) Network power losses in kW can be derived from Equation (3.27) as Equation (4.15);

$$\text{network power loss} = \sum_{s\in S}\rho_s \sum_{(ij\in B)} P_{(ij,s)}^{loss} \quad (4.15)$$

where S and s are set and index of scenarios, respectively and ρ_s is occurrence probability of scenario s.

The outcomes out of a thousand simulation scenarios will be selected according to their probabilities, consisting of ten scenarios. The daily profiles are represented with fifteen minutes time intervals, depending on the varying values of the input data. In other words, the studied deterministic results will be extended to ten different scenarios for increasing the accuracy of the results. In the previous chapter where the deterministic approach was considered, the results were represented for 96 samples only (horizon of 15 minutes). Results are expected to be improved by accuracy with consideration of the probabilistic forecasts over 15 minute horizons.

Table 4-2, represents the probabilities the ten scenario probabilities for given load and PV profiles composed. The sum of all probabilities is equal to 1, where the expected value is the weighted sum of the random variable values, with probabilities for each random variable.

Table 4-2. Ten scenario probabilities for load and PV profiles

Scenario number	Probabilities
1	0.314947
2	0.306518
3	0.194149
4	0.052861
5	0.048938
6	0.031003
7	0.021069
8	0.014038
9	0.007882
10	0.008594

Figure 4-9 represents the ten PV power output scenarios reduced from 1000 set of scenarios generated by the Monte Carlo simulations. Correspondingly, Figure 4-10 represents the ten load profile scenarios after the executed MCS. Scenarios are condensed to ten PV and load

scenarios with the given probabilities. These characteristic profiles will be appended to the results in Section 5.4.

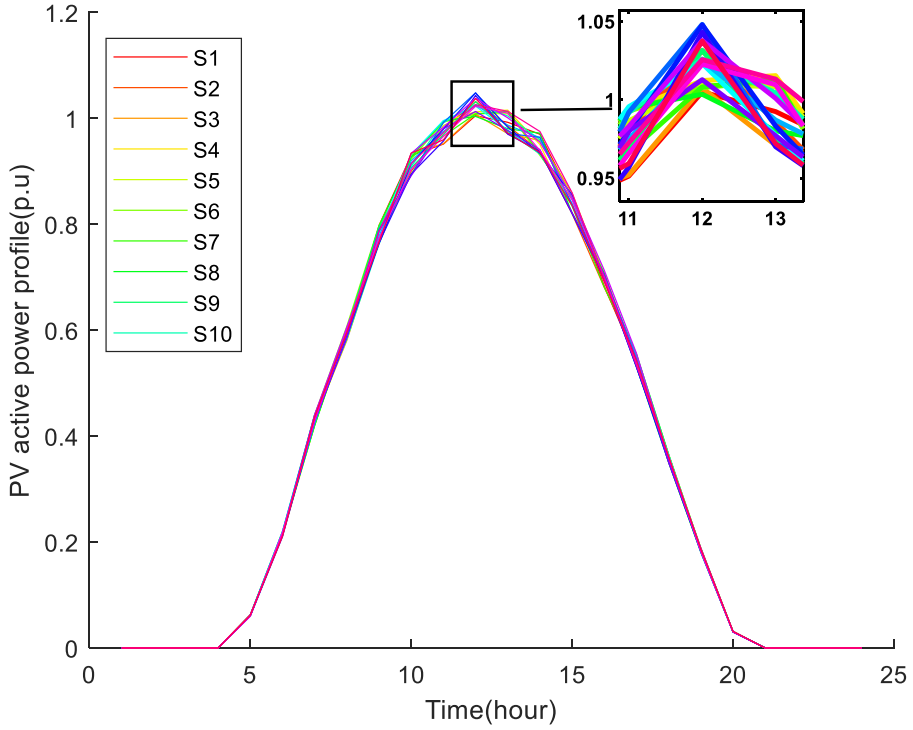

Figure 4-9. Ten PV generation output scenarios

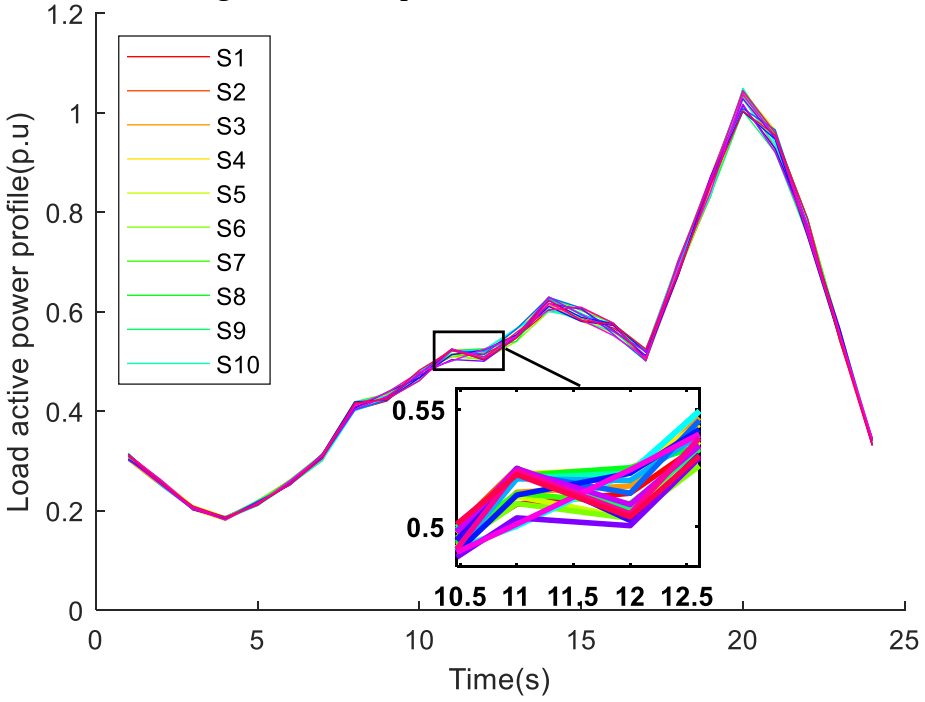

Figure 4-10.Ten load profile scenarios

4.5. Chapter Summary

The chapter concludes by presenting the stochastic assessment concerning the local voltage controller's potential in preserving satisfactory voltage regulation under high PV penetrated ADNs. The method has advantages by being producible and extendable. Beta distribution and Gaussian distribution are selected for demonstrating the uncertainties of the solar generation and the system loads, respectively. A scenario-based method was applied to solve uncertainties with a Monte Carlo simulation computational technique. With stochastic analysis where distributions of outputs are produced, the Monte Carlo simulation is used to generate uncertainties to reflect the stochastic behaviour of load and PV profiles. By considering the influences of uncertainties, the improved MCS method delivers an advanced HC evaluation.

It should be highlighted that using the scenario reduction technique following MCS technique has significantly reduced the complexity of the computation in probabilistic power flow studies. The simulation studies are provided in the simulation results, Section 5.4.

5. SIMULATION RESULTS FOR 33 NODE RADIAL AND 69 NODE RADIAL & MESHED TEST SYSTEMS

5.1. Introduction

In this chapter, the enhancement of the proposed controller in distribution systems is investigated. PF-power and Q-voltage methods are compared with proposed controller simulation studies, performed in DIgSILENT Power Factory software. The simulations are performed on the 33 node and 69 node radial test systems. Also, to observe the application of the proposed control on a meshed network, the modification of the 69 node meshed test system is considered. This study focuses mostly on the voltage rise and overloading limitations for the system components caused by very high PV generation in peak times of the day.

The ADN is investigated with increased generation of PV systems and low load consumption scenarios. The simulation studies are conducted by running 24-hour advanced load flow and Quasi-Dynamic simulations. Moreover, a DIgSILENT Programming Language (DPL) script is improved to allow flexibility while running the program and group the components to be deactivated. During the simulations, all PV systems use the same strategy and have the same PV power output and load profile.

The inputs of the proposed method are real-time measurements, including active power of PV inverters P_{pv}, reactive power of PV inverters Q_{pv} and PCC voltage V_{PCC}. The local control provides fast response compared to other voltage regulation methods. Following the test systems description, a daily case study evaluates the performance of the proposed scheme. Then, an assessment study derives the PV hosting capacity in the deployed test systems. In addition to deterministic simulations, all abovementioned simulations are repeated with the stochastic method and presented.

5.2. The studied test systems description

The study examines the proposed method's effectiveness through comprehensive simulations on Baran & Wu 33-node and 69-node test feeders [155], [156]. The 33-node test system is presented in Figure 5-1 with PVs integrated into each node [155]. Both test systems are hypothetical test systems, but then verified through many researchers and used in the literature for several studies, especially with high integration of PVs [157]. DIgSILENT Power Factory 2020 software is used to execute the Quasi Dynamic simulation studies, to reduce the processing time of the dynamic simulations [134]. The quasi dynamic simulation offers multiple load-flow calculations with user-defined time-step over a twenty four hour time scale. In the study, 15 minutes time steps are selected as the scale, the feeders' lines and loads data can be accessed through the Appendix A.

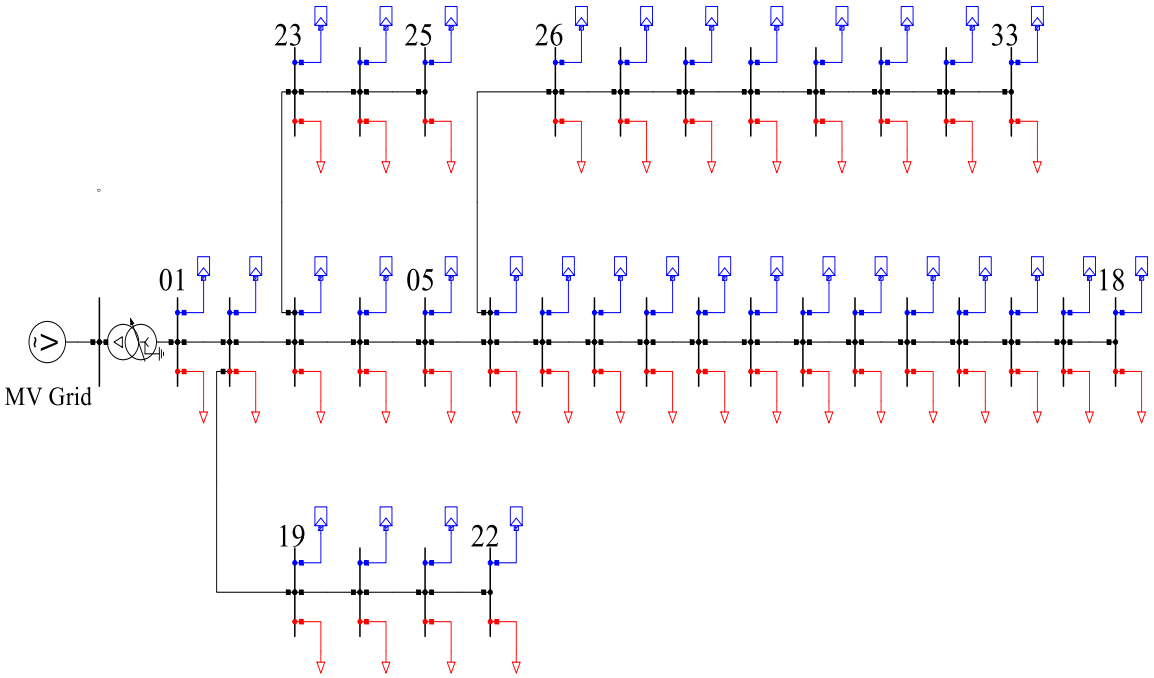

Figure 5-1. The single line diagram of the 33 node test feeder

5.2.1. PV and Load Profiles

With the increased integration of PVs into the distribution network, the PV power output and varying load demand will play a significant role over the system. PV and load data changes

over the time, as well as showing different characteristics over months. It also varies according to the weekdays and weekends. The overall characteristics of the PVs within the distribution network can be considered to have a similar generation profile. In this regard, the PV and load profiles used in the network will be described according to UK standards [158].

5.2.1.1. PV Profile

PV profile refers to the power output of the system changing with solar irradiance. For simplicity, a linear relationship is considered between the active power profile and solar irradiance. The solar radiance data is obtained from a real-time monitored profile, from the practical PV outcome over a summer day [159]. Every residential-scale PV unit is equipped with an inverter that can control the voltage within its unit. Figure 5-2 illustrates the PV profile over a sunny summer day. The base power of this profile is the PVs nominal active power.

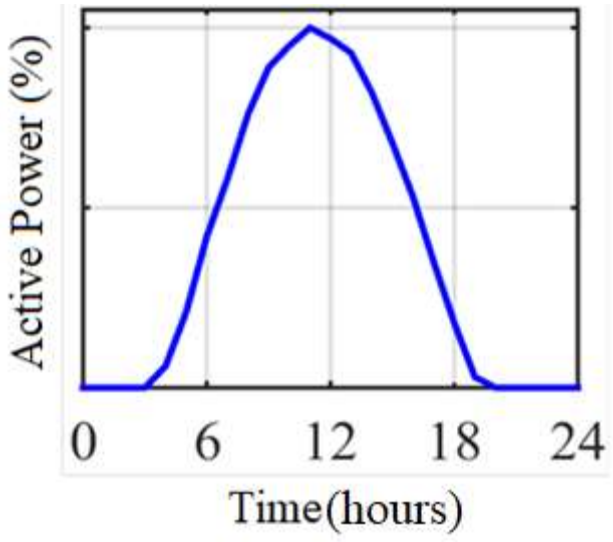

Figure 5-2. PV active power profile over a day (time in hours)

5.2.1.2. Load Profile

Load profile denotes to the time-dependent load active power data over a period (daily, weekly or monthly). In this study, the load profile is taken from a residential level load and has daily

(24 hours) time series [160]. All loads in the system will be assumed to have a power factor of 0.95 lagging. In the studied test systems, all loads are assumed to have similar characteristics and thus their influences on system is considered alike.

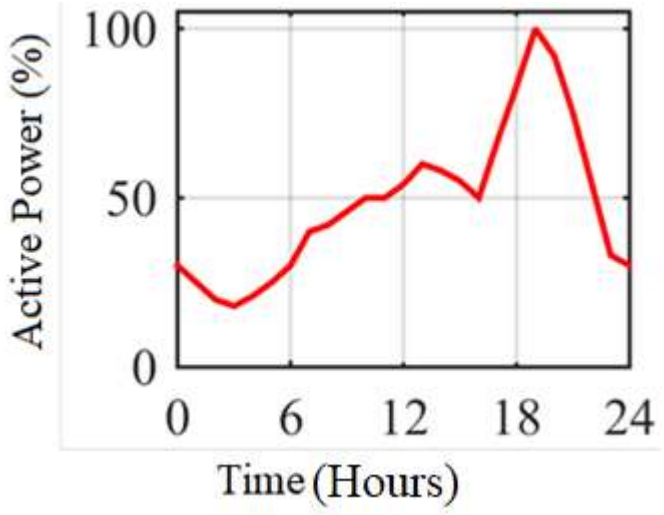

Figure 5-3. Load profile over a day (time in hours)

In this study, Figure 5-3 shows the typical load data selected for the load profile in test system. The reason of the load profile description is to obtain a mathematical representation, which portrays the actual load behaviour. The base power of all load profile are transformed to PVs nominal active power, in order to adjust the values into a single form. The base power of this profile is the loads' nominal power and further data (active and reactive power values) according to each load is listed in Appendix A , Table A2.

5.2.2. The 33-Bus Test System

The 33-bus test system is portrayed in Figure 5-4 with the representation of zonal control strategy explained in Section 3.3.2. To model a high PV penetration level case, it is assumed that each node of the feeder is equipped with PV system which has a nominal apparent power of 10 kW. The nominal power factor of the PV systems is selected as 0.9 [161].

The test feeders are supplied by MV grid through three-phase transformers. The transformers are equipped with OLTC tap changers. The OLTCs automatically adjust voltage magnitude of the transformers LV bus at 1.0 per unit using steps of ±10, with 1% voltage change per step. The lower and upper bounds of the OLTCs are 0.9 and 1.1 per unit, respectively. The tap changers controller time constant is set to 120 seconds [162]. Further details regarding the system components can be obtained from the Appendix A: 33 and 69 Node Test System Data.

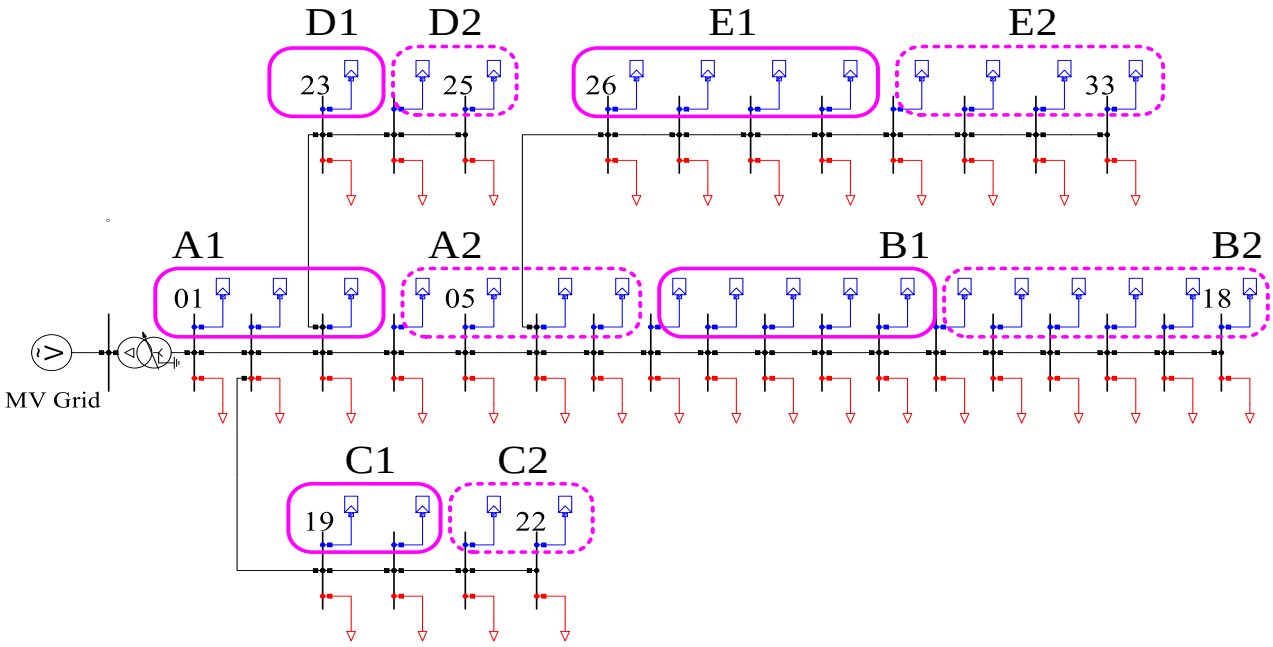

Figure 5-4 The single line diagram of the studied 33-node test feeder with zonal management

5.2.3. The 69-Bus Test System

The 69-bus test system will be presented by two different system representations, radial and meshed, respectively. The following assumptions are applied to both radial and meshed systems. By selecting the transformers' nominal powers, the system base power is 6,150 kVA for both of the 69-node test feeders. Transformer settings are the same with 33 bus test system. In order to model a high PV penetration level case, it is assumed that each node of the feeder

is equipped with PV system which has a nominal apparent power of 10 kW. The nominal power factor of the PV systems is selected as 0.9 [163].

5.2.3.1. Radial 69-Bus Test System

The proposed methodology is firstly studied on the radial test system, where the 69-bus test system is portrayed in Figure 5-5. The PV systems working according to the proposed controller are shown with the pink color whereas the rest of PVs work under the Q-voltage strategy.

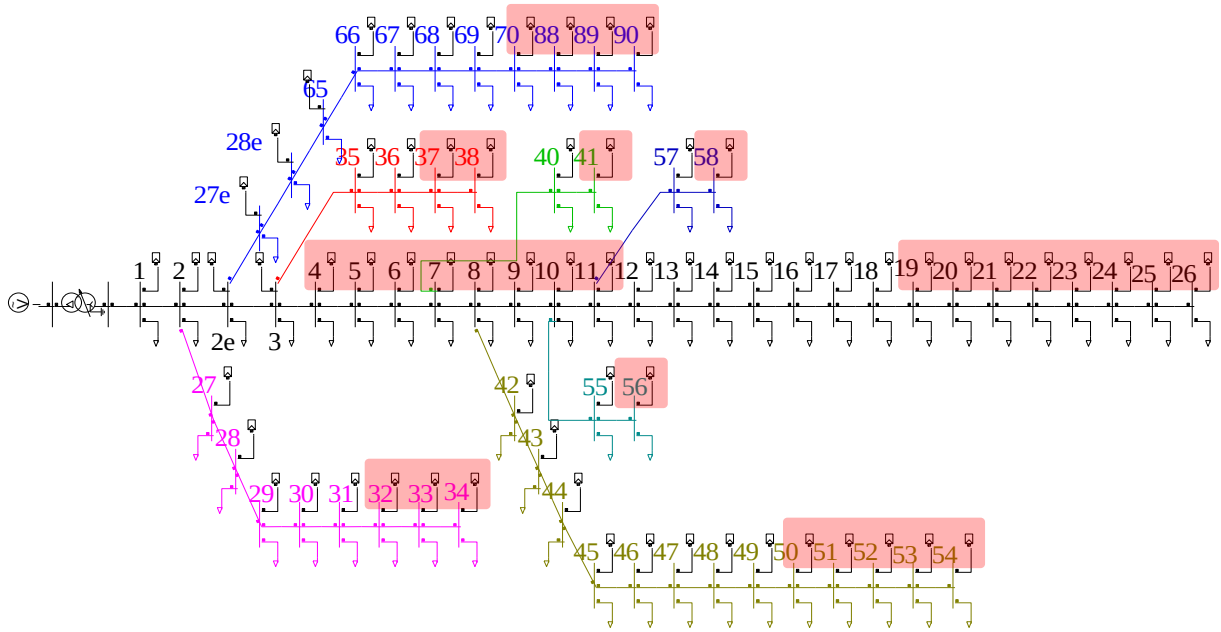

Figure 5-5 The single line diagram of the radial 69-node test feeder

5.2.3.2. Meshed 69-bus network topology

To further investigate practicality of the suggested approach, the proposed methodology has been applied on the meshed 69-node test feeder. As the potential of the future networks can also consist of meshed topologies, a meshed structure is also worth for taking into consideration for the simulation studies. For this purpose, Figure 5-6, represents the single line diagram of

the meshed test system where the dotted trace show from which points the grid is connected. This section proves the reconfiguration of the benchmark test feeder is possible. Following, the results will be compared for this specific case with radial test feeder.

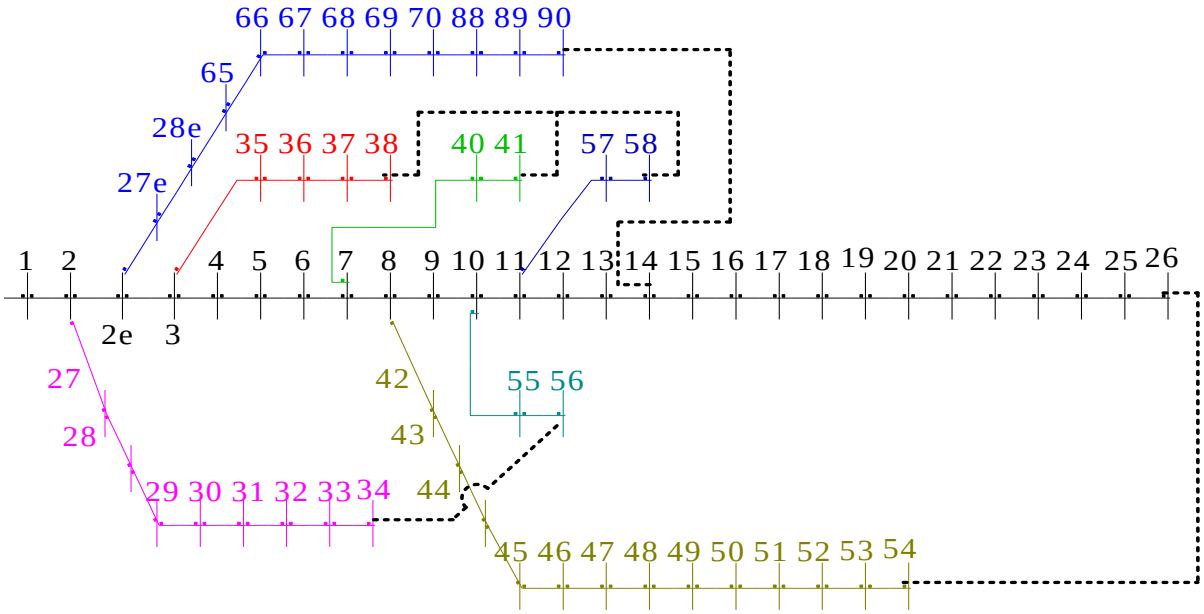

Figure 5-6 The single line diagram of the meshed 69-node test feeder

With the simulations executed, the effectiveness of the proposed control strategy in increasing the standard distribution networks hosting capacity will be studied by comparing the abovementioned test systems by different aspects (i.e. size and topology of the test system). This will be concluded by comparing the listed results presented in further sections in Table 5-2 and Table 5-3. In case of the meshed 69-node system, the suggested approach will investigated through its ability in reducing reactive power flow through the network electrical bottlenecks in comparison to the conventional strategy. Following, the results will be compared for this specific case with radial test feeder.

5.3. Test System Simulation Results

5.3.1. The 33-node test system simulation results

In this section, effectiveness of the proposed method is compared with the PF-power and Q-voltage strategies through simulation results applied on the 33-node feeder. In this regard, three discrepant scenarios are considered. At the first scenario, reactive power for all the PV units are controlled via PF-power scheme. The Q-voltage method modulates the PVs reactive power in the second scenario. The parameters of these two conventional approaches are listed in the given in Table 5-1.

Table 5-1. The parameters of the conventional characteristics (p.u.)

The parameters of the PF-power characteristic				
$\boldsymbol{PF_{pvn}}$	$\boldsymbol{PF_{over}}$	$\boldsymbol{PF_{under}}$	$\boldsymbol{P_{over}}$	$\boldsymbol{P_{under}}$
0.9	PF_{pvn}	$-PF_{pvn}$	$0.2PF_{pvn}S_{pvn}$	$PF_{pvn}S_{pvn}$

Parameters of the Q-voltage characteristic					
$\boldsymbol{Q_{lim}}$	$\boldsymbol{Q_{over}}$	$\boldsymbol{Q_{under}}$	$\boldsymbol{V_{min}}$	$\boldsymbol{V_{max}}$	$\boldsymbol{V_{ref}}$
$\sqrt{\boldsymbol{S_{pvn}^2 - P_{pv}^2}}$	Q_{lim}	$-Q_{lim}$	0.9	1.1	1

In the third scenario, the feeder is divided into 5 zones using the algorithm explained in 3.3. Voltage Sensitivity Studies as shown in Figure 5-4. In this case, the suggested framework manages the reactive power of the PV units located in groups A1, B1, C1, D1 and E1. On the other hand, the PV in groups A2 to E2 operate with the Q-voltage characteristic.

The achieved results with the PVs nominal apparent power of 250 kVA are shown from Figure 5-7 to Figure 5-14. The results are derived through load flow calculations over the specific dispatch interval of 15 minutes. The active and reactive power variables are shown in the percentage of the system base power, which is the transformer nominal apparent power, 5,750 kVA. In addition, the transformer and branch loadings are presented in percentage of their nominal capacity. The voltage variation at the most critical node of the 33 bus feeder, i.e. bus 18, is portrayed in Figure 5-7.

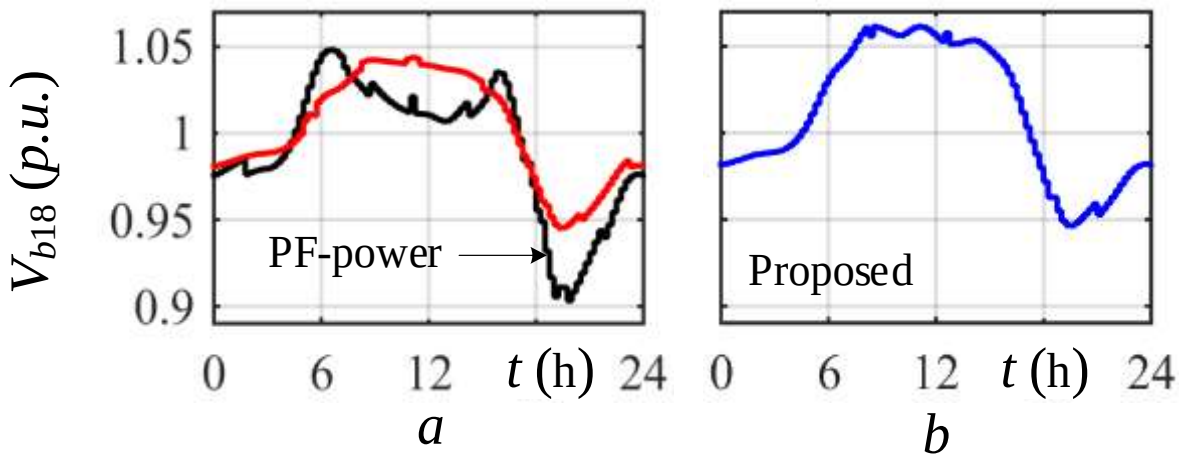

Figure 5-7.The voltage amplitude at the bus 18 **(a)** The PF-power (black) and the Q-voltage (red) scenarios, **(b)** The proposed scenario (p.u.)

The MV grid's reactive power and the network losses are plotted in Figure 5-8.a and Figure 5-8.b, respectively. It is observed that the proposed strategy reduces the maximum of these quantities during a day, significantly.

On the other hand, the loading of the feeder transformer and line 8 are depicted in Figure 5-9. It can be observed that the proposed technique also results in substantial reduction in the transformer and line loadings.

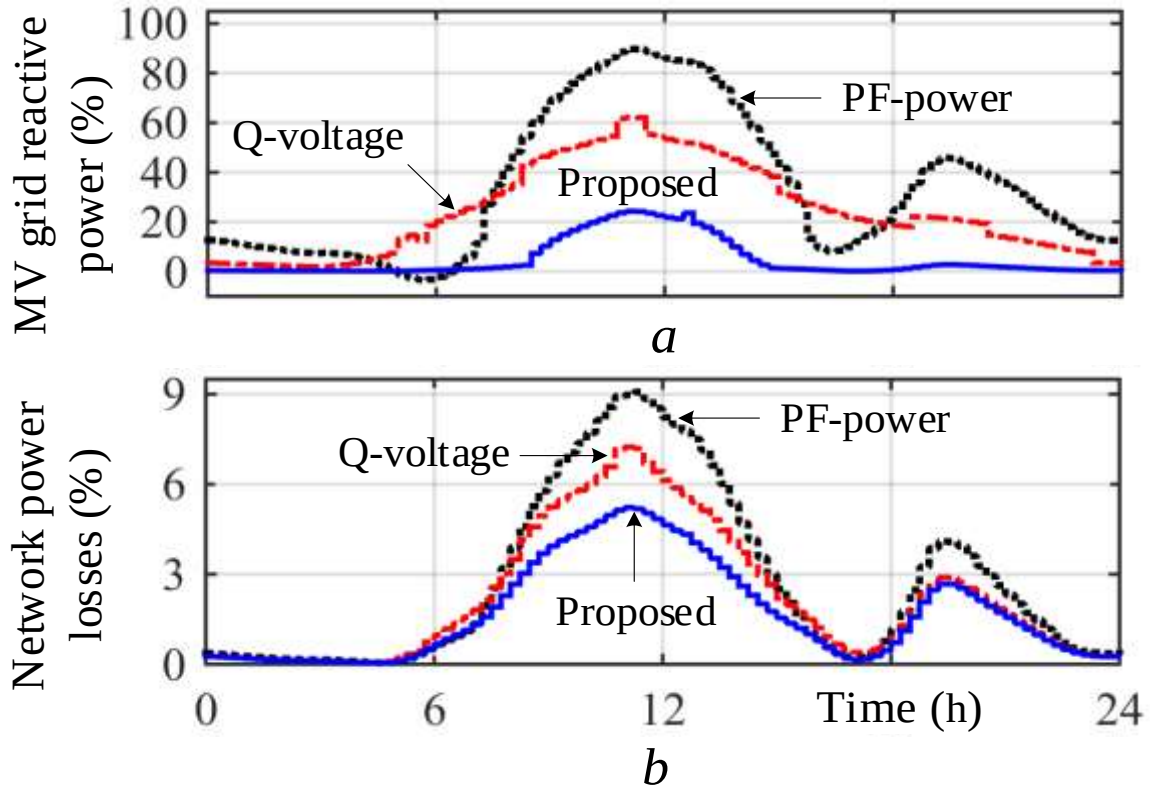

Figure 5-8. The 33-node test feeder results with thirty three 250 kVA PV systems (a) The MV grid reactive power generation, (b) The test feeder active power losses

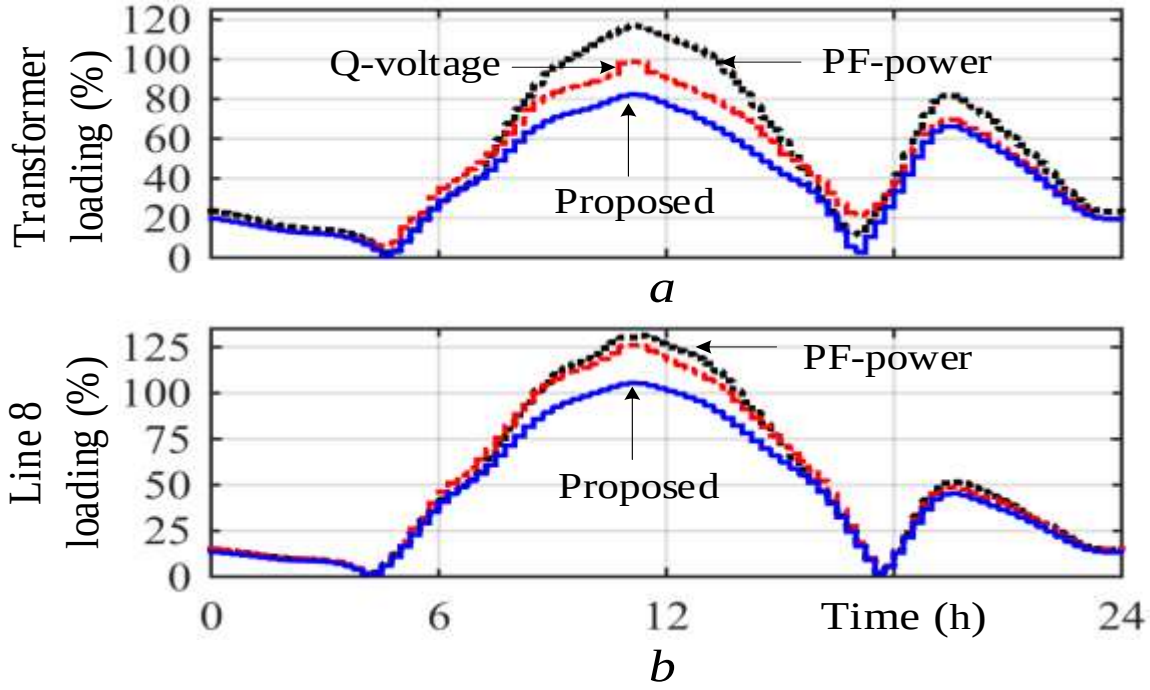

Figure 5-9.The 33-node test feeder results with thirty three 250 kVA PV systems (a) The transformer loading, (b) The line 8 loading

The grouped PVs reactive power variation for the proposed scenario is illustrated in Figure 5-10. It is precise that the PV units located in the first groups (solid traces) supply the reactive power for the PV units located in the second groups (dotted traces). Additionally, the former groups generate part of the loads reactive power demand.

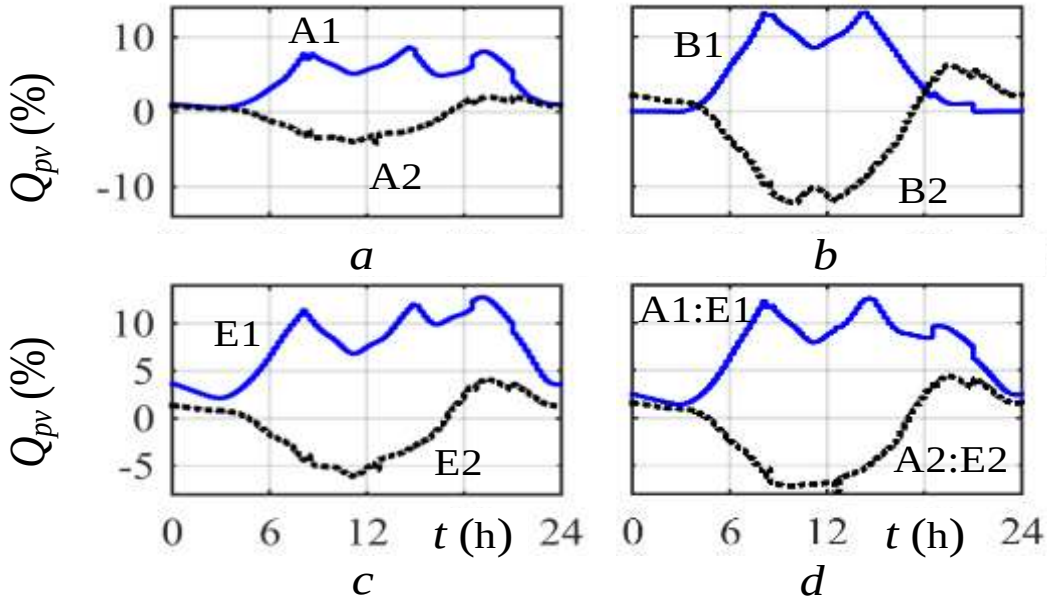

Figure 5-10. The 33-node test feeder results with thirty three 250 kVA PV systems: the PVs reactive power using the proposed scenario (a) The group A1 and A2, (b) The group B1 and B2, (c) The group E1 and E2, (d) The one-third of total of the groups A to E

For further investigation of the results, the reactive power flow in the first lateral of the network C1 is investigated and evaluated for the Q-voltage and the suggested scenario as shown in Figure 5-11. These flows, represented in percentage of the system base power, are pertinent to PVs maximum active power generation instant.

In the Q-voltage case, all the four PVs consume reactive power like the loads. Therefore, the lateral draws 2.5% reactive power from the main feeder. In the proposed method, the available capacity of the first two PV units is used to locally generate reactive power. Consequently, the drawn reactive power from the main feeder decreases to zero neglecting losses.

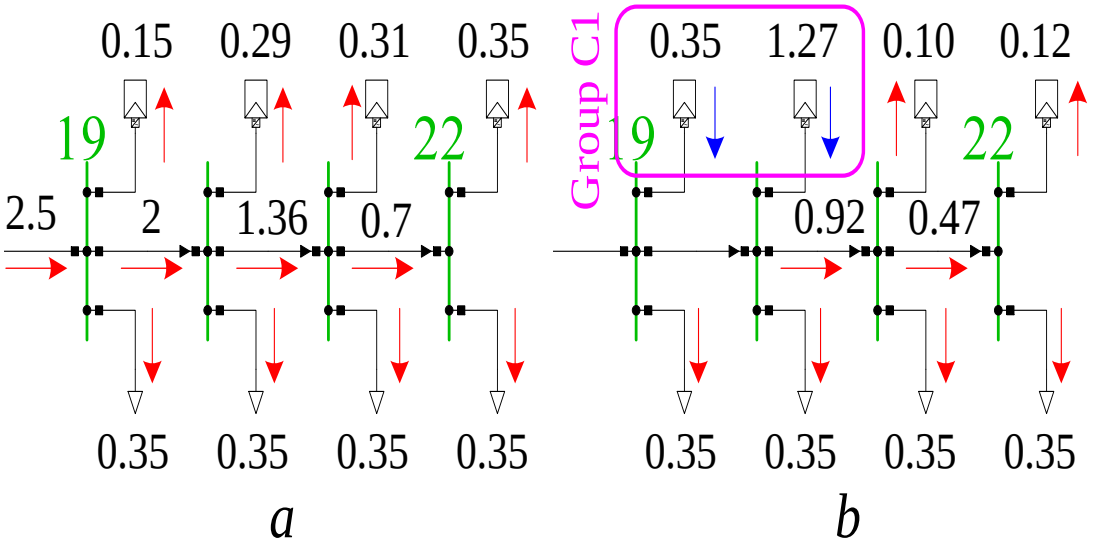

Figure 5-11. The 33-node test feeder results with thirty three 250 kVA PV systems: the reactive power flow at PVs maximum generation time (a) The Q-voltage scenario, (b) The proposed scenario

5.3.1.1. Active and Reactive Power Results

This section will present the capability of the proposed system to enhance the voltage control of the system. It is important to consider the reactive power generation and consumption for maximum generation and maximum load demand scenarios. Therefore, the bar diagram in Figure 5-12 (a) shows the cumulative reactive power generation and consumption for the considered scenarios at midday hours.

In the PF-power case, the PVs consume their possible maximum reactive power, i.e. 60%. This provides a considerable voltage support, however, it puts a high burden on the MV grid. This burden is reduced by 30% when the Q-voltage controller governs the PVs reactive power. In the case of the proposed scenario, the reactive power balance is achieved with less dependency to the MV grid. Figure 5-12 (b) provides this comparison for the maximum loads demand time interval. To keep the bus voltages above the permissible lower limit, the PVs supply half of the loads' reactive power when the Q-voltage strategy is deployed.

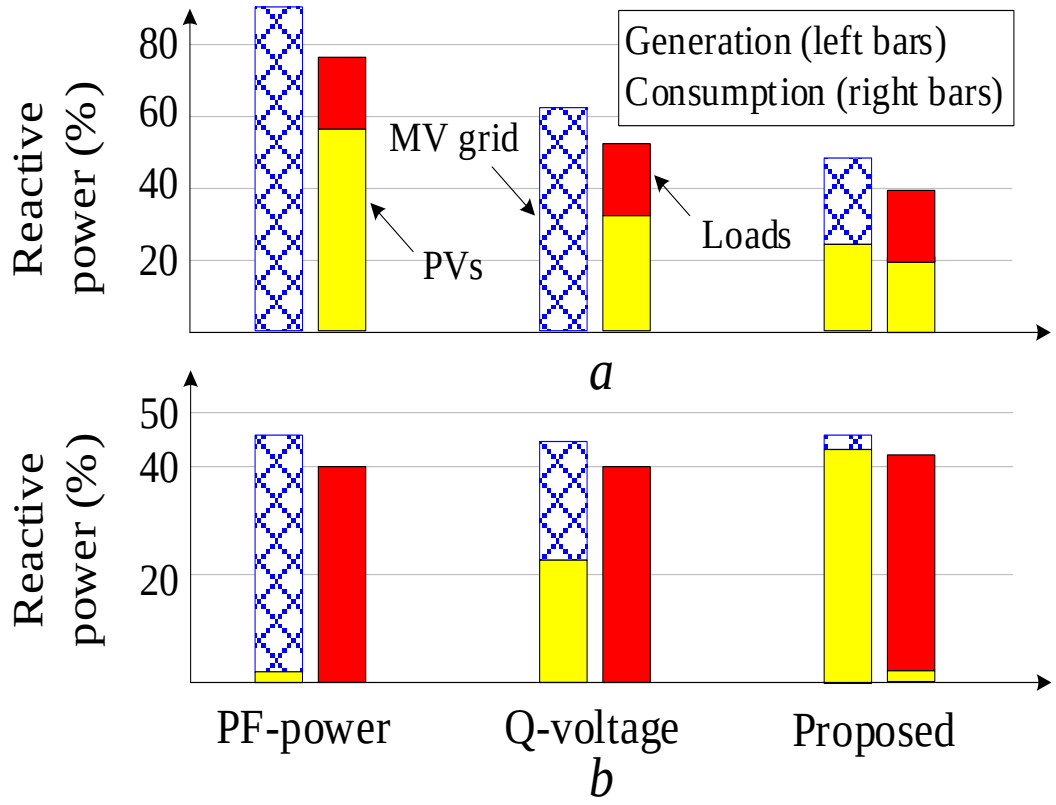

Figure 5-12. The 33-node test feeder results with thirty three 250 kVA PV systems: the reactive power generation and consumption in percentage (a) For maximum PVs generation time, (b) For maximum loads demand time

5.3.1.2. Tap positions

The greater voltage deviation occurs due to weather conditions in one day, it may cause the total number of tap-changes to exceed the allowable value and shorten the OLTC service life. However, in the proposed method, the OLTC tap-position only changes four times, which effectively reduces the number of tap-changes. Moreover, the total number of tap-changes per day is much less than the maximum allowable value.

In the proposed scenario, the PVs located at the first groups deploy their remaining reactive power capability to supply the loads in addition to the network voltage support. Therefore, all of the reactive power demand is approximately supplied by the PV units. The performance of

the reactive power control scenarios from the transformer tap changing point of view is investigated in Figure 5-13 and Figure 5-14.

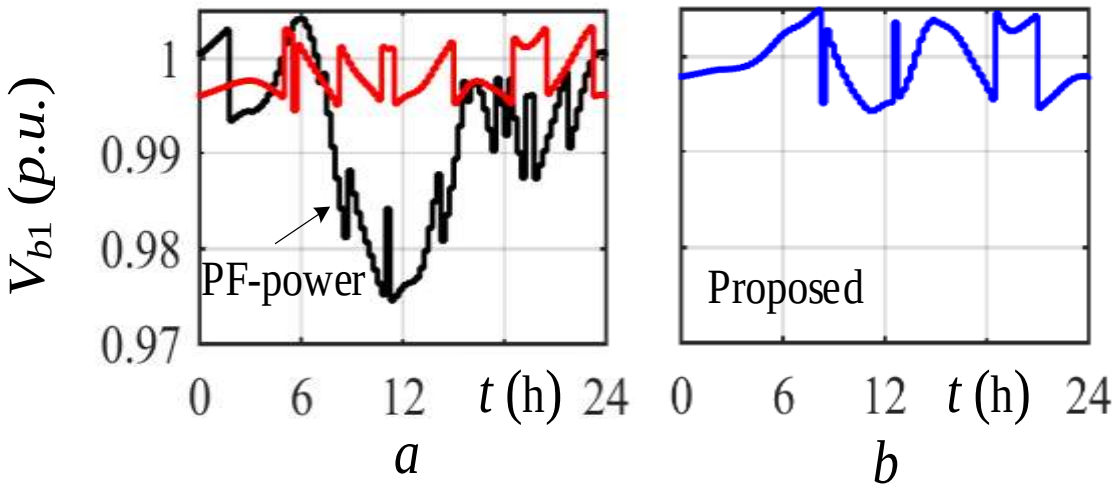

Figure 5-13. The 33-node test feeder results with thirty three 250 kVA PV systems: the voltage amplitude at the bus 1 (a) The PF-power and the Q-voltage scenarios, (b) The proposed scenario

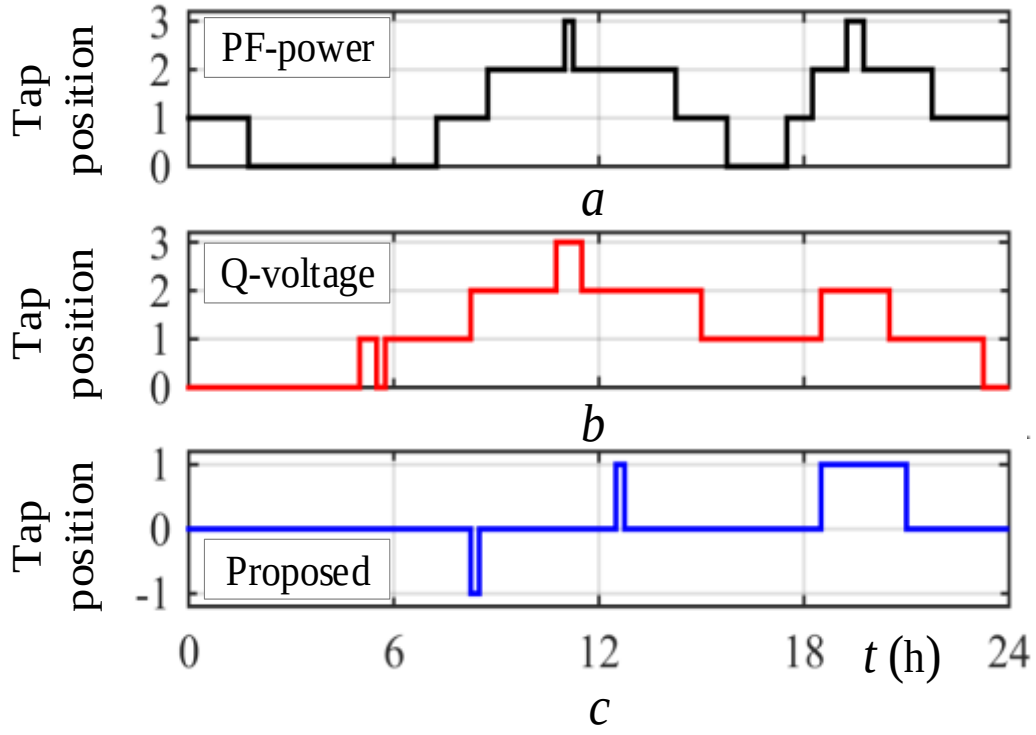

Figure 5-14. The 33-node test feeder results with thirty three 250 kVA PV systems: the tap position of the feeder transformer (a) The PF-power scenario, (b) The Q-voltage scenario, (c) The proposed scenario

The voltage amplitude at the LV-side of the transformer is presented in Figure 5-13. However, the voltage profile shows a slightly higher trend compared to Q-voltage scenario, yet it's still regulated within the permissible voltage limits. The transformer tap positions are provided in Figure 5-14. As can be seen, the OLTC experiences fewer tap changes when the proposed technique is deployed.

5.3.1.3. Hosting Capacity Simulations

After accomplishing the power studies and tap position considerations, hereinafter, the 33-node feeder hosting capacity is determined. Here, the network hosting capacity is defined as the amount of PV capacity that can be connected to the network without system constraints violation [164]. In this context, the maximum and minimum voltage constraints are defined as follows [79], in Equation (3.1) and (3.2), where the boundaries of $Vmax$ and $Vmin$ are 1.1 and 0.9 per unit in this study, respectively. Additionally, the transformer loading constraint is equal to the maximum loading of the transformer over a day. Similarly, a branch flow constraint is also defined regarding the network lines loading.

To determine the PV hosting capacity for the 33-node network, load flow calculations are derived over 24 hours over the time intervals of 15 minutes for the PVs nominal apparent power ranged from 75 to 350 kVA with 25 kVA increment steps. The derived constraints versus the cumulative PVs apparent power (in percentage of the system base power) are illustrated in Figure 5-15.a to Figure 5-15.c. In addition, the determined hosting capacities are listed in Table 5.2 for the three scenarios.

Table 5-2. The PV hosting capacity of the 33-node test feeder (in percentage of the system base power 5750 kW)

control method	**Hosting capacity subject to constraint**		
	Max. voltage	Trans. loading	Branch flow
PF-power	215	114	100
Q-voltage	286	132	107
Proposed	187	150	**124**

Ignoring the loading constraints, the Q-voltage approach gives the largest hosting capacity. On the other hand, the proposed algorithm has the largest hosting capacity considering the loading constraints. Particularly, it increases the PVs hosting capacity by 16% in comparison with that of the Q-voltage case, proving the system can embrace more PV capacity for future studies. Finally, the total number of the OLTC tap operations over 24 hours is provided in Figure 5-15.d. As can be clearly observed, the suggested method results in fewer tap changes where it eliminates unnecessary tap changes, compared to the standard voltage control strategies,

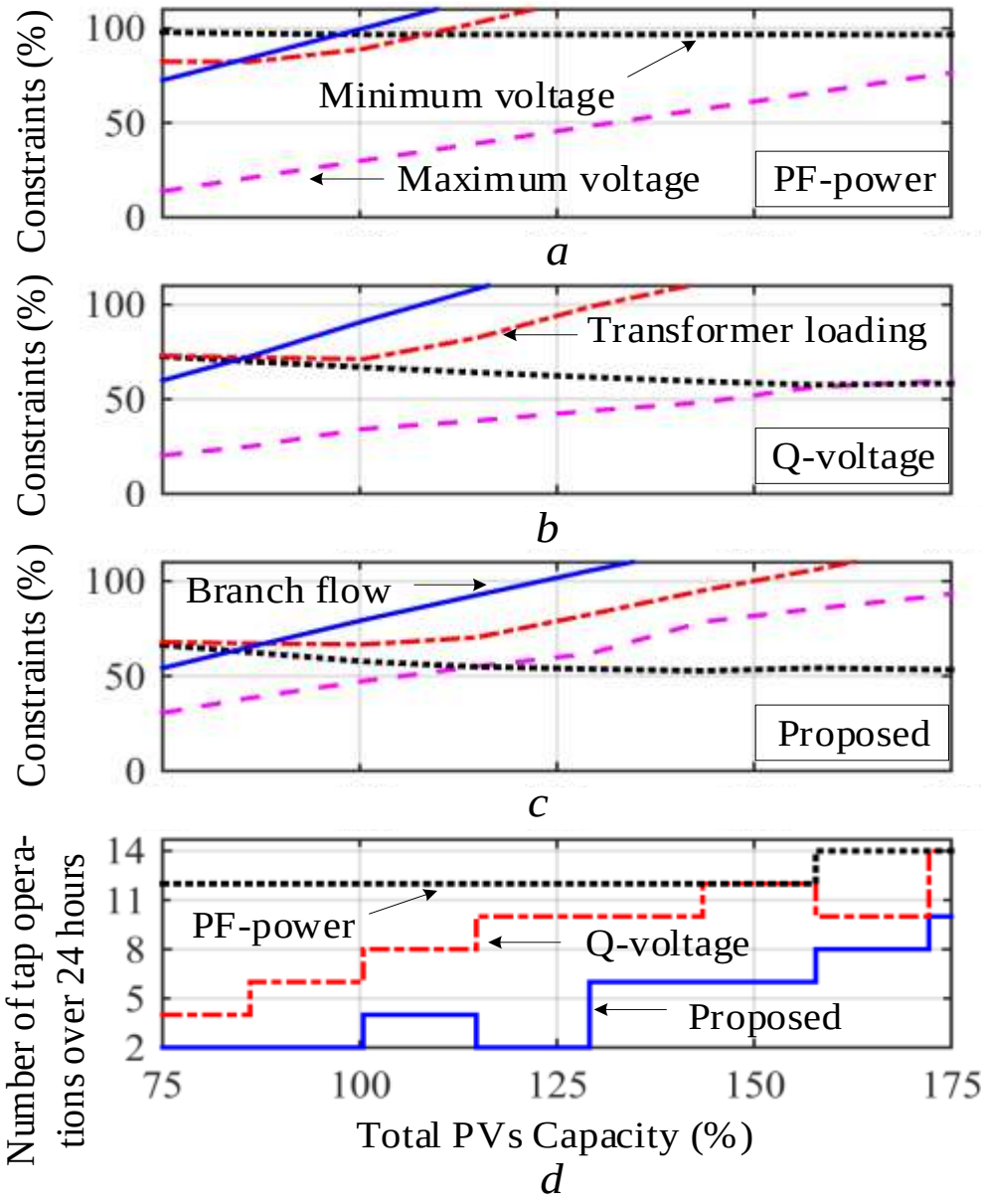

Figure 5-15. The 33-node test feeder: (a) The constraints for the PF-power scenario, (b) The constraints for the Q-voltage scenario, (c) The constraints for the proposed scenario, (d) The number of transformer tap operations over a day

5.3.2. The 69-node test system simulation results

In order to verify the generality of the proposed scheme, simulation studies on the 69-node feeder has also been carried out. In this regard, simulation results have been provided for both radial and meshed configurations of the test network. The diagram of the radial 69-node feeder was shown in Figure 5-5, while its meshed configuration also depicted in Figure 5-6. In the

proposed strategy, the PV units highlighted in the work, deploy the Q-voltage local controller and the rest are equipped with the suggested local controller.

5.3.2.1. Hosting Capacity Simulations

The network constraints along with the daily OLTC tap operations for the radial and meshed configurations are demonstrated in Figure 5-16 and Figure 5-17, respectively. The horizontal axis represents the total PVs apparent power in percentage of the system base power, i.e., transformer apparent power, 6,150 kVA.

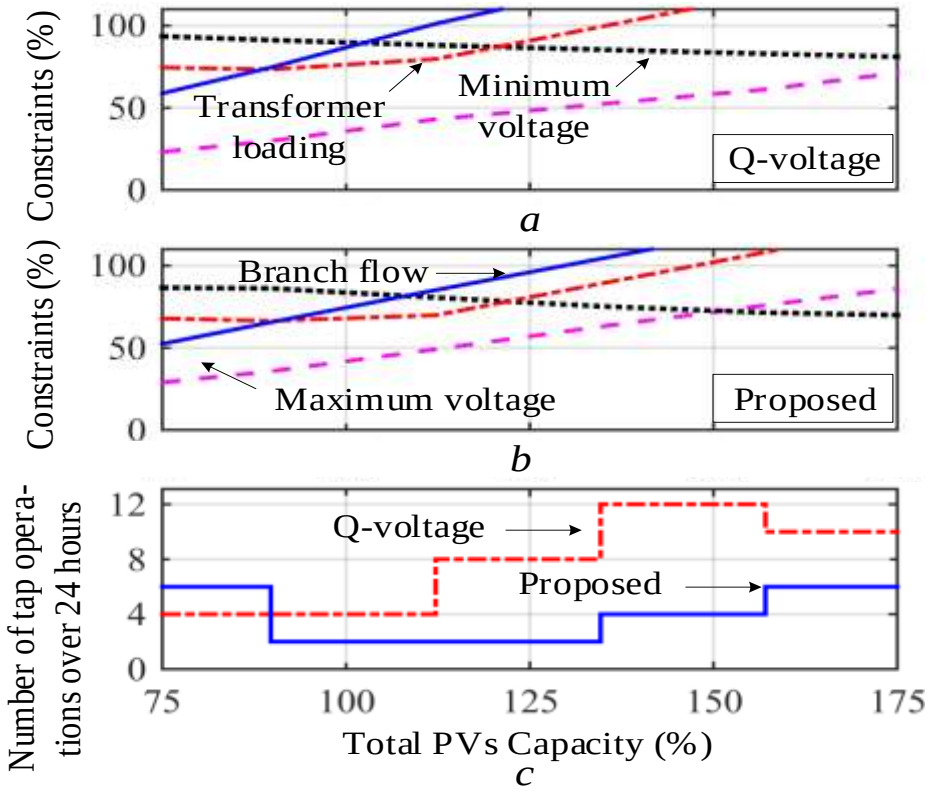

Figure 5-16. The radial 69-node test feeder: (a) The constraints for the Q-voltage scenario, (b) The constraints for the proposed scenario (c) The number of transformer tap operations over a day

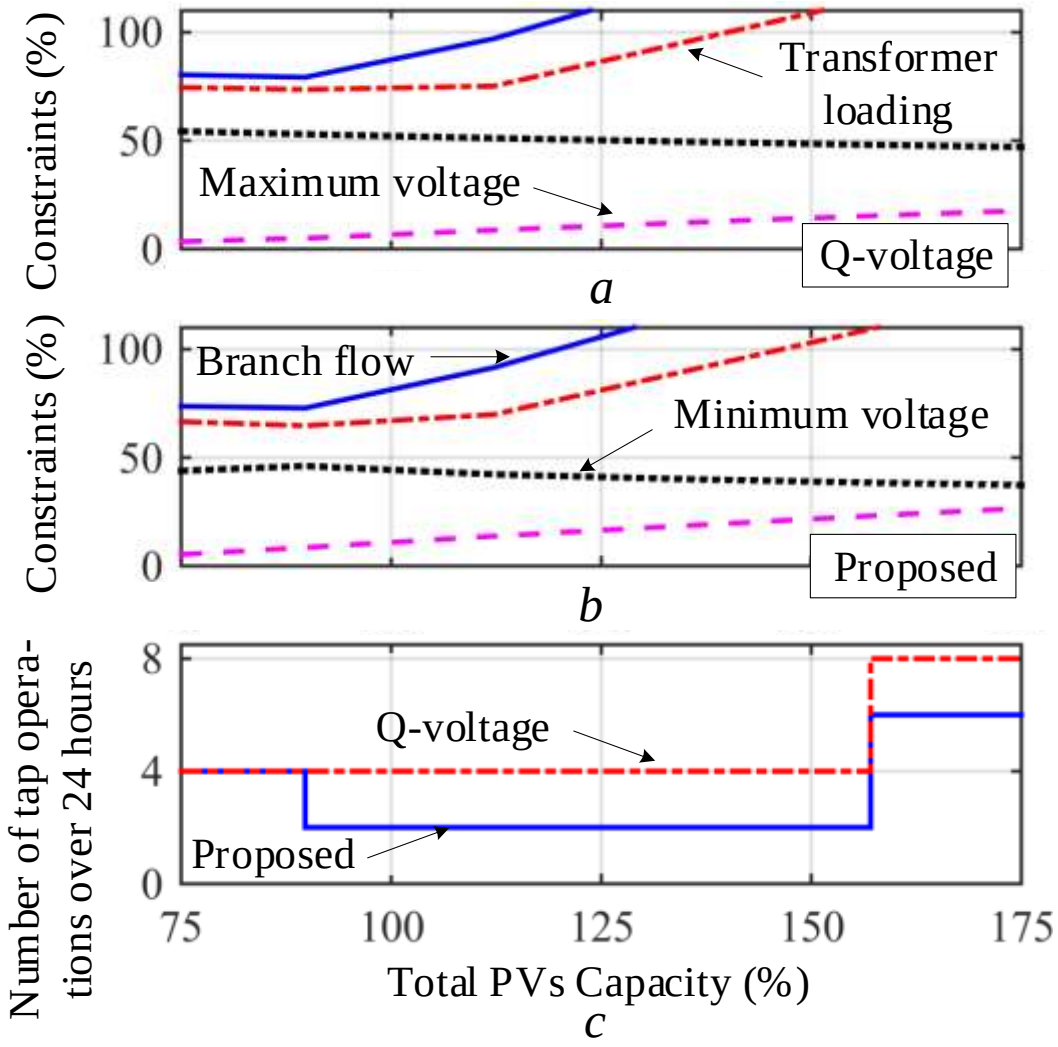

Figure 5-17. The meshed 69-node test feeder: (a) The constraints for the Q-voltage scenario, (b) The constraints for the proposed scenario (c) The number of transformer tap operations over a day

The achieved results are shown for the Q-voltage and the proposed scenarios. Accordingly, the hosting capacities of the 69-node feeder are listed in Table 5-3, for the radial and meshed configurations.

Table 5-3. The PV hosting capacity of the 69-node test feeders (in percentage of the system base power 6,150 kW)

control method	**Network configuration**	**Hosting capacity subject to constraint**		
		Max. voltage	Trans. loading	Branch flow
Q-voltage	Radial	270	135	110
	Meshed	1,000	140	114
Proposed	Radial	190	148	**129**
	Meshed	560	146	**120**

Several observations are in order from Table 5-3. First, the devised scheme can increase the network hosting capacity even in the meshed feeder. However, the achieved hosting capacity with the radial feeder is slightly larger than that of the meshed one.

Second, for the PVs capacities further than 90% of the system base power, the proposed method results in fewer OLTC tap operations in comparison with that of the Q-voltage approach. It is also interesting to point out that the effectiveness of the proposed and/or the Q-voltage strategies are roughly independent of the feeders' topology by comparing Figure 5-16 with Figure 5-15. It's worth to highlight this is a very important outcome, since the future network studies can be made based on this consideration.

5.3.2.2. Power loss Simulations

The maximum power losses of the radial and meshed 69-node feeders, over a day, is illustrated in Figure 5-18.a and b, respectively. It is deduced that the power losses can be approximately reduced by half using the meshed network. Besides, it can be observed that the proposed methodology offers lower system power losses in comparison with that of the conventional Q-voltage strategy.

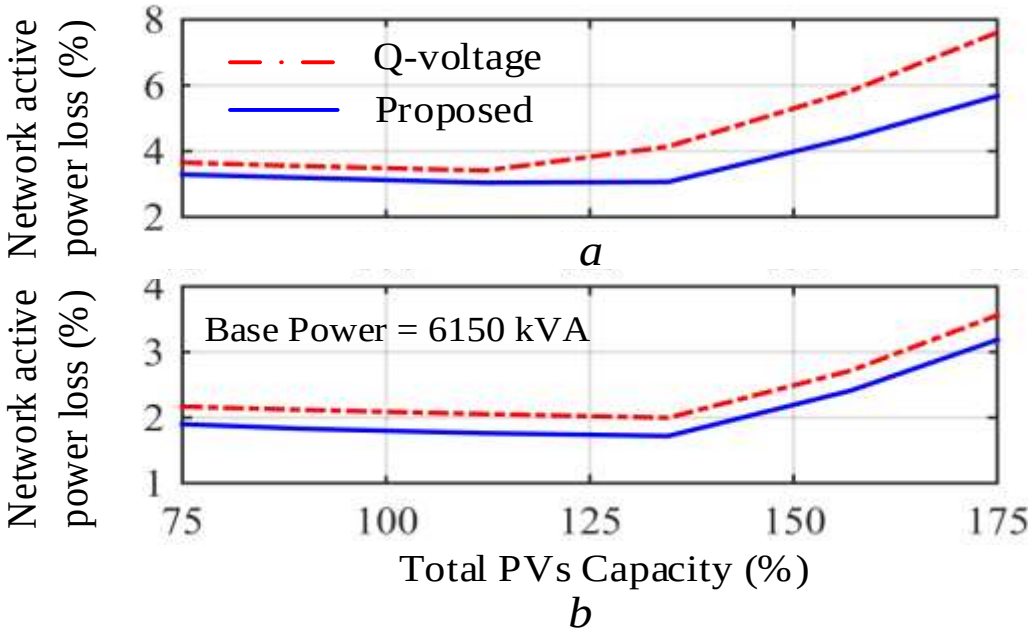

Figure 5-18. The maximum power losses of the 69-node test feeder: (a) The radial configuration (b) The meshed configuration

5.4. Stochastic Evolution Simulation Results

This section presents the stochastic assessment results of selected input parameters to enhance the accuracy of the simulation results in Section 5.3. , with advanced probabilistic methods. Stochastic approaches were used for the test networks to calculate the probability distribution of PV power output and load demand inputs, as explained in Chapter 4.

The distributions of the stochastic variables can be approached by a discrete distribution with a limited number of scenarios with the corresponding probabilities. An extensive collection of scenarios are created with the Monte Carlo simulation technique by using the Roulette Wheel Mechanism (RWM). To accurately decrease the number of scenarios and handle the stochastic problem, scenario reduction algorithm is applied. Out of one thousand scenarios with infinite probabilities, these scenarios are reduced to ten set of scenarios with backward scenario reduction method. On the basis of demonstrating the results with selected uncertainties, the effectiveness of the suggested approach for increasing the DN hosting capacity is demonstrated through different case studies on 33 node and 69 node test feeders. The figures illustrate the results of the system with the reduced ten different probability scenarios. Here, each PV power output and load demand scenario was represented as a single probability, given in Table 4-2.

5.4.1. Generated Scenario Results

The stochastic assessment results are represented over the specific dispatch interval of 15 minutes, resulting in 96 data points over a day, on the 33 node test system. The achieved results with the PVs nominal apparent power of 250 kVA are represented. The active and reactive power variables are shown in the percentage of the system base power 5750 kVA. It should be noted that the results are shown for 24 hours over a day, although, there are 96 evaluated data points. The generated scenario results are represented only on 33 node system because the PV generation and load demand profiles are quite similar within these networks, whereas the

further comparisons will be evaluated for both test systems. Figure 5-19 illustrates the voltage amplitude at the critical bus 18, where the voltage tends to have an increased magnitude, especially in peak PV generation time. The alteration among scenarios also show difference at this point. Figure 5-20 presents the bus 1, at the LV-side of the transformer. As seen, the voltage deviation shows difference among number of scenarios. For none of the simulations, the overvoltage limit (110% of nominal) is exceeded with the proposed voltage control method.

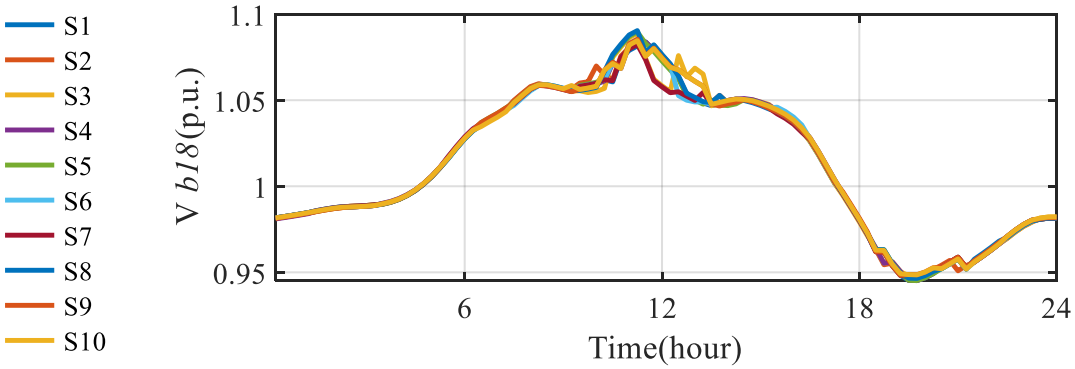

Figure 5-19. The voltage amplitude at the bus 18 with generated scenarios with proposed voltage control strategy

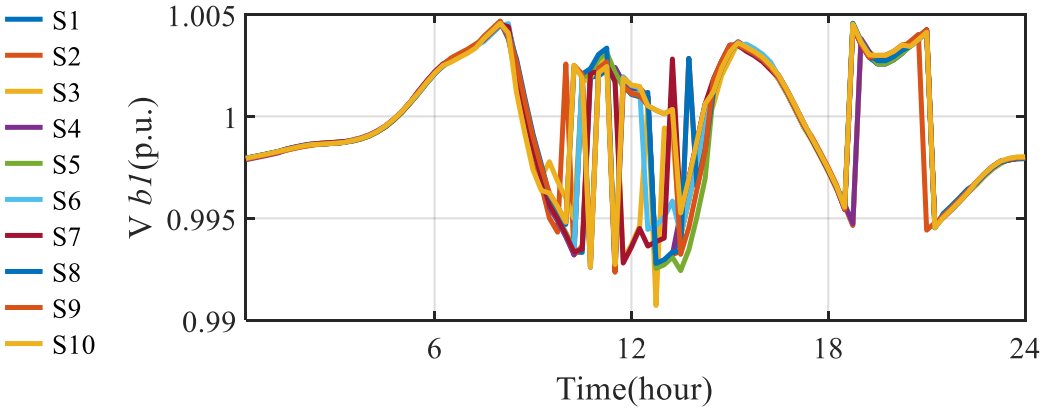

Figure 5-20. The voltage amplitude at the bus 1 with generated scenarios with proposed voltage control strategy

Figure 5-21 illustrates the grid losses in kW, where some scenarios have possible higher grid losses in the peak generation times. Similarly, Figure 5-22 illustrates the MV grid reactive power generated by the upstream network. It is obvious that in some scenarios, the MV grid reactive power support would be needed more and for a longer time scale.

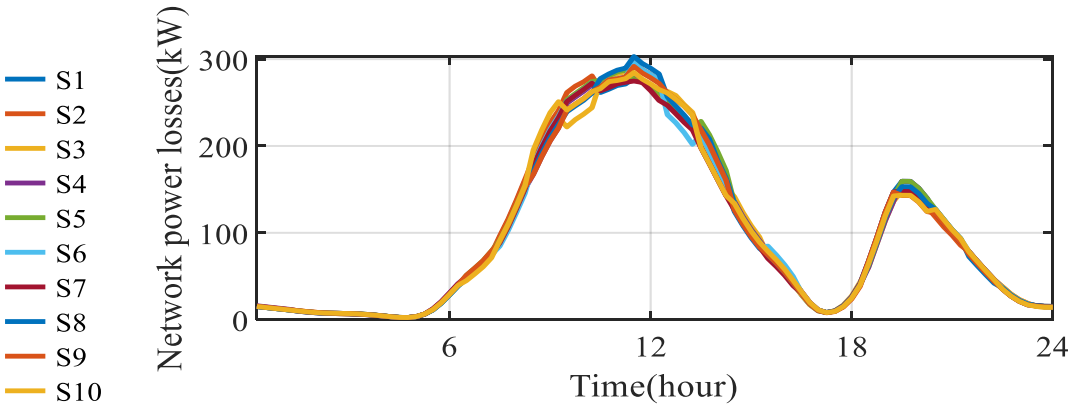

Figure 5-21. The 33-node test feeder results with thirty three 250 kVA PV systems, active power losses (kW) in the system with generated scenarios

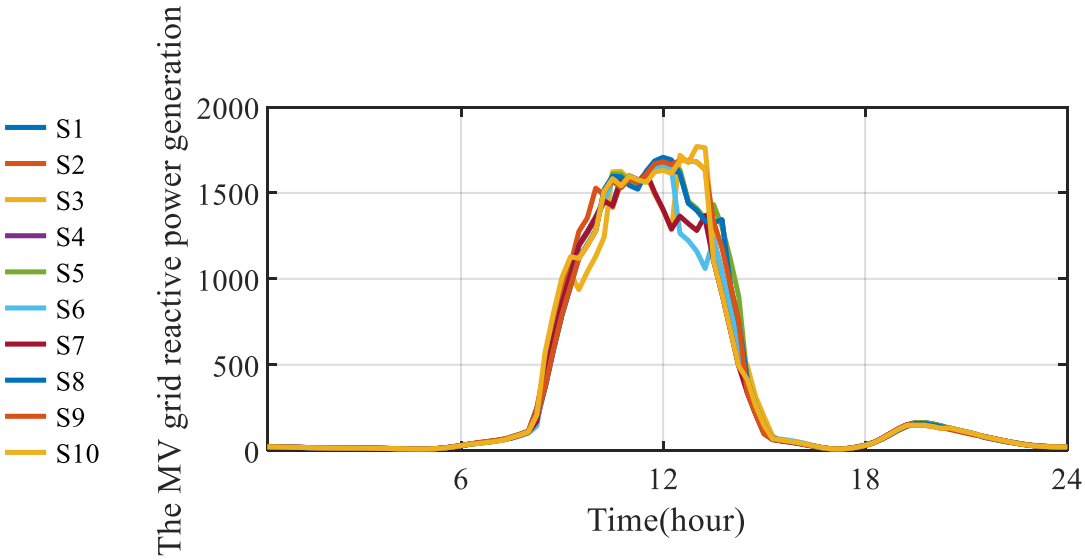

Figure 5-22. The MV grid reactive power generation (kVAr)

Figure 5-23 represents the transformer loading at the beginning of the feeder. Figure 5-24 illustrates the loading of line 8, as it is referred being the critical bus in the 33 node test system, previously. Overall, the transformer loading results are aligned within the permissible limits.

However for the line loadings, in some scenarios, there is a small probability that loadings may exceed the limits provided.

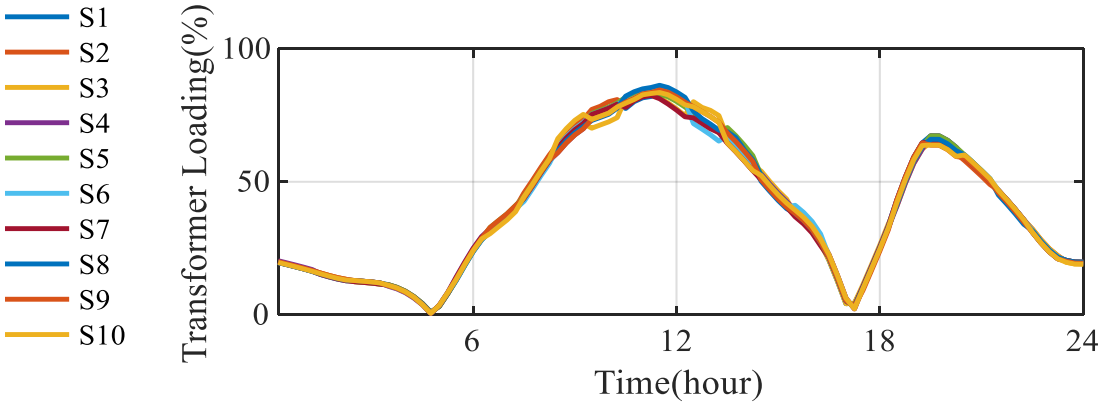

Figure 5-23 The 33-node test feeder results with thirty three 250 kVA PV systems, transformer loading results with generated scenarios

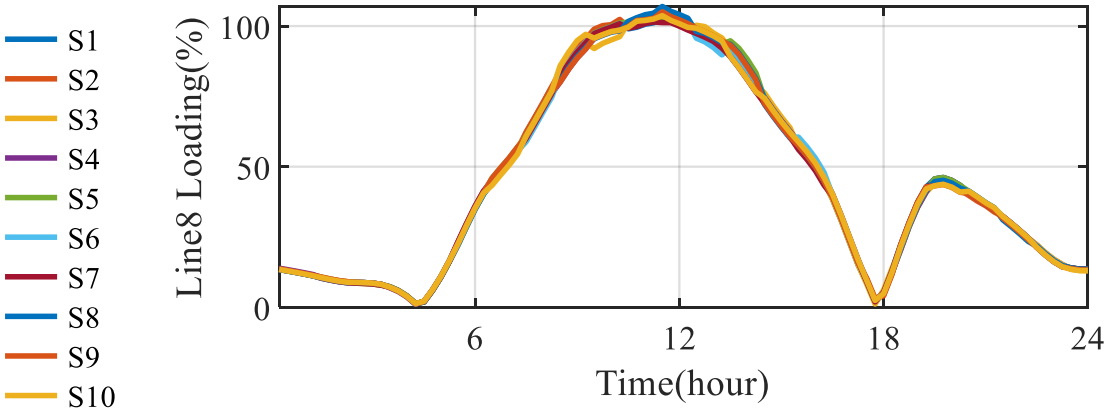

Figure 5-24. The 33-node test feeder results with thirty three 250 kVA PV systems, line 8 loading results with generated scenarios

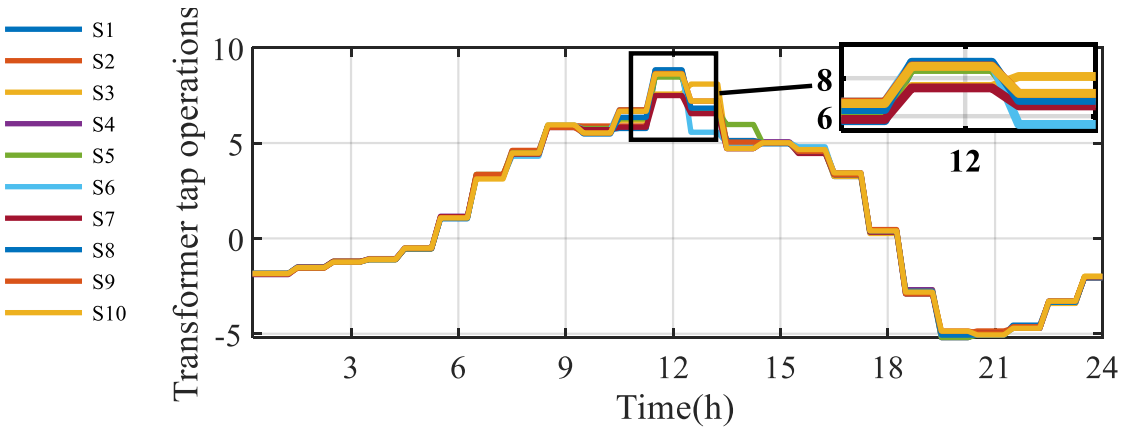

Figure 5-25. The 33-node test feeder results with thirty three 250 kVA PV systems, tap changes per day transformer of the feeder with generated scenarios

Finally, Figure 5-25 illustrates the tap changers over the day. As can be seen, there might be up to three tap change differences between some scenario cases. This would be a vital consideration before addressing the tap changer operations in a practical high penetrated PV test system. So that, the simulation results reveal the importance of evaluating the stochastic analysis results. Next section will compare the expected value of stochastic analysis with deterministic results.

5.4.2. Deterministic and Expected Value Results comparisons

This section will compare the evaluated deterministic results in Section 5.3. , with the stochastic assessment expected value results. Expected value is a generalization of the weighted average, which is the arithmetic mean of a large number of independent realizations of random variable. The 33 node test system is evaluated with the stochastic expected value of proposed voltage controller and deterministic study results.

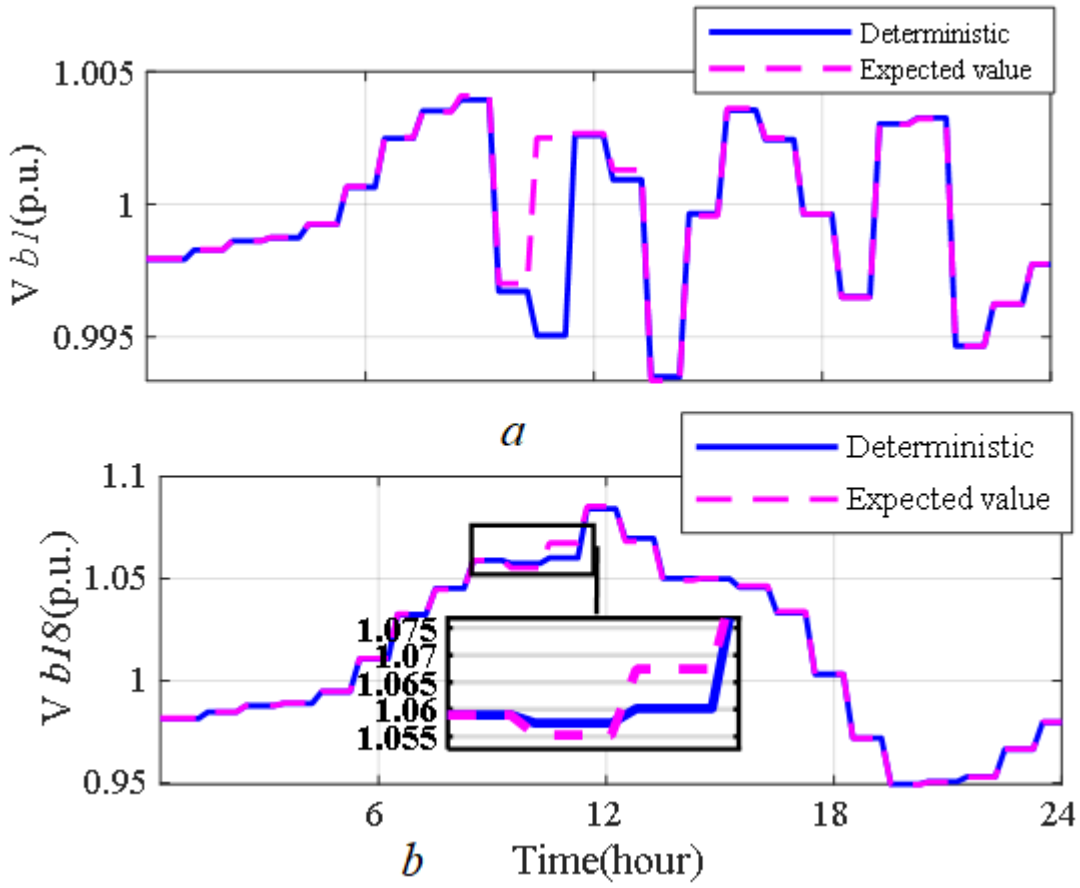

Figure 5-26 The 33-node test feeder voltage magnitude results by deterministic and expected values (a) Bus1, (b) Bus18

Figure 5-26 illustrates the voltage magnitudes at the bus "Bus1" at the transformer LV side and the critical bus "Bus 18". While the simulation results demonstrate similar trends with deterministic results over the most of the day, it becomes significantly different for the peak generation times. Figure 5-27 illustrates the active power losses over the 33 node test feeder. Lastly, Figure 5-28 illustrates the transformer and line loading with the expected value and deterministic results. With the expected results, there is a small probability that line loadings may exceed the limits provided.

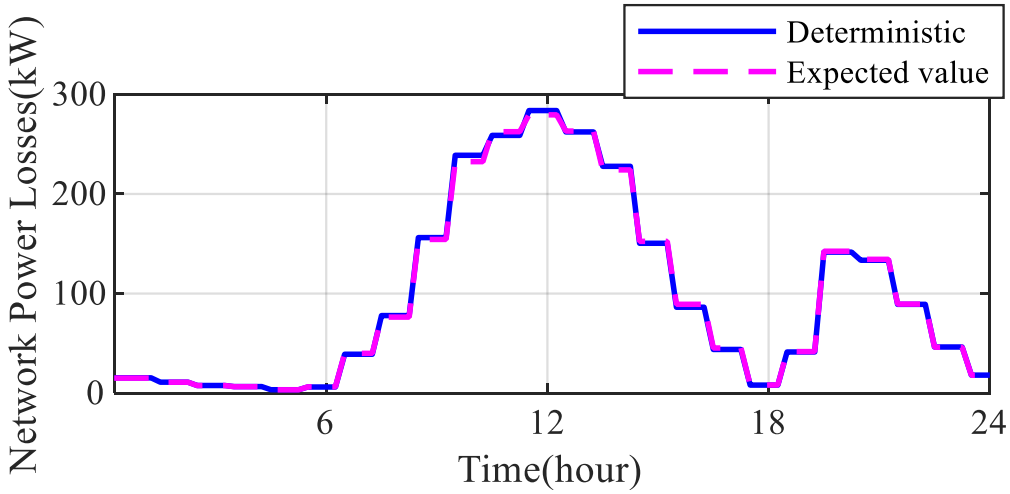

Figure 5-27. The 33-node test feeder network power losses results by deterministic and expected values (kW)

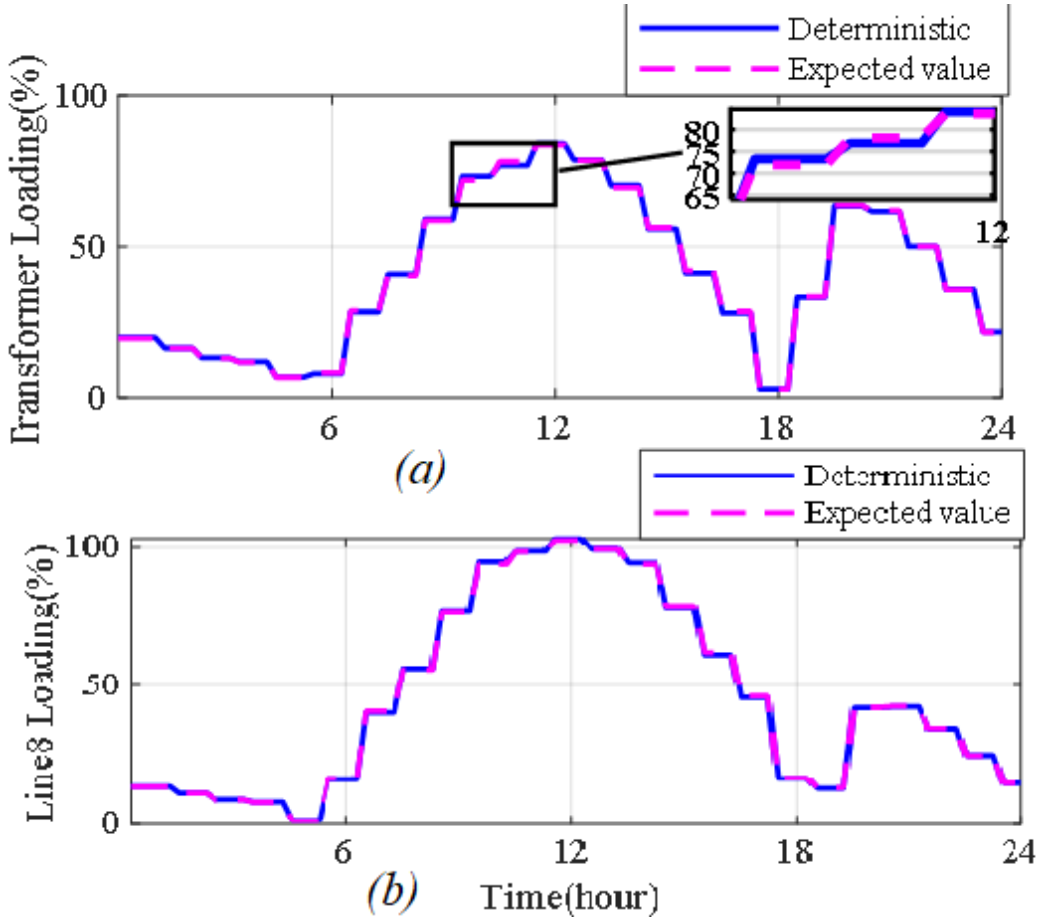

Figure 5-28. The 33-node test feeder results by deterministic and expected values with thirty three 250 kVA PV systems (a) The transformer loading, (b) The line 8 loading

5.4.3. Expected Value Results Comparison with Existing Voltage Control Methodologies

It is a necessity to compare the evaluated stochastic assessment results with the expected values of the existing voltage control techniques to reveal the effectiveness of the proposed technique. Thus, this section will illustrate the PF-Power, Q-Voltage and proposed voltage control methods comparison over their expected values, on the 33 node test feeder.

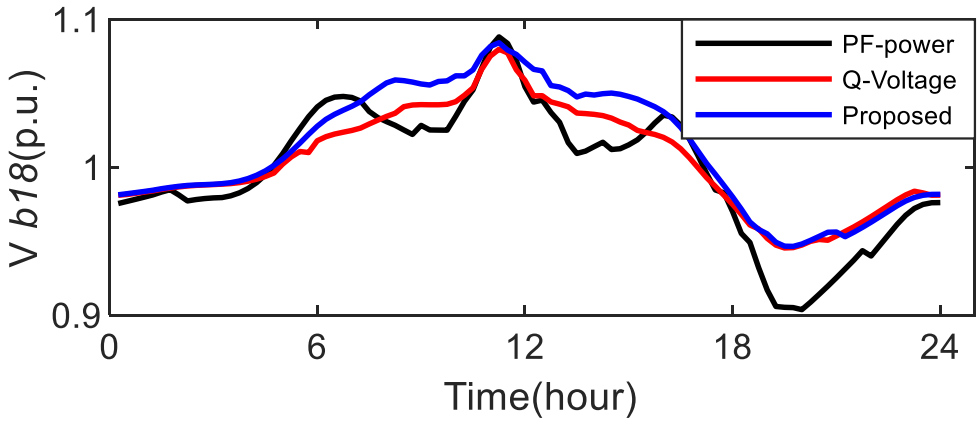

Figure 5-29. Voltage amplitude at the (critical) bus 18 for expected values

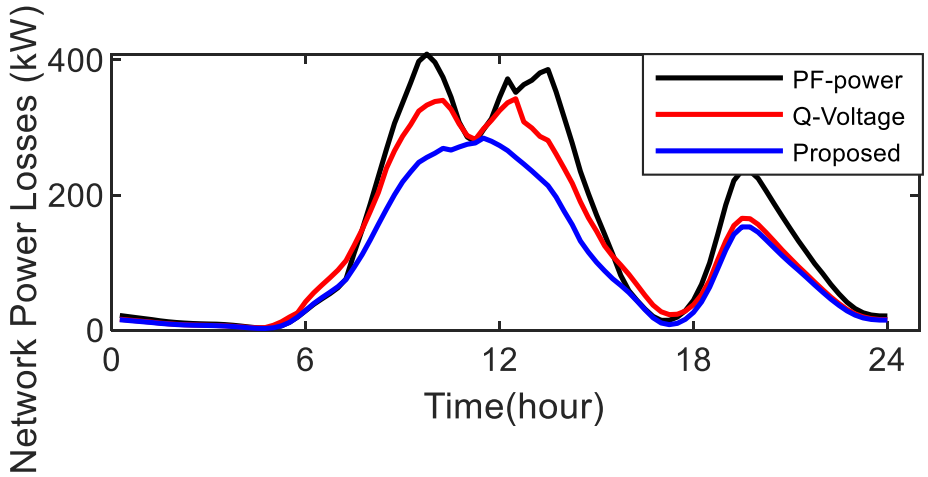

Figure 5-30. The 33-node test feeder network power losses (kW) for expected values

The voltage variation at the most critical node of the 33 bus feeder, i.e. bus 18, is portrayed in Figure 5-29. For the voltage profiles, similar to the results in deterministic studies, the voltage

on the bus 18 is slightly higher over the day. From further numerical studies, this result appears to be reasonable, thus it is preserved within the critical voltage limits. Figure 5-30 presents the network power losses in terms of active power, compared with three discrepant scenarios. Another interesting aspect is the decrease of losses in standard voltage control techniques, while the generation is increased, thereby can be explained by the excessive reactive power consumption. However, network power losses are much lower in the proposed stochastic results over the daily trend.

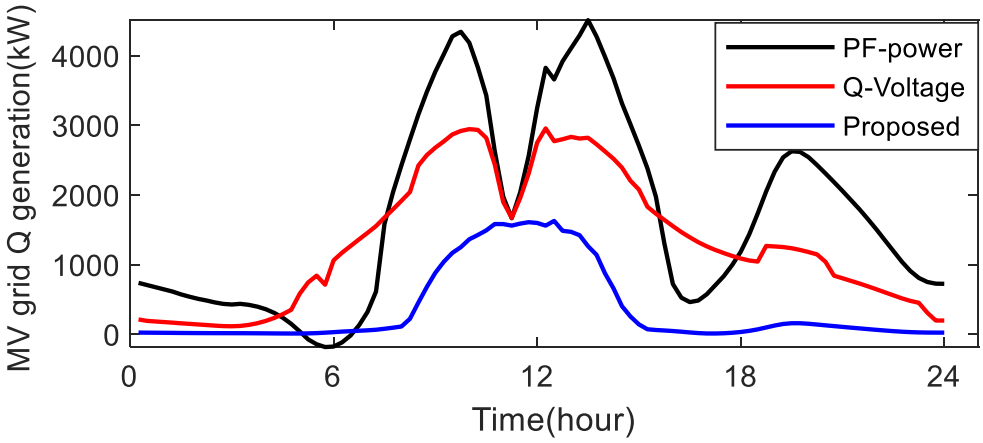

Figure 5-31. The 33-node test feeder MV grid reactive power generation for expected values

In Figure 5-31, there is a massive difference for the MV grid reactive power requirement from the upstream network, regarding the proposed controller. As seen, the PF-power and Q-voltage strategies require an excessive amount of reactive power support from the upstream network. However, the proposed controller results in a significant reduction in MV grid reactive power support, being able to generate the desired reactive power within its own PV units. Figure 5-32 illustrates the transformer and line 8 loadings for the studied test system. For the lines, both PF-power and Q-voltage strategies violates the safety limit, and further, comes quite close by violating the strict voltage limits of the system. It is clear that the time of the over-loading coincide with the period of highest solar generation in standard voltage control techniques.

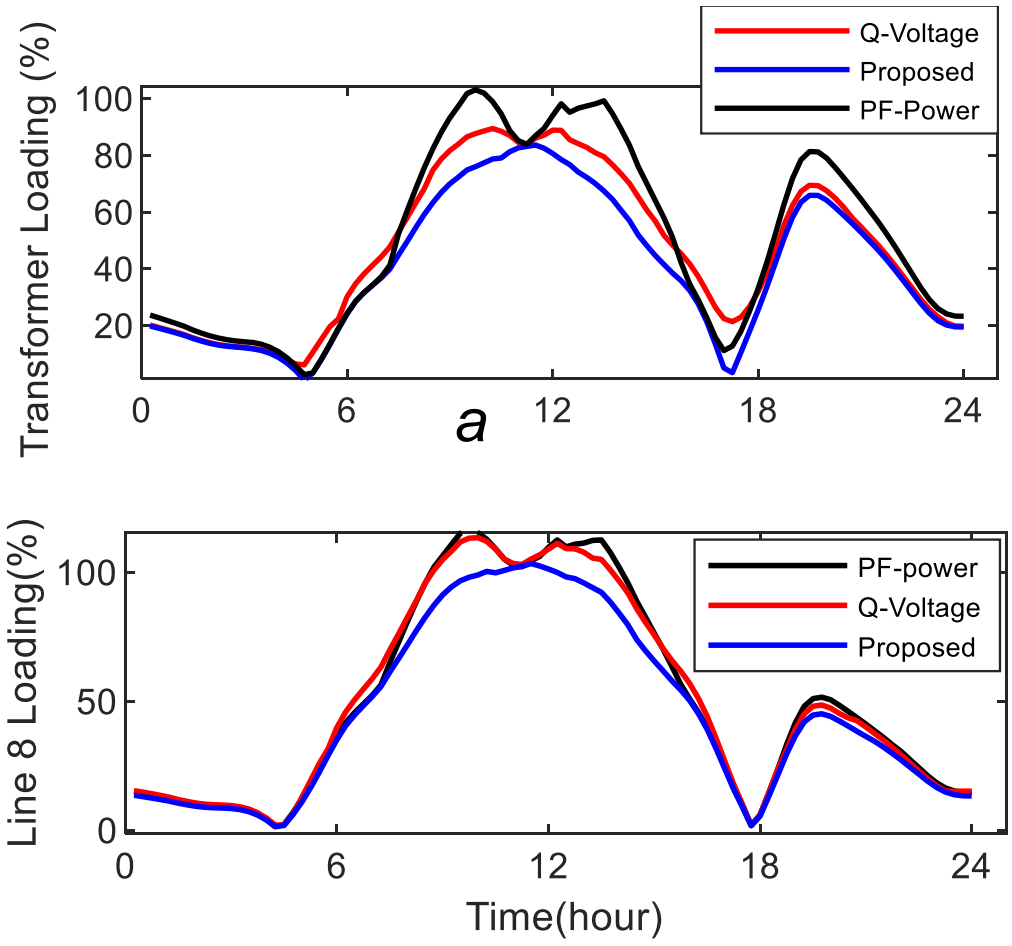

Figure 5-32. The 33-node test feeder results with thirty three 250 kVA PV systems for expected values (a) The transformer loading, (b) The line 8 loading

Table 5-4the enhanced PV hosting capacity with expected values of proposed method compared to the conventional control methods is given in Table 5-4. The hosting capacity defined by maximum voltage is lower compared to deterministic results, due to the increase in the load demand and slight decrease in PV generated power with generated scenarios. For the loading constraints, the proposed strategy, will allow more PV units to be integrated without violating the limits. For conventional voltage control methodologies, it is anticipated that PVs may cause the grid components to be overloaded under the several scenario considerations. Thus, when loading constraints are observed under several predicted scenarios, it is obvious that the proposed strategy, is the most effective method to increase the hosting capacity.

Table 5-4. The PV hosting capacity of the 33-node test feeder with the expected values (in percentage of the system base power 5750 kW)

control method	Hosting capacity subject to constraint		
	Max. voltage	Trans. loading	Branch flow
PF-power	210	112	100
Q-voltage	280	132	105
Proposed	205	152	**120**

From the expanded evaluations by stochastic assessment, the results demonstrate that, the proposed method is a reliable and robust way to increase the PV capacity within the network without surpassing the constraints defined in the grid codes.

5.5. Chapter Summary

To demonstrate the proposed strategy's applicability on different occasions, the first step to investigate the effectiveness of the proposed scheme, is to apply simulations on the 33-node test system with deterministic calculations. Second step, the simulations are extended by using a broader test system, i.e., 69-node test feeder, not only the radial network but also the meshed one. The achieved results are added into the simulation results in addition to that of the 33-node system. Third step, ten different scenarios are generated for load profile and PV generation output by stochastic scenario generation and reduction techniques, from a wide variety of probabilities database. The deterministic results are compared with the derived ten different stochastic assessment results.

For the deterministic studies, the simulation results on the radial and meshed test feeders verify the practicality of the proposed voltage control method. The proposed method resulted in 35% reduction in transformer and 20% reduction in line loadings, respectively, over the conventional Q-control method. Also at the PVs maximum generation time, the reactive power flow from PVs towards the upstream network is reduced 70% and 33%, respectively, over PF-

Power and Q-Voltage strategies. The tap changer positions with OLTCs experienced fewer tap changes with the proposed controller over the day. The results prove that, when the transformer loading and branch flow constraints are taken into consideration, the hosting capacity enhancement is greater by about 20%, for the proposed method. Comparative results of the 69-node feeder with that of the 33-node, reveals that the new method can increase the distribution network hosting capacity almost by 15% of the feeder transformer nominal power, regardless of the studied network.

As a further consideration, the stochastic assessment results are executed on 33 node test system. The studies were conducted for ten different scenarios considering load profile and PV power generation output as uncertain variables. The expected value, which is the summation over the probabilities of given ten scenarios, is compared with the deterministic results. Active power losses decreased by %50 and %40 compared to PF-power and Q-voltage strategy, respectively. There is a major reduction over the MW reactive power supplied to the studied 33- node test system, for the proposed controller (%75 less than PF-power and %65 less than Q-voltage). Hosting capacity expected value observations show that the proposed approach increases the hosting capacity by 20% in comparison to PF-power case.

For the distribution system studies, the proposed strategy will contribute to the integration of more PV units. With the proposed strategy, especially at higher penetration levels a significant reduction can be expected by the excessive reactive power flow, and 70 percent less requirement from the MV network reactive power. Thus, the proposed methodology can assist in maintaining grid limitations, even when increasing the penetration of PVs far beyond the levels currently applied to the electric grid,

6. CONCLUSIONS AND FUTURE WORK

The main goal of this thesis is to propose a novel decentralised voltage control for achieving the desired level of additional hosting capacity for the distribution network feeder. The issues about centralized control, i.e. the need extensive monitoring and communication makes decentralised control more attractive which presents compact solutions and local strategies. Firstly, the impact of the standard local voltage controllers Power Factor-P and Q-Voltage strategies are studied and evaluated by sensitivity studies with high penetration levels of PVs. The aim is to enhance reactive power control by improving the performance of conventional local voltage control strategies.

This study derives a novel entirely local reactive power management method for the PV systems to improve the distribution feeders hosting capacity. In this strategy, a feeder is divided into several zones. To this end, a simple algorithm has been developed which aims to minimise the reactive power flow through the network electrical bottlenecks. Firstly, the network data that includes the line parameters and the feeder transformer is loaded. Secondly, all the loads are disconnected from the network. Then, one PV system is connected to each node of the feeder. It is assumed that all the PV systems are initially equipped with the conventional Q-voltage local controllers. Afterwards, the feeder transformer loading is checked. If it's not fully loaded, the nominal power of the PVs will be increased until the transformer reaches its full load operation. Subsequently, the algorithm finds the network electrical bottlenecks according to the line loadings. Next, the closest PV systems, which are neighbouring the bottlenecks towards the feeder downstream, will be equipped with the proposed local controller. Then, the

reactive power flow through the bottlenecks should be checked. If it is not minimized, the next PV units must be equipped with the suggested controller.

First of all, the proposed control strategy is tested without loads to observe the overvoltage problem. All the nodes in the distribution feeder are equipped with a PV unit to represent the high penetration issue. Sensitivity studies are performed to select the most appropriate local control strategy from the literature, to support the novel approach. The PF-power and Q-voltage method leads to 1% increment in feeder transformer capacity and provides 0.4% and 0.5% voltage reduction, respectively. The outcomes of the sensitivity studies revealed that Q-voltage strategy shows 25% more efficient control than PF-power. Thus, Q-voltage was used as the supporting method to the proposed controller.

The proposed network voltage support strategy deploys zonal reactive power management to regulate the voltage in the distribution network. In this strategy, a distribution feeder is divided into several zones. To this end, a computationally efficient algorithm has been developed, aiming to minimize the reactive power flow, which is measured every 15 minutes, through the network electrical bottlenecks. In the zones located at the end of feeder laterals, the PV systems support the grid voltage through a standard local voltage-dependent reactive power regulator (Q-voltage). Alternatively, each PV unit located in the zones neighbouring the bottlenecks is equipped with the proposed local controller. These PV units try to minimise the reactive power flow at their up-stream branch.

Extensive studies were carried out for increasing the accuracy of all the results obtained in deterministic results. The stochastic evaluation of the uncertain variables is executed to improve the performance of the decentralised controller with consideration of the variable nature of PVs and loads in the distribution network. On one hand, mainly in the literature, the studies mentioned and used a deterministic model of PV power production, not fully

considering the stochastic character of the energy sources. On the other hand, in the proposed method, PV output power and load demand are the two parameters to be modelled in a stochastic manner with probability density functions. Computational burden and extensive time are the outcomes of modelling the stochastic nature of PVs with the existing methods. Through the scenario generation method, the stochastic nature of the proposed problem will be decomposed into a deterministic solution. This research has found that with the stochastic assessment of the uncertain variables, the hosting capacity of the feeder can reach more accurate results in terms of grid losses, transformer loading and upstream network support.

In the suggested voltage control approach, all the controllers are implemented locally for each PV unit. Thus, the communication devices are eliminated, mitigating the investment cost significantly. The simulation results on the radial and meshed test feeders verify the practicality of the proposed method. When calculating the hosting capacity, the maximum voltage, transformer loading and branch flow are the three metrics to measure the efficiency of the proposed method. The results on the 33 node test system, prove that the developed controller can increase the system hosting capacity by about 20% of the systems base power in comparison with the existing controllers. Furthermore, using the proposed method considerably decreased the network active power loss. Moreover, the transformer tap changer experiences reduced tap operations (20 less tap changes) over a day using the suggested technique. The proposed algorithm increases the PVs hosting capacity by 16% in comparison with that of the Q-voltage case, proving the system can embrace more PV capacity for future studies. As a result, the voltage is within permissible limits alongside the voltage control ability, and feeder hosting capacity is enhanced to allow further PV integration.

To investigate practicality of the suggested approach, the proposed methodology has been applied on both meshed and radial 69-node test feeders. Interestingly, it has been observed that

effectiveness of the proposed controlling strategy in increasing the standard distribution networks is roughly independent of the studied test system. In case of meshed 69-node system, the suggested approach preserves its ability and superiority in reducing reactive power flow through the network electrical bottlenecks in comparison to the conventional strategy. However, the achieved hosting capacity in the meshed configuration (120% of the system base power) is somehow lower than that of the radial feeder (129% of the system base power).

The stochastic assessment results are also in line with the deterministic results, highlighting the importance of more studies for including stochastic behaviour of PVs and loads. The studies were conducted for ten different scenarios considering load profile and PV power generation output as uncertain variables. The expected value, which is the summation over the probabilities of given ten scenarios, is compared with the deterministic results. Active power losses decreased by %50 and %40 compared to PF-power and Q-voltage strategy, respectively. A major reduction was observed over the MW reactive power supplied to the studied 33- node test system, for the proposed controller (%75 less than PF-power and %65 less than Q-voltage). Hosting capacity expected value observations show that the proposed approach increases the hosting capacity by 20% in comparison to PF-power case.

One of the biggest outcomes of this work is that the hosting capacity enhancement occurs regardless of the studied network. So that, the results have revealed that the system hosting capacity can be increased without overloading the transformers and lines in the system, with mitigating the overvoltage issues with the proposed controller and constraint considerations in this thesis. The simulation results on the radial and meshed test feeders verify the practicality of the proposed voltage control method. The results prove that the developed controller can increase the system hosting capacity by about 20% of the systems base power in comparison with the existing controllers. The main contributions are summarised in next section.

6.1. Contributions of the Thesis

The main contributions of this thesis can be summarized as follows:

1. The simultaneous use of proposed control can significantly mitigate overvoltage issues and increase hosting capacity of the feeder. Decentralized control provides several advantages like high efficiency, network losses reduction, local power grid support and the voltage profile enhancement. The decentralized strategies combine the benefits of centralized and distributed methods through zonal control and inter-zonal coordination in the portioned ADNs. The proposed approach has been applied to two different small- and large-scale radial and meshed systems and attains superior performance in comparison with other traditional decentralized techniques.

2. The network partitioning is a crucial part of the proposed reactive power control framework for active distribution feeders. In this study, a practical and straightforward algorithm is developed to find the candidate PV systems to be clustered for real-world distribution multi-lateral feeders. The approach mainly divides a multi-lateral distribution feeder into several zones to equip the PV systems located in half of these zones with the proposed local reactive power control strategy. On the other hand, the rest of the zones follow the Q-voltage controller strategy. This allocation provides a further control structure that provides reactive power control with the PV inverters in ADNs.

3. The algorithm finds the network electrical bottlenecks in according to the line loadings. The closest PV systems, which are neighbouring the bottlenecks towards the feeder downstream, will be equipped with the proposed local controller. Then, the reactive power flow through the bottlenecks should be investigated. If the power flow is still not minimized, in addition, the next PV units are equipped with the suggested controller. This process will repeat towards optimizing the objective function.

4. Comprehensive simulations are performed to elaborate on the developed algorithm. The effectiveness of the proposed scheme has been investigated using a more extensive test system, i.e., 69-node test feeder, not only the radial network but also the meshed one. The achieved results are appended into the simulation results in addition to that of the 33-node system. Comparative outcomes of the 69-node feeder with that of the 33-node, reveals that the new method can increase the distribution network hosting capacity from 100% to effectively 125% of the feeder transformer nominal power, regardless of the studied network.

5. To further investigate the practicality of the suggested approach, the proposed methodology has been applied on both meshed and radial 69-node test feeder, and the results are illustrated. Interestingly, studies showed that the effectiveness of the proposed controlling strategy in the standard distribution networks is roughly independent of the studied test system. In the case of meshed 69-node system, the suggested approach preserves its ability and superiority in reducing reactive power flow through the network electrical bottlenecks in comparison to the conventional strategy. However, the achieved hosting capacity in the meshed configuration (120% of the

system base power) is somehow lower than that of the radial feeder (129% of the system base power).

6. Stochastic assessment of the uncertain parameters is practised to improve the accuracy of the simulations. Most of the decentralized control approaches in the literature use simple resolution PV and load forecast. The proposed stochastic process will allow both customers and operators to understand the benefits of using more advanced techniques for the decentralized control of PVs. Following the detailed stochastic analysis, it is expected that the distribution system operators should also consider uncertainty in their decisions when assuming voltage control by inverters. This would further contribute to identify standards in the grid codes, suitable for higher PV penetration levels.

7. In future networks the customers are offered to have flexible control, like demand response, resulting to the popularity of decentralized control. Decentralized control provides several advantages such as, high efficiency, reduce the transmission & distribution grid losses, provide support to the local power grid and enhance the voltage profile. The communication between distributed controllers is also much more cost effective and promising from less computational burden.

Accordingly, the feeder hosting capacity is enhanced while equipment loadings remain in their permissible limits. Moreover, the network power loss is decreased due to the local reactive power management. Furthermore, the proposed approach provides superior coordination between the PV systems controller and the transformer feeder tap changing mechanism. Another important parameter is the voltage control speed, where the proposed methodology has an improved response time in comparison to the centralised control methods which use communication infrastructure. From this point of view, the proposed strategy is a flexible tool

to make a trade-off between various benefits. As a result, the proposed controller can enhance the resiliency of the system and provide additional capacity in the system to accommodate more penetration of DERs in the system.

6.2. Future Work

Future work will extend the developed formulation to consider the stochastic nature of the PV power and load demands in an active micro-grid network with other distributed generators and battery energy storages. With the future power system, there is a big importance to investigate the distribution network with the technical and economic aspects of flexibility in energy systems. Since the DERs have an impact on voltage profile and power flow direction, reliability decrease caused by dynamic connection/reconnection of individual DERs, this is also penetration reasoned impacts on ADNs. Another important component of the future ADNs is the energy storage devices. Next section will describe the further integration of inverter based generation, and their possible participation in future work. After that, the microgrid application will be elaborated.

6.2.1. Further integration of inverter based generation

In the presented PhD work, the focus intended to tackle the challenges of high penetration of PVs in distribution level. Considering the current challenges, the simulations were addressed by considering only PVs, in this study. However, it is obvious that the future power system will also heavily consist of more DERs in the distribution network [165]. In distribution level, in addition to PVs, there are also more generic DERs like WTs and BESSs. Further work is needed to understand the increased penetration effect of the DERs on the distribution level.

With the future low inertia scenario, there is a big importance to investigate the distribution network with the technical and economic aspects of flexibility in energy systems. Since the DERs have an impact on voltage profile and power flow direction, reliability decrease caused by dynamic connection/reconnection of individual DERs, this is also penetration reasoned impacts on microgrids. With the further integration of DERs into the distribution systems, the correlation between PVs and other DERs should also be taken into consideration.

6.2.1.1. Battery Energy Storage System

The energy storage systems can improve the operations of the network because this equipment gives the distribution network operators (DNOs) a solution for network upgrade deferral [166]. This deferral can be achieved through the coordination between storages and other renewable resources (e.g., PV systems). In this regard, numerous energy management strategies have been developed in the literature [36], [166], [167]. However, these management strategies were out of the scope of the PhD study. The superior performance of the proposed reactive power control strategy will be maintained considering other service providers, e.g. storage systems. The proposed controlling methodology is improved as much as necessary to achieve excellent results even without storage devices. Still, it is highly possible to investigate battery applications in future studies on the proposed method.

Aiming to increase the distribution network's hosting capacity, BESS may not be an economically viable solution [52]. Although having an individual BESS with PVs can cope with the overvoltage problem and improve the hosting capacity, it is complicated to coordinate them for voltage regulation and to integrate them in the ancillary service market. Because of the high investment cost of storage systems, some research focused on optimizing the size and place of a central BESS. To this end, an optimal sizing and placement method using a quadratic power control is deployed in [168]. A multi-variable non-linear constrained optimization

problem is solved for a central BESS in LV grids to improve the hosting capacity of rooftop PVs. It is concluded that a device that provides only reactive power control (e.g., D-STATCOM or thyristor-controlled reactor (TCR)) might improve the hosting capacity of distribution grids with much lower investment cost rather than a central BESS. Also another technical report showed that batteries with common self-consumption controllers do not contribute to the hosting capacity as they are unable to reduce peak PV generation [169].

On the other hand, the contributions from BESS can be both from the economic and technical aspects when there is not enough generation to meet the demand in the system. Economically, BESS can help the price trading when purchasing electricity during the period of low cost and then selling at a high cost. BESS can help to flatten and stabilise the PV generation output variations and can support the upstream network in case of insufficient capacity. It can also support the power quality and reliability improvement, providing provision to PV systems. To achieve the overall maximum fulfilment, the capacity of PVs and BESS need be co-optimised.

Evaluating the ideal location of the batteries along with the DERs, controllable loads and demand response is also critical in the LV distribution network. The impact of penetration levels of converter connected units in the distribution system should be also analysed under discrepant battery locations. Especially in case of largescale applications, battery storage systems can enhance the benefits from the integration of distributed energy sources, aid power quality management, and reduce distribution network expansion costs [51]. From this point of view, battery storage should be included in the future work of this study to meet the power needs of consumers reliably and economically. In the case of battery storages added to the system, the proposed voltage control strategy will be obviously needed to contribute to the reduction of the charge/discharge cycles of the battery, so that even larger levels of PV can be integrated with smaller battery capacities. When used together with proposed controller, the extra headroom would allow batteries to provide ancillary services at low cost. This brings the

proposed strategy to a technical and economical solutions for the advanced voltage control of ADNs.

6.2.2. Microgrid application

With the evolution of power grid towards non-synchronous generation, the inertia is more decoupled from the grid. As the rotational inertia decreases, the stability of the system also becomes more vulnerable to disturbances, generation losses. Hence, there is a need for extra support to preserve the strength of the new distribution system. The introduced control capabilities should allow microgrids already interconnected to the upstream network, also to operate when isolated from the main grid in case of faults or other external disturbances. Overall, the control application is the crucial feature that distinguishes microgrids from distribution networks with DERs.

A microgrid application study was presented in the authors work given in 1.4.3, and would be improved on future studies. Microgrids are capable of coordinating DERs and loads in a decentralised way without the need for a centralised scheme. Main challenges to be taken into account are the uncertainties due to unstable demand from loads and generation from renewable energy sources. The load profile varies with time and season. The future work microgrid studies are intended to focus on the evaluation of the effect of DERs' dynamic behaviours and frequency response following the islanded-mode and/or frequency excursion. In Appendix C, a practical European MV-LV network is demonstrated with the dynamics of the system. The main target is to observe the microgrid system under load increment and loss of generation events also with high penetration of DERs. The microgrid test system was modelled based on the CIGRE's "Benchmark Systems for Network Integration of Renewable and Distributed Energy Resources", [170].

Presented in Figure C-1, firstly a low-voltage (MV/LV) distribution microgrid system is presented. The 20 kV MV upstream network is converted to 0, 4 kV (LV) by 0.5 MVA rated power and 20/0.4 kV rated voltage transformer. The lines are modelled in two topology namely overhead and underground lines (all the parameters can be found in Appendix C). Grounding resistances are not applied to the system because a significant change isn't observed in the load flow analysis. The loads are in three models including residential, industrial and commercial loads. The bus/plate/pole representations are made as residential buses/plates from R0 to R18, industrial buses as I0, I1, I2 and commercial buses/ poles from C0 to C20. First of all the analyses are conducted under load flow analysis to see the systems steady state behaviour. Afterwards, the time domain RMS studies are conducted.

In grid connected mode, microgrid frequency is the same as that of the main grid, where in islanded mode the frequency regulation should be defined independently. In this case the integration of some additional control approaches like inertia emulation for the wind turbine, can increase the reference power to the turbine, which provides flexibility after the disturbance. Inertia emulators are designed to be deployed in wind energy conversion system for the sake of frequency support. Consequently, the kinetic energy stored in the wind turbine's shaft can be released following the frequency excursion in order to help frequency restoration process. The inertia emulator allows a rapid active power contribution by obtaining a high $\frac{dP}{dt}$, which makes a significant change. Inertia emulator will be added to the wind turbine dynamics to investigate the overall effects of injecting inertial power to the distribution network to help frequency restoration process. The inertia emulator can reduce the settling time and can decrease the frequency nadir of the system. In Figure C-2, the additional power support from the rotor is added to reference power value.

REFERENCES

[1] T. J. Tengku Hashim, A. Mohamed, and H. Shareef, “A review on voltage control methods for active distribution networks,” *Prz. Elektrotechniczny*, vol. 88, no. 6, pp. 304–312, 2012.

[2] F. Andrén, B. Bletterie, S. Kadam, P. Kotsampopoulos, and C. Bucher, “On the Stability of Local Voltage Control in Distribution Networks with a High Penetration of Inverter-Based Generation,” *IEEE Trans. Ind. Electron.*, vol. 62, no. 4, pp. 2519–2529, 2015, doi: 10.1109/TIE.2014.2345347.

[3] A. Ehsan and Q. Yang, “State-of-the-art techniques for modelling of uncertainties in active distribution network planning: A review,” *Applied Energy*, vol. 239. pp. 1509–1523, 2019, doi: 10.1016/j.apenergy.2019.01.211.

[4] National Grid, “System Operability Framework Executive Summary: Regional Trends and Insights,” 2018. [Online]. Available: https://www.nationalgrideso.com/sites/eso/files/documents/SOF Report- Regional Trends and Insights.pdf.

[5] IRENA, “Renewable Energy Capacity Highlights 31 March 2020,” *Irena*, vol. 00, no. March 2020, pp. 1–3, 2020, [Online]. Available: www.irena.org/publications.

[6] REN21, “Renewables 2020 Global Status Report,” 2020. [Online]. Available: http://www.ren21.net/resources/publications/.

[7] National Grid, “Future Energy Scenarios Navigation,” 2020. [Online]. Available: https://www.nationalgrideso.com/future-energy/future-energy-scenarios/fes-2020-documents.

[8] DIgSILENT, “PowerFactory 2020, User Manual,” Germany, 2020.

[9] A. Samadi, E. Shayesteh, R. Eriksson, B. Rawn, and L. Söder, “Multi-objective coordinated droop-based voltage regulation in distribution grids with PV systems,” *Renew. Energy*, vol. 71, pp. 315–323, 2014, doi: 10.1016/j.renene.2014.05.046.

[10] D. Wolter, M. Zdrallek, M. Stötzel, C. Schacherer, I. Mladenovic, and M. Biller, “Impact of meshed grid topologies on distribution grid planning and operation,” *CIRED - Open Access Proc. J.*, vol. 2017, no. 1, pp. 2338–2341, 2017, doi: 10.1049/oap-cired.2017.0708.

[11] National Grid, “System Operability Framework Summary,” *UK Electr. Transm.*, 2017, [Online]. Available: https://www.nationalgrideso.com/document/63476/download.

[12] K. Prakash, A. Lallu, F. R. Islam, and K. A. Mamun, “Review of Power System Distribution Network Architecture,” in *2016 3rd Asia-Pacific World Congress on Computer Science and Engineering (APWC on CSE)*, 2016, pp. 124–130, doi: 10.1109/APWC-on-CSE.2016.030.

[13] Á. Molina-García, R. A. Mastromauro, T. García-Sánchez, S. Pugliese, M. Liserre, and S. Stasi, “Reactive Power Flow Control for PV Inverters Voltage Support in LV Distribution Networks,” *IEEE Trans. Smart Grid*, vol. 8, no. 1, pp. 447–456, 2017,

doi: 10.1109/TSG.2016.2625314.

[14] E. Lakervi and E. J. Holmes, *A review of " Electricity Distribution Network Design ,"* Second Edi. IEE Power Series 21, 1996.

[15] G. Celli, F. Pilo, G. Pisano, V. Allegranza, R. Cicoria, and A. Iaria, "Meshed vs. radial MV distribution network in presence of large amount of DG," *2004 IEEE PES Power Syst. Conf. Expo.*, vol. 2, pp. 709–714, 2004, doi: 10.1109/psce.2004.1397664.

[16] F. R. Islam, K. Prakash, K. A. Mamun, A. Lallu, and H. R. Pota, "Aromatic network: A novel structure for power distribution system," *IEEE Access*, vol. 5, pp. 25236–25257, 2017, doi: 10.1109/ACCESS.2017.2767037.

[17] R. Tonkoski, L. A. C. Lopes, and T. H. M. El-Fouly, "Coordinated Active Power Curtailment of Grid Connected PV Inverters for Overvoltage Prevention," *IEEE Trans. Sustain. Energy*, vol. 2, no. 2, pp. 139–147, 2011, doi: 10.1109/TSTE.2010.2098483.

[18] N. Mahmud and A. Zahedi, "Review of control strategies for voltage regulation of the smart distribution network with high penetration of renewable distributed generation," *Renew. Sustain. Energy Rev.*, vol. 64, pp. 582–595, 2016, doi: 10.1016/j.rser.2016.06.030.

[19] S. J. Kang, J. Kim, J. W. Park, and S. M. Baek, "Reactive power management based on voltage sensitivity analysis of distribution system with high penetration of renewable energies," *Energies*, vol. 12, no. 8, 2019, doi: 10.3390/en12081493.

[20] P. Kotsampopoulos, N. Hatziargyriou, B. Bletterie, and G. Lauss, "Review, analysis and recommendations on recent guidelines for the provision of ancillary services by Distributed Generation," in *2013 IEEE International Workshop on Inteligent Energy Systems (IWIES)*, 2013, pp. 185–190, doi: 10.1109/IWIES.2013.6698583.

[21] Y. P. Agalgaonkar, B. C. Pal, and R. A. Jabr, "Voltage Control in Distribution System Considering the Impact of PV Generation using MPPT Controller on Tap Changers and Autonomous Regulators," *IEEE Trans. Power Syst.*, vol. 29, no. 1, pp. 1–10, 2016, [Online]. Available: http://www.ijatir.org/uploads/356214IJATIR12904-660.pdf.

[22] T. Stetz, F. Marten, and M. Braun, "Improved Low Voltage Grid-Integration of Photovoltaic Systems in Germany," *IEEE Trans. Sustain. Energy*, vol. 4, no. 2, pp. 534–542, 2013, doi: 10.1109/TSTE.2012.2198925.

[23] A. M. M. Nour, A. Y. Hatata, A. A. Helal, and M. M. El-Saadawi, "Review on voltage-violation mitigation techniques of distribution networks with distributed rooftop PV systems," *IET Generation, Transmission and Distribution*, vol. 14, no. 3. pp. 349–361, 2020, doi: 10.1049/iet-gtd.2019.0851.

[24] M. Selcen Ayaz, M. Malekpour, R. Azizipanah-Abarghooee, and V. Terzija, "Local photovoltaic reactive power controller for increasing active distribution networks hosting capacity," *IET Gener. Transm. Distrib.*, vol. 14, no. 22, pp. 5152 –5162, Sep. 2020, doi: 10.1049/iet-gtd.2020.0649.

[25] M. H. J. Bollen and S. K. Rönnberg, "Hosting capacity of the power grid for renewable electricity production and new large consumption equipment," *Energies*, 2017, doi: 10.3390/en10091325.

[26] S. E. Razavi *et al.*, “Impact of distributed generation on protection and voltage regulation of distribution systems: A review,” *Renew. Sustain. Energy Rev.*, vol. 105, no. February, pp. 157–167, 2019, doi: 10.1016/j.rser.2019.01.050.

[27] M. M. Haque and P. Wolfs, “A review of high PV penetrations in LV distribution networks: Present status, impacts and mitigation measures,” *Renew. Sustain. Energy Rev.*, vol. 62, pp. 1195–1208, 2016, doi: 10.1016/j.rser.2016.04.025.

[28] K. De Brabandere, B. Bolsens, J. Van Den Keybus, A. Woyte, J. Driesen, and R. Belmans, “A voltage and frequency droop control method for parallel inverters,” *PESC Rec. - IEEE Annu. Power Electron. Spec. Conf.*, vol. 4, no. 4, pp. 2501–2507, 2004, doi: 10.1109/PESC.2004.1355222.

[29] Z. Wang, H. Chen, J. Wang, and M. Begovic, “Inverter-less hybrid voltage/var control for distribution circuits with photovoltaic generators,” *IEEE Trans. Smart Grid*, vol. 5, no. 6, pp. 2718–2728, 2014, doi: 10.1109/TSG.2014.2324569.

[30] D. Mende, Y. Fawzy, D. Premm, and S. Stevens, “Increasing the Hosting Capacity of Distribution Networks for Distributed Generation Using Reactive Power Control - Potentials and Limits,” Nov. 2012.

[31] J. Hossain and H. R. Pota, *Robust Control for Grid Voltage Stability: High Penetration of Renewable Energy*, vol. 1987. 2014.

[32] N. Karthikeyan, B. R. Pokhrel, J. R. Pillai, and B. Bak-Jensen, “Coordinated voltage control of distributed PV inverters for voltage regulation in low voltage distribution networks,” *2017 IEEE PES Innov. Smart Grid Technol. Conf. Eur. ISGT-Europe 2017 - Proc.*, vol. 2018-Janua, no. i, pp. 1–6, 2018, doi: 10.1109/ISGTEurope.2017.8260279.

[33] A. M. Garcia, R. A. Mastromauro, and M. Liserre, “A combined centralized/decentralized voltage regulation method for PV inverters in LV distribution networks,” *IEEE Power Energy Soc. Gen. Meet.*, vol. 2014-Octob, no. October, pp. 0–4, 2014, doi: 10.1109/PESGM.2014.6938817.

[34] N. Karthikeyan, B. R. Pokhrel, J. R. Pillai, and B. Bak-Jensen, “Coordinated voltage control of distributed PV inverters for voltage regulation in low voltage distribution networks,” in *2017 IEEE PES Innovative Smart Grid Technologies Conference Europe (ISGT-Europe)*, 2017, pp. 1–6, doi: 10.1109/ISGTEurope.2017.8260279.

[35] L. Wang, F. Bai, R. Yan, and T. K. Saha, “Real-Time Coordinated Voltage Control of PV Inverters and Energy Storage for Weak Networks With High PV Penetration,” *IEEE Trans. Power Syst.*, vol. 33, no. 3, pp. 3383–3395, 2018, doi: 10.1109/TPWRS.2018.2789897.

[36] M. Zeraati, M. E. H. Golshan, and J. M. Guerrero, “Distributed Control of Battery Energy Storage Systems for Voltage Regulation in Distribution Networks With High PV Penetration,” *IEEE Trans. Smart Grid*, vol. 9, no. 4, pp. 3582–3593, 2018, doi: 10.1109/TSG.2016.2636217.

[37] A. Mohamed and T. J. Tengku Hashim, “Coordinated Voltage Control in Active Distribution Networks -,” in *Electric Distribution Network Management and Control*, A. Arefi, F. Shahnia, and G. Ledwich, Eds. Singapore: Springer Singapore, 2018, pp.

85–109.

[38] T. Senjyu, Y. Miyazato, A. Yona, N. Urasaki, and T. Funabashi, “Optimal distribution voltage control and coordination with distributed generation,” *IEEE Trans. Power Deliv.*, vol. 23, no. 2, pp. 1236–1242, 2008, doi: 10.1109/TPWRD.2007.908816.

[39] N. Nimpitiwan and N. C. Chaiyabut, “Centralized control of system voltage/reactive power using genetic algorithm,” 2007, doi: 10.1109/ISAP.2007.4441598.

[40] A. G. Madureira and J. A. Peças Lopes, “Coordinated voltage support in distribution networks with distributed generation and microgrids,” *IET Renew. Power Gener.*, vol. 3, no. 4, pp. 439–454, 2009, doi: 10.1049/iet-rpg.2008.0064.

[41] E. Demirok, P. C. González, K. H. B. Frederiksen, D. Sera, P. Rodriguez, and R. Teodorescu, “Local reactive power control methods for overvoltage prevention of distributed solar inverters in low-voltage grids,” *IEEE J. Photovoltaics*, vol. 1, no. 2, pp. 174–182, 2011, doi: 10.1109/JPHOTOV.2011.2174821.

[42] J. Ishaq, Y. T. Fawzy, T. Buelo, B. Engel, and R. Witzmann, “Voltage control strategies of low voltage distribution grids using photovoltaic systems,” *2016 IEEE Int. Energy Conf. ENERGYCON 2016*, pp. 1–7, 2016, doi: 10.1109/ENERGYCON.2016.7513881.

[43] S. Hashemi and J. Østergaard, “Efficient Control of Energy Storage for Increasing the PV Hosting Capacity of LV Grids,” *IEEE Trans. Smart Grid*, vol. 9, no. 3, pp. 2295–2303, 2018, doi: 10.1109/TSG.2016.2609892.

[44] G. Wang *et al.*, “A Review of Power Electronics for Grid Connection of Utility-Scale Battery Energy Storage Systems,” *IEEE Trans. Sustain. Energy*, vol. 7, no. 4, pp. 1778–1790, 2016, doi: 10.1109/TSTE.2016.2586941.

[45] J. C. Vasquez, R. Mastromauro, J. Guerrero, and M. Liserre, “Voltage Support Provided by a Droop-Controlled Multifunctional Inverter,” *Ind. Electron. IEEE Trans.*, vol. 56, pp. 4510–4519, Dec. 2009, doi: 10.1109/TIE.2009.2015357.

[46] K. Turitsyn, P. Sulc, S. Backhaus, and M. Chertkov, “Distributed control of reactive power flow in a radial distribution circuit with high photovoltaic penetration,” *IEEE PES Gen. Meet. PES 2010*, no. June 2014, 2010, doi: 10.1109/PES.2010.5589663.

[47] D. L. Schultis, “Comparison of local volt/var control strategies for PV hosting capacity enhancement of low voltage feeders,” *Energies*, vol. 12, no. 8, 2019, doi: 10.3390/en12081560.

[48] K. W. Joung, T. Kim, and J. W. Park, “Decoupled frequency and voltage control for stand-alone microgrid with high renewable penetration,” *IEEE Trans. Ind. Appl.*, vol. 55, no. 1, pp. 122–133, 2019, doi: 10.1109/TIA.2018.2866262.

[49] M. Yazdanian and A. Mehrizi-Sani, “Distributed control techniques in microgrids,” *IEEE Trans. Smart Grid*, vol. 5, no. 6, pp. 2901–2909, 2014, doi: 10.1109/TSG.2014.2337838.

[50] “Studie zur Ermittlung der Technischen Mindesterzeugung des Konventionellen Kraftwerksparks zur Gewährleistung der Systemstabilität in den Deutschen Übertragungsnetzen bei Hoher Einspeisung aus Erneuerbaren Energien,” 2012.

[51] M. Yekini Suberu, M. Wazir Mustafa, and N. Bashir, “Energy storage systems for renewable energy power sector integration and mitigation of intermittency,” *Renew. Sustain. Energy Rev.*, vol. 35, pp. 499–514, 2014, doi: https://doi.org/10.1016/j.rser.2014.04.009.

[52] C. Parthasarathy, H. Hafezi, H. Laaksonen, and K. Kauhaniemi, “Modelling and simulation of hybrid PV BES systems as flexible resources in smartgrids - Sundom smart grid case,” 2019, doi: 10.1109/PTC.2019.8810579.

[53] S. Alyami, Y. Wang, C. Wang, J. Zhao, and B. Zhao, “Adaptive real power capping method for fair overvoltage regulation of distribution networks with high penetration of PV systems,” *IEEE Trans. Smart Grid*, 2014, doi: 10.1109/TSG.2014.2330345.

[54] P. Jahangiri and D. C. Aliprantis, “Distributed Volt/VAr control by PV inverters,” *IEEE Trans. Power Syst.*, 2013, doi: 10.1109/TPWRS.2013.2256375.

[55] E. Dall’Anese, S. V. Dhople, and G. B. Giannakis, “Optimal dispatch of photovoltaic inverters in residential distribution systems,” *IEEE Trans. Sustain. Energy*, 2014, doi: 10.1109/TSTE.2013.2292828.

[56] A. Nassif and X. Long, “Mitigating overvoltage scenarios caused by large penetration of distributed energy resources,” 2016, doi: 10.1109/EPEC.2016.7771699.

[57] R. Azizipanah, “Wide - Area Monitoring based Smart Frequency Control in Future Low - Variable Inertia Systems with CCGT / Wind / PV / BES / Load A Thesis submitted to the University of Manchester for the degree of in the Faculty of Science & Engineering Rasoul Azizipanah,” 2018.

[58] K. E. Antoniadou-Plytaria, I. N. Kouveliotis-Lysikatos, P. S. Georgilakis, and N. D. Hatziargyriou, “Distributed and Decentralized Voltage Control of Smart Distribution Networks: Models, Methods, and Future Research,” *IEEE Trans. Smart Grid*, vol. 8, no. 6, pp. 2999–3008, 2017, doi: 10.1109/TSG.2017.2679238.

[59] G. Mokhtari, G. Nourbakhsh, and A. Ghosh, “Smart Coordination of Energy Storage Units (ESUs) for Voltage and Loading Management in Distribution Networks,” *IEEE Trans. Power Syst.*, vol. 28, no. 4, pp. 4812–4820, 2013, doi: 10.1109/TPWRS.2013.2272092.

[60] F. Olivier, P. Aristidou, D. Ernst, and T. Van Cutsem, “Active Management of Low-Voltage Networks for Mitigating Overvoltages Due to Photovoltaic Units,” *IEEE Trans. Smart Grid*, 2016, doi: 10.1109/TSG.2015.2410171.

[61] A. Andreotti, A. Petrillo, S. Santini, A. Vaccaro, and D. Villacci, “A decentralized architecture based on cooperative dynamic agents for online voltage regulation in smart grids,” *Energies*, vol. 12, no. 7, 2019, doi: 10.3390/en12071386.

[62] G. C. Kryonidis, C. S. Demoulias, and G. K. Papagiannis, “A new voltage control scheme for active medium-voltage (MV) networks,” *Electric Power Systems Research*, vol. 169. pp. 53–64, 2019, doi: 10.1016/j.epsr.2018.12.014.

[63] J. Ding, Q. Zhang, S. Hu, Q. Wang, and Q. Ye, “Clusters partition and zonal voltage regulation for distribution networks with high penetration of PVs,” *IET Gener. Transm. Distrib.*, 2018, doi: 10.1049/iet-gtd.2018.6255.

[64] J. Von Appen, T. Stetz, M. Braun, and A. Schmiegel, “Local voltage control strategies for PV storage systems in distribution grids,” *IEEE Trans. Smart Grid*, vol. 5, no. 2, pp. 1002–1009, 2014, doi: 10.1109/TSG.2013.2291116.

[65] X. Huang, H. Liu, B. Zhang, J. Wang, and X. Xu, “Research on local voltage control strategy based on high-penetration distributed PV systems,” *J. Eng.*, vol. 2019, no. 18, pp. 5044–5048, 2019, doi: 10.1049/joe.2018.9245.

[66] H. Zhu and H. J. Liu, “Fast local voltage control under limited reactive power: Optimality and stability analysis,” *IEEE Trans. Power Syst.*, 2016, doi: 10.1109/TPWRS.2015.2504419.

[67] A. Einfalt, F. Zeilinger, R. Schwalbe, B. Bletterie, and S. Kadam, “Controlling active low voltage distribution grids with minimum efforts on costs and engineering,” 2013, doi: 10.1109/IECON.2013.6700374.

[68] H. G. Yeh, D. F. Gayme, and S. H. Low, “Adaptive VAR control for distribution circuits with photovoltaic generators,” *IEEE Trans. Power Syst.*, vol. 27, no. 3, pp. 1656–1663, 2012, doi: 10.1109/TPWRS.2012.2183151.

[69] A. Singhal, V. Ajjarapu, J. C. Fuller, and J. Hansen, “Real-Time Local Volt/VAR Control Under External Disturbances with High PV Penetration,” *IEEE Trans. Smart Grid*, vol. 3053, no. c, pp. 1–11, 2018, doi: 10.1109/TSG.2018.2840965.

[70] A. Samadi, L. Soder, E. Shayesteh, and R. Eriksson, “Static Equivalent of Distribution Grids With High Penetration of PV Systems,” *IEEE Trans. Smart Grid*, vol. 6, no. 4, pp. 1763–1774, 2015, doi: 10.1109/TSG.2015.2399333.

[71] N. Prabaharan, A. Rini Ann Jerin, E. Najafi, and K. Palanisamy, “‘6 - An overview of control techniques and technical challenge for inverters in micro grid,’” in *Woodhead Publishing Series in Energy*, Woodhead Publishing, 2018, pp. 97–107.

[72] A. T. Procopiou, “Active management of PV-rich low voltage networks,” p. 199, 2017.

[73] F. Zhang *et al.*, “The reactive power voltage control strategy of PV systems in low-voltage string lines,” 2017, doi: 10.1109/PTC.2017.7980995.

[74] M. Braun, T. Stetz, T. Reimann, B. Valov, and G. Arnold, “Optimal Reactive Power Supply in Distribution Networks - Technological and Economic Assessment for PV-Systems,” *Pvsec2009*, 2009, doi: 10.4229/24thEUPVSEC2009-5AO.7.5.

[75] P. S. Georgilakis and N. D. Hatziargyriou, “A review of power distribution planning in the modern power systems era: Models, methods and future research,” *Electr. Power Syst. Res.*, vol. 121, pp. 89–100, 2015, doi: 10.1016/j.epsr.2014.12.010.

[76] A. Krishnan and R. P. Broadwater, “Robustness and Stability Analysis with a Heavily-Meshed Distribution Network Robustness and Stability Analysis with a Heavily-Meshed Distribution Network,” 2019.

[77] M. A. Shuvra and B. Chowdhury, “Reconfigurable and flexible voltage control strategy using smart PV inverters with integrated energy storage for advanced distribution systems,” *IET Smart Grid*, 2020, doi: 10.1049/iet-stg.2019.0018.

[78] M. N. I. Sarkar, L. G. Meegahapola, and M. Datta, “Reactive power management in renewable rich power grids: A review of grid-codes, renewable generators, support devices, control strategies and optimization Algorithms,” *IEEE Access*, vol. 6, pp. 41458–41489, 2018, doi: 10.1109/ACCESS.2018.2838563.

[79] Y. P. Agalgaonkar, B. C. Pal, and R. A. Jabr, “Distribution voltage control considering the impact of PV generation on tap changers and autonomous regulators,” *IEEE Trans. Power Syst.*, 2014, doi: 10.1109/TPWRS.2013.2279721.

[80] E. Demirok, P. C. González, K. H. B. Frederiksen, D. Sera, P. Rodriguez, and R. Teodorescu, “Local reactive power control methods for overvoltage prevention of distributed solar inverters in low-voltage grids,” *IEEE J. Photovoltaics*, vol. 1, no. 2, pp. 174–182, 2011, doi: 10.1109/JPHOTOV.2011.2174821.

[81] National Grid Electricity System Operator, “The Grid Code (Uk),” no. 5, pp. 0–1014, 2020.

[82] British Standard Institution, “BS EN 50160:2010+A1:2015 Voltage characteristics of electricity supplied by public electricity networks,” 2010.

[83] UK Statutory Instruments, *The electricity safety, quality and continuity regulations 2002*. 2002.

[84] California ISO, “Energy and environmental goals drive change,” *Tech. Rep.*, p. 4, 2016, [Online]. Available: www.caiso.com.

[85] E. P. Systems and V. Ratings, “ANSI C84.1-2006 American National Standard,” *Power*, 2006.

[86] X. Yingcheng and T. Nengling, “Review of contribution to frequency control through variable speed wind turbine,” *Renew. Energy*, vol. 36, no. 6, pp. 1671–1677, 2011, doi: 10.1016/j.renene.2010.11.009.

[87] E.ON Netz GmbH, “Grid connection regulations for high and extra high voltage,” 2006.

[88] M. Mohseni and S. M. Islam, “Review of international grid codes for wind power integration: Diversity, technology and a case for global standard,” *Renew. Sustain. Energy Rev.*, vol. 16, no. 6, pp. 3876–3890, Aug. 2012, doi: 10.1016/j.rser.2012.03.039.

[89] B. Noone, “PV Integration On Australian Distribution Networks,” no. September, 2013, [Online]. Available: http://apvi.org.au/wp-content/uploads/2013/12/APVA-PV-and-DNSP-Literature-review-September-2013.pdf.

[90] T. Stetz, F. Marten, and M. Braun, “Improved low voltage grid-integration of photovoltaic systems in Germany,” *IEEE Trans. Sustain. Energy*, vol. 4, no. 2, pp. 534–542, 2013, doi: 10.1109/TSTE.2012.2198925.

[91] A. Samadi, R. Eriksson, L. Söder, B. G. Rawn, and J. C. Boemer, “Coordinated Active Power-Dependent Voltage Regulation in Distribution Grids With PV Systems,” *IEEE Trans. Power Deliv.*, vol. 29, no. 3, pp. 1454–1464, 2014, doi: 10.1109/TPWRD.2014.2298614.

[92] O. H. Abdalla and A. A. A. Mostafa, “Technical Requirements for Connecting Solar Power Plants to Electricity Networks,” in *Innovation in Energy Systems - New Technologies for Changing Paradigms*, 2019, p. 13.

[93] M. Knudsen, “The Path to 25% Silicon Solar Cell Efficiency: History of Silicon Cell Evolution,” *Prog. Photovoltaics Res. Appl.*, vol. 17, no. November 2011, pp. 183–189, 2011, doi: 10.1002/pip.

[94] SMA, “Solar Inverters,” 2020. .

[95] Verband der Elektrotechnik, “Generators connected to the LV distribution network-technical requirements for the connection to and parallel operation with low-voltage distribution networks, VDE-AR-N 4105,” 2011. https://www.vde-verlag.de/standards/0100492/vde-ar-n-4105-anwendungsregel-2018-11.html (accessed Aug. 28, 2020).

[96] J. Hu, Z. Li, J. Zhu, and J. M. Guerrero, “Voltage Stabilization: A Critical Step Toward High Photovoltaic Penetration,” *IEEE Ind. Electron. Mag.*, 2019, doi: 10.1109/MIE.2019.2906844.

[97] M. Karimi, H. Mokhlis, K. Naidu, S. Uddin, and A. H. A. Bakar, “Photovoltaic penetration issues and impacts in distribution network - A review,” *Renew. Sustain. Energy Rev.*, vol. 53, pp. 594–605, 2016, doi: 10.1016/j.rser.2015.08.042.

[98] S. Hashemi and J. Østergaard, “Methods and strategies for overvoltage prevention in low voltage distribution systems with PV,” *IET Renewable Power Generation*. 2017, doi: 10.1049/iet-rpg.2016.0277.

[99] Energinet, “Ancillary Services From New Technologies Technical Potentials and Market Integration,” no. December, 2019.

[100] C. Xiao, B. Zhao, M. Ding, Z. Li, and X. Ge, “Zonal voltage control combined day-ahead scheduling and real-time control for distribution networks with high proportion of PVs,” *Energies*, 2017, doi: 10.3390/en10101464.

[101] Y. Xu, W. Jiang, and X. Cheng, “Partitioning for reactive voltage based on spectral clustering and pilot nodes selection,” *Dianli Xitong Baohu yu Kongzhi/Power Syst. Prot. Control*, 2016, doi: 10.7667/PSPC160052.

[102] E. E. Pompodakis, I. A. Drougakis, I. S. Lelis, and M. C. Alexiadis, “Photovoltaic systems in low-voltage networks and overvoltage correction with reactive power control,” *IET Renew. Power Gener.*, 2016, doi: 10.1049/iet-rpg.2014.0282.

[103] M. Bollen and F. Hassan, *Integration of Distributed Generation in the Power System*. 2011.

[104] A. Dukpa, I. Duggal, B. Venkatesh, and L. Chang, “Optimal participation and risk mitigation of wind generators in an electricity market,” *IET Renew. Power Gener.*, 2010, doi: 10.1049/iet-rpg.2009.0016.

[105] A. Azizivahed, M. Barani, S. E. Razavi, S. Ghavidel, L. Li, and J. Zhang, “Energy storage management strategy in distribution networks utilised by photovoltaic resources,” *IET Gener. Transm. Distrib.*, 2018, doi: 10.1049/iet-gtd.2018.5221.

[106] A. Procopiou and K. Petrou, “Advanced Planning of PV-Rich Distribution Networks Deliverable 3: Traditional Solutions,” no. February, pp. 1–95, 2020.

[107] L. F. Ochoa, A. Keane, and G. P. Harrison, “Minimizing the reactive support for distributed generation: Enhanced passive operation and smart distribution networks,” *IEEE Trans. Power Syst.*, 2011, doi: 10.1109/TPWRS.2011.2122346.

[108] P. N. Vovos and J. W. Bialek, “Direct incorporation of fault level constraints in optimal power flow as a tool for network capacity analysis,” *IEEE Trans. Power Syst.*, 2005, doi: 10.1109/TPWRS.2005.856975.

[109] C. J. Dent, L. F. Ochoa, G. P. Harrison, and J. W. Bialek, “Efficient secure AC OPF for network generation capacity assessment,” *IEEE Trans. Power Syst.*, 2010, doi: 10.1109/TPWRS.2009.2036809.

[110] R. Bacher, “Power System Models, Objectives and Constraints in Optimal Power Flow Calculations,” *Optim. Plan. Oper. Electr. Power Syst.*, pp. 217–263, 1993, doi: 10.1007/978-3-662-12646-2_8.

[111] W. Zheng, W. Wu, B. Zhang, H. Sun, and Y. Liu, “A Fully Distributed Reactive Power Optimization and Control Method for Active Distribution Networks,” *IEEE Trans. Smart Grid*, vol. 7, no. 2, pp. 1021–1033, 2016, doi: 10.1109/TSG.2015.2396493.

[112] Y. Chai, L. Guo, C. Wang, Z. Zhao, X. Du, and J. Pan, “Network Partition and Voltage Coordination Control for Distribution Networks With High Penetration of Distributed PV Units,” *IEEE Trans. Power Syst.*, vol. 33, no. 3, pp. 3396–3407, 2018, doi: 10.1109/TPWRS.2018.2813400.

[113] B. Zhao, Z. Xu, C. Xu, C. Wang, and F. Lin, “Network Partition-Based Zonal Voltage Control for Distribution Networks with Distributed PV Systems,” *IEEE Trans. Smart Grid*, vol. 9, no. 5, pp. 4087–4098, 2018, doi: 10.1109/TSG.2017.2648779.

[114] F. Zheng, M. Ding, and J. Zhang, “Modelling and simulation of grid-connected PV system in DIgSILENT/PowerFactory,” in *IET Conference Publications*, 2013, vol. 2013, no. 623 CP, pp. 1–6, doi: 10.1049/cp.2013.1867.

[115] M. Aien, M. Rashidinejad, and M. Fotuhi-Firuzabad, “On possibilistic and probabilistic uncertainty assessment of power flow problem: A review and a new approach,” *Renewable and Sustainable Energy Reviews*. 2014, doi: 10.1016/j.rser.2014.05.063.

[116] EPRI, “Practical Guidance on the Use of Probabilistic Risk Assessment in Risk-Informed Applications with a Focus on the Treatment of Uncertainty,” 2012.

[117] Q. P. Zheng, J. Wang, and A. L. Liu, “Stochastic Optimization for Unit Commitment—A Review,” *IEEE Trans. Power Syst.*, vol. 30, no. 4, pp. 1913–1924, 2015, doi: 10.1109/TPWRS.2014.2355204.

[118] W. El-Khattam, Y. G. Hegazy, and M. M. A. Salama, “Investigating distributed generation systems performance using Monte Carlo simulation,” *IEEE Trans. Power Syst.*, 2006, doi: 10.1109/TPWRS.2006.873131.

[119] J. A. Martinez and G. Guerra, “A parallel Monte Carlo method for optimum allocation

of distributed generation," *IEEE Trans. Power Syst.*, 2014, doi: 10.1109/TPWRS.2014.2317285.

[120] G. Carpinelli, P. Caramia, and P. Varilone, "Multi-linear Monte Carlo simulation method for probabilistic load flow of distribution systems with wind and photovoltaic generation systems," *Renew. Energy*, 2015, doi: 10.1016/j.renene.2014.11.028.

[121] M. Rossi, G. Vigano, D. Moneta, and D. Clerici, "Stochastic evaluation of distribution network hosting capacity: Evaluation of the benefits introduced by smart grid technology," 2017, doi: 10.23919/AEIT.2017.8240490.

[122] A. Navarro-Espinosa and L. F. Ochoa, "Probabilistic Impact Assessment of Low Carbon Technologies in LV Distribution Systems," *IEEE Trans. Power Syst.*, 2016, doi: 10.1109/TPWRS.2015.2448663.

[123] J. Xiao, Y. Li, X. Qiao, Y. Tan, Y. Cao, and L. Jiang, "Enhancing Hosting Capacity of Uncertain and Correlated Wind Power in Distribution Network With ANM Strategies," *IEEE Access*, 2020, doi: 10.1109/access.2020.3030705.

[124] M. Deakin, C. Crozier, D. Apostolopoulou, T. Morstyn, and M. McCulloch, "Stochastic hosting capacity in LV distribution networks," *arXiv*. 2019.

[125] J. Wang, M. Shahidehpour, and Z. Li, "Security-Constrained Unit Commitment With Volatile Wind Power Generation," *IEEE Trans. Power Syst.*, vol. 23, pp. 1319–1327, 2008.

[126] F. J. Ruiz-Rodriguez, J. C. Hernández, and F. Jurado, "Probabilistic load flow for radial distribution networks with photovoltaic generators," *IET Renew. Power Gener.*, vol. 6, no. 2, pp. 110–121, 2012, doi: 10.1049/iet-rpg.2010.0180.

[127] Y. Guo, Y. Fang, and P. P. Khargonekar, "Risk-Constrained Optimal Energy Management for Smart Microgrids BT - Stochastic Optimization for Distributed Energy Resources in Smart Grids," Y. Guo, Y. Fang, and P. P. Khargonekar, Eds. Cham: Springer International Publishing, 2017, pp. 57–73.

[128] S. Talari, M. Yazdaninejad, and M. R. Haghifam, "Stochastic-based scheduling of the microgrid operation including wind turbines, photovoltaic cells, energy storages and responsive loads," *IET Gener. Transm. Distrib.*, 2015, doi: 10.1049/iet-gtd.2014.0040.

[129] H. Heitsch and W. Römisch, "Scenario reduction algorithms in stochastic programming," *Comput. Optim. Appl.*, 2003, doi: 10.1023/A:1021805924152.

[130] A. Alarcon-Rodriguez, G. Ault, and S. Galloway, "Multi-objective planning of distributed energy resources: A review of the state-of-the-art," *Renewable and Sustainable Energy Reviews*. 2010, doi: 10.1016/j.rser.2010.01.006.

[131] M. Mazidi, A. Zakariazadeh, S. Jadid, and P. Siano, "Integrated scheduling of renewable generation and demand response programs in a microgrid," *Energy Convers. Manag.*, vol. 86, pp. 1118–1127, 2014, doi: 10.1016/j.enconman.2014.06.078.

[132] R. Zárate-Miñano, M. Anghel, and F. Milano, "Continuous wind speed models based on stochastic differential equations," *Appl. Energy*, vol. 104, pp. 42–49, 2013, doi: 10.1016/j.apenergy.2012.10.064.

[133] M. Ghofrani, A. Arabali, M. Etezadi-Amoli, and M. S. Fadali, “A framework for optimal placement of energy storage units within a power system with high wind penetration,” *IEEE Trans. Sustain. Energy*, vol. 4, no. 2, pp. 434–442, 2013, doi: 10.1109/TSTE.2012.2227343.

[134] B. Stephen, A. J. Mutanen, S. Galloway, G. Burt, and P. Jarventausta, “Enhanced load profiling for residential network customers,” *IEEE Trans. Power Deliv.*, vol. 29, no. 1, pp. 88–96, 2014, doi: 10.1109/TPWRD.2013.2287032.

[135] K. N. Hasan, R. Preece, and J. V. Milanović, “Existing approaches and trends in uncertainty modelling and probabilistic stability analysis of power systems with renewable generation,” *Renewable and Sustainable Energy Reviews*. 2019, doi: 10.1016/j.rser.2018.10.027.

[136] A. Saberian, H. Hizam, M. A. M. Radzi, M. Z. A. Ab Kadir, and M. Mirzaei, “Modelling and prediction of photovoltaic power output using artificial neural networks,” *Int. J. Photoenergy*, 2014, doi: 10.1155/2014/469701.

[137] S. . Sulaiman, R. . Abdul, and I. Musirin, “Partial Evolutionary ANN for Output Prediction of a Grid-Connected Photovoltaic System,” *Int. J. Comput. Electr. Eng.*, 2009, doi: 10.7763/ijcee.2009.v1.7.

[138] Y. K. Wu, C. R. Chen, and H. Abdul Rahman, “A novel hybrid model for short-term forecasting in PV power generation,” *Int. J. Photoenergy*, 2014, doi: 10.1155/2014/569249.

[139] M. Q. Raza, M. Nadarajah, and C. Ekanayake, “On recent advances in PV output power forecast,” *Solar Energy*. 2016, doi: 10.1016/j.solener.2016.06.073.

[140] A. Bracale, G. Carpinelli, and P. De Falco, “A Probabilistic Competitive Ensemble Method for Short-Term Photovoltaic Power Forecasting,” *IEEE Trans. Sustain. Energy*, 2017, doi: 10.1109/TSTE.2016.2610523.

[141] M. J. Sanjari and H. B. Gooi, “Probabilistic Forecast of PV Power Generation Based on Higher Order Markov Chain,” *IEEE Trans. Power Syst.*, 2017, doi: 10.1109/TPWRS.2016.2616902.

[142] R. H. Inman, H. T. C. Pedro, and C. F. M. Coimbra, “Solar forecasting methods for renewable energy integration,” *Progress in Energy and Combustion Science*. 2013, doi: 10.1016/j.pecs.2013.06.002.

[143] D. W. van der Meer, J. Widén, and J. Munkhammar, “Review on probabilistic forecasting of photovoltaic power production and electricity consumption,” *Renewable and Sustainable Energy Reviews*. 2018, doi: 10.1016/j.rser.2017.05.212.

[144] T. Niknam, R. Azizipanah-Abarghooee, and M. R. Narimani, “An efficient scenario-based stochastic programming framework for multi-objective optimal micro-grid operation,” *Appl. Energy*, 2012, doi: 10.1016/j.apenergy.2012.04.017.

[145] K. P. Kumar and B. Saravanan, “Recent techniques to model uncertainties in power generation from renewable energy sources and loads in microgrids – A review,” *Renewable and Sustainable Energy Reviews*. 2017, doi: 10.1016/j.rser.2016.12.063.

[146] M. Barukčić, Hederić, M. Hadžiselimović, and S. Seme, “A simple stochastic method

for modelling the uncertainty of photovoltaic power production based on measured data," *Energy*, 2018, doi: 10.1016/j.energy.2018.09.134.

[147] R. Singh, B. C. Pal, and R. A. Jabr, "Statistical representation of distribution system loads using Gaussian mixture model," *IEEE Trans. Power Syst.*, vol. 25, no. 1, pp. 29–37, 2010, doi: 10.1109/TPWRS.2009.2030271.

[148] P. Chakraborty, M. Marwah, M. Arlitt, and N. Ramakrishnan, "Fine-grained photovoltaic output prediction using a Bayesian ensemble," in *Proceedings of the National Conference on Artificial Intelligence*, 2012, vol. 1, pp. 274–280, [Online]. Available: https://www.scopus.com/inward/record.uri?eid=2-s2.0-84868273830&partnerID=40&md5=ee58a227aefb38f25ea371f7e2d6bac2.

[149] L. Holmes, B. Illowsky, and S. Dean, *Introductory Business Statistics*. Minneapolis, MN: Open Textbook Library, 2017.

[150] MATLAB, "Incomplete beta function," 2006. https://uk.mathworks.com/help/matlab/ref/betainc.html.

[151] L. Wu, M. Shahidehpour, and T. Li, "Stochastic security-constrained unit commitment," *IEEE Trans. Power Syst.*, 2007, doi: 10.1109/TPWRS.2007.894843.

[152] S. Abedi, G. Hossein, S. Hossein, and M. Farhadkhani, "Improved Stochastic Modeling: An Essential Tool for Power System Scheduling in the Presence of Uncertain Renewables," in *New Developments in Renewable Energy*, 2013.

[153] J. Dupačová, N. Gröwe-Kuska, and W. Römisch, "Scenario reduction in stochastic programming An approach using probability metrics," *Math. Program. Ser. B*, 2003, doi: 10.1007/s10107-002-0331-0.

[154] H. Siahkali and M. Vakilian, "Stochastic unit commitment of wind farms integrated in power system," *Electr. Power Syst. Res.*, 2010, doi: 10.1016/j.epsr.2010.01.003.

[155] M. E. Baran and F. F. Wu, "Network reconfiguration in distribution systems for loss reduction and load balancing," *IEEE Trans. Power Deliv.*, vol. 4, no. 2, pp. 1401–1407, 1989, doi: 10.1109/61.25627.

[156] H. D. Chiang and R. Jean-Jumeau, "Optimal network reconfigurations in distribution systems: Part 2: Solution algorithms and numerical results," *IEEE Trans. Power Deliv.*, 1990, doi: 10.1109/61.58002.

[157] S. H. Dolatabadi, M. Ghorbanian, P. Siano, and N. D. Hatziargyriou, "An Enhanced IEEE 33 Bus Benchmark Test System for Distribution System Studies," *IEEE Trans. Power Syst.*, p. 1, 2020, doi: 10.1109/TPWRS.2020.3038030.

[158] T. Bobmann and I. Staffell, "The shape of future electricity demand: Exploring load curves in 2050s Germany and Britain," *Energy*, vol. 90, pp. 1317–1333, 2015, doi: 10.1016/j.energy.2015.06.082.

[159] H. Sangrody, M. Sarailoo, N. Zhou, N. Tran, M. Motalleb, and E. Foruzan, "Weather forecasting error in solar energy forecasting," *IET Renew. Power Gener.*, vol. 11, no. 10, pp. 1274–1280, 2017, doi: 10.1049/iet-rpg.2016.1043.

[160] Western Power Distribution, "Changing Load Profiles," 2018.

[161] H. Xin, Z. Qu, J. Seuss, and A. Maknouninejad, “A self-organizing strategy for power flow control of photovoltaic generators in a distribution network,” *IEEE Trans. Power Syst.*, 2011, doi: 10.1109/TPWRS.2010.2080292.

[162] H. E. Farag, E. F. El-Saadany, and R. Seethapathy, “A two ways communication-based distributed control for voltage regulation in smart distribution feeders,” *IEEE Trans. Smart Grid*, 2012, doi: 10.1109/TSG.2011.2167355.

[163] A. T. Procopiou and L. F. Ochoa, “On the limitations of volt-var control in pv-rich residential lv networks: A UK case study,” 2019, doi: 10.1109/PTC.2019.8810797.

[164] F. Ding, B. Mather, and P. Gotseff, “Technologies to increase PV hosting capacity in distribution feeders,” in *IEEE Power and Energy Society General Meeting*, 2016, vol. 2016-Novem, doi: 10.1109/PESGM.2016.7741575.

[165] T. Adefarati and R. C. Bansal, “Chapter 2 - Energizing Renewable Energy Systems and Distribution Generation,” A. Taşcıkaraoğlu and O. B. T.-P. to a S. P. S. Erdinç, Eds. Academic Press, 2019, pp. 29–65.

[166] S. R. Deeba, R. Sharma, T. K. Saha, D. Chakraborty, and A. Thomas, “Evaluation of technical and financial benefits of battery-based energy storage systems in distribution networks,” *IET Renew. Power Gener.*, 2016, doi: 10.1049/iet-rpg.2015.0440.

[167] A. Azizivahed *et al.*, “Energy management strategy in dynamic distribution network reconfiguration considering renewable energy resources and storage,” *IEEE Trans. Sustain. Energy*, 2020, doi: 10.1109/TSTE.2019.2901429.

[168] P. Hasanpor Divshali and L. Soder, “Improving Hosting Capacity of Rooftop PVs by Quadratic Control of an LV-Central BSS,” *IEEE Trans. Smart Grid*, vol. 10, no. 1, pp. 919–927, 2019, doi: 10.1109/TSG.2017.2754943.

[169] A. Procopiou and K. Petrou, “Advanced Planning of PV-Rich Distribution Networks Deliverable 3: Traditional Solutions,” 2020.

[170] K. Strunz, E. Abbasi, R. Fletcher, N. Hatziargyriou, R. Iravani, and G. Joos, *Benchmark Systems for Network Integration of Renewable and Distributed Energy Resources*. 2014.

[171] National Grid, “System Operability Framework Summary,” *UK Electr. Transm.*, 2017.

[172] E. Demirok, S. Kjær, D. Sera, and R. Teodorescu, *Three-Phase Unbalanced Load Flow Tool for Distribution Networks*. 2012.

[173] I. H. Altas and A. M. Sharaf, “A novel maximum power fuzzy logic controller for photovoltaic solar energy systems,” *Renew. Energy*, 2008, doi: 10.1016/j.renene.2007.03.002.

[174] M. Veerachary, T. Senjyu, and K. Uezato, “Neural-network-based maximum-power-point tracking of coupled-inductor interleaved-boost-converter-supplied PV system using fuzzy controller,” 2003, doi: 10.1109/TIE.2003.814762.

[175] P. Gabrielli, F. Fürer, G. Mavromatidis, and M. Mazzotti, “Robust and optimal design of multi-energy systems with seasonal storage through uncertainty analysis,” *Appl. Energy*, vol. 238, no. December 2018, pp. 1192–1210, 2019, doi:

10.1016/j.apenergy.2019.01.064.

[176] Y. Guo and C. Zhao, “Islanding-Aware Robust Energy Management for Microgrids,” *IEEE Trans. Smart Grid*, vol. 9, no. 2, pp. 1301–1309, 2018, doi: 10.1109/TSG.2016.2585092.

[177] K. S. Ayyagari, R. Gonzalez, Y. Jin, M. Alamaniotis, S. Ahmed, and N. Gatsis, “Artificial Neural Network-Based Adaptive Voltage Regulation in Distribution Systems using Data-Driven Stochastic Optimization,” 2019, doi: 10.1109/ECCE.2019.8912702.

[178] A. Chaturvedi, K. Prasad, and R. Ranjan, “Use of interval arithmetic to incorporate the uncertainty of load demand for radial distribution system analysis,” *IEEE Trans. Power Deliv.*, 2006, doi: 10.1109/TPWRD.2005.848436.

[179] K. Clark, N. W. Miller, and J. J. Sanchez-Gasca, “Modeling of GE wind turbine-generators for grid studies,” *Gen. Electr. Int. Tech. Rep.*, no. April, p. 46, 2010.

APPENDICES

Appendix A: 33 and 69 Node Test System Data

The lines nominal current I_{ln} is selected in such a way that the lines loading condition under the nominal system demand is at most 50%. In addition, the minimum lines nominal currents are assumed to be 70 Ampere [156].

The single line diagrams of the 33 node and 69 node test systems can be found in Figure 5-1 and Figure 5-5, respectively.

Table A-1. Parameters of the test feeders' transformers

Network	S_{trn} (kVA)	V_{hvn} (kV)	V_{lvn} (kV)	uk (%)	Re(uk)	Vector group
33-node	5750	66	12.66	6	0.96	Dyn11
69-node	6150	66	12.66	6	0.96	Dyn11

Table A-2. Loads nominal powers for the 33-node test feeder

Load	Bus	P_{ld}(kW)	Q_{ld} (kvar)
Load 02	2	100	60
Load 03	3	90	40
Load 04	4	120	80
Load 05	5	60	30
Load 06	6	60	20
Load 07	7	200	100
Load 08	8	200	100
Load 09	9	60	20
Load 10	10	60	20
Load 11	11	45	30
Load 12	12	60	35
Load 13	13	60	35
Load 14	14	120	80
Load 15	15	60	10
Load 16	16	60	20
Load 17	17	60	20
Load 18	18	90	40
Load 19	19	90	40
Load 20	20	90	40
Load 21-22	21,22	90	40
Load 23	23	90	50
Load 24	24	420	200
Load 25	25	420	200
Load 26	26	60	25
Load 27	27	60	25
Load 28	28	60	20
Load 29	29	120	70
Load 30	30	200	600
Load 31	31	150	70
Load 32	32	210	100
Load 33	33	60	40

Table A-3. The lines data for the 33-node test feeder

Line No.	Bus 1	Bus 2	R_l (Ω)	X_l (Ω)	I_{ln} (A)	Line No.	Bus 1	Bus 2	R_l (Ω)	X_l (Ω)	I_{ln} (A)
01	1	2	0.09	0.05	400	**17**	17	18	0.73	0.57	70
02	2	3	0.49	0.25	400	**18**	2	19	0.16	0.16	70
03	3	4	0.37	0.19	270	**19**	19	20	1.50	1.36	70
04	4	5	0.38	0.19	260	**20**	20	21	0.41	0.48	70
05	5	6	0.82	0.71	260	**21**	21	22	0.71	0.94	70
06	6	7	0.19	0.62	115	**22**	3	23	0.45	0.31	115
07	7	8	0.71	0.24	115	**23**	23	24	0.90	0.71	115
08	8	9	1.03	0.74	70	**24**	24	25	0.90	0.70	70
09	9	10	1.04	0.74	70	**25**	26	6	0.20	0.10	138
10	10	11	0.20	0.07	70	**26**	26	27	0.28	0.14	138
11	11	12	0.37	0.13	70	**27**	27	28	1.06	0.93	138
12	12	13	1.47	1.16	70	**28**	28	29	0.80	0.70	115
13	13	14	0.54	0.71	70	**29**	29	30	0.51	0.26	115
14	14	15	0.59	0.53	70	**30**	30	31	0.97	0.96	70
15	15	16	0.75	0.55	70	**31**	31	32	0.31	0.36	70
16	16	17	1.29	1.72	70	**32**	32	33	0.34	0.53	70

Table A-4. Loads nominal powers for the 69-node test feeder

Load	Bus	P_{ld}(kW)	Q_{ld} (kvar)	Load	Bus	P_{ld}(kW)	Q_{ld} (kvar)
Load 05	5	2.60	2.20	**Load 36**	36	26.0	18.55
Load 06	6	40.40	30.00	**Load 38**	38	24.0	17.0
Load 07	7	75.00	54.00	**Load 39**	39	24.0	17.0
Load 08	8	30.00	22.00	**Load 40**	40	1.20	1.0
Load 09	9	28.00	19.00	**Load 42**	42	6.0	4.30
Load 10	10	145.00	104.00	**Load 44**	44	39.22	26.30
Load 11	11	145.00	104.00	**Load 45**	45	39.22	26.30
Load 12	12	8.00	5.00	**Load 47**	47	79.0	56.40
Load 13	13	8.00	5.50	**Load 48**	48	384.70	274.50
Load 15	15	45.50	30.00	**Load 49**	49	384.70	274.50
Load 16	16	60.00	35.00	**Load 50**	50	40.50	28.30
Load 17	17	60.00	35.00	**Load 51**	51	3.60	2.70
Load 19	19	1.00	0.60	**Load 52**	52	4.35	3.50
Load 20	20	114.00	81.00	**Load 53**	53	26.40	19.00
Load 21	21	5.00	3.50	**Load 54**	54	24.0	17.20
Load 23	23	28.0	20.0	**Load 58**	58	100.0	72.0
Load 25	25	14.0	10.0	**Load 60**	60	1244.0	888.0
Load 26	26	14.0	10.0	**Load 61**	61	32.0	23.0
Load 27	27	26.0	18.6	**Load 63**	63	227.0	162.0
Load 28	28	26.0	18.6	**Load 64**	64	59.0	42.0
Load 32	32	14.0	10.0	**Load 65**	65	18.0	13.0
Load 33	33	9.50	14.00	**Load 66**	66	18.0	13.0
Load 34	34	6.00	4.00	**Load 67**	67	28.0	20.0
Load 35	35	26.0	18.55	**Load 68**	68	28.0	20.0

Table A-5. The lines data for the 69-node test feeder

line No.	bus 1	bus 2	R_l (Ω)	X_l (Ω)	I_{ln} (A)	line No.	bus 1	bus 2	R_l (Ω)	X_l (Ω)	I_{ln} (A)
1	LV	1	0.0005	0.0012	450	**36**	27e	02e	0.0044	0.0108	70
2	1	2	0.0005	0.0012	450	**37**	28e	27e	0.0640	0.1565	70
3	2	02e	0.0000	0.0000	450	**38**	65	28e	0.1053	0.1230	70
4	02e	3	0.0015	0.0036	450	**39**	66	65	0.0304	0.0355	70
5	3	4	0.0251	0.0294	320	**40**	66	67	0.0018	0.0021	70
6	4	5	0.3660	0.1864	320	**41**	67	68	0.7283	0.8509	70
7	5	6	0.3811	0.1941	320	**42**	68	69	0.3100	0.3623	70
8	6	7	0.0922	0.0470	320	**43**	69	70	0.0410	0.0478	70
9	7	8	0.0493	0.0251	320	**44**	70	88	0.0092	0.0116	70
10	8	9	0.8190	0.2707	115	**45**	88	89	0.1089	0.1373	70
11	9	10	0.1872	0.0619	115	**46**	89	90	0.0009	0.0012	70
12	10	11	0.7114	0.2351	70	**47**	35	3	0.0034	0.0084	115
13	11	12	1.0300	0.3400	70	**48**	35	36	0.0851	0.2083	115
14	12	13	1.0440	0.3450	70	**49**	36	37	0.2898	0.7091	115
15	13	14	1.0580	0.3496	70	**50**	37	38	0.0822	0.2011	70
16	14	15	0.1966	0.0650	70	**51**	7	40	0.0928	0.0473	70
17	15	16	0.3744	0.1238	70	**52**	40	41	0.3319	0.1114	70
18	16	17	0.0047	0.0016	70	**53**	8	42	0.1740	0.0886	208
19	17	18	0.3276	0.1083	70	**54**	42	43	0.2030	0.1034	208
20	18	19	0.2106	0.0696	70	**55**	43	44	0.2842	0.1447	208
21	19	20	0.3416	0.1129	70	**56**	44	45	0.2813	0.1433	208
22	20	21	0.0140	0.0046	70	**57**	45	46	1.5900	0.5337	208
23	21	22	0.1591	0.0526	70	**58**	46	47	0.7837	0.2630	208
24	22	23	0.3463	0.1145	70	**59**	47	48	0.3042	0.1006	208
25	23	24	0.7488	0.2475	70	**60**	48	49	0.3861	0.1172	208
26	24	25	0.3089	0.1021	70	**61**	49	50	0.5075	0.2585	208
27	25	26	0.1732	0.0572	70	**62**	50	51	0.0974	0.0496	70
28	2	27	0.0044	0.0108	70	**63**	51	52	0.1450	0.0738	70

29	27	28	0.0640	0.1565	70	**64**	52	53	0.7105	0.3619	70
30	28	29	0.3978	0.1315	70	**65**	53	54	1.0410	0.5302	70
31	29	30	0.0702	0.0232	70	**66**	10	55	0.2012	0.0611	70
32	30	31	0.3510	0.1160	70	**67**	55	56	0.0047	0.0014	70
33	31	32	0.8390	0.2816	70	**68**	11	57	0.7394	0.2444	70
34	32	33	1.7080	0.5646	70	**69**	57	58	0.0047	0.0016	70
35	33	34	1.4740	0.4873	70						

Appendix B: Extensive Studies

B1. The voltage and reactive power relation

Voltage concept fits in the local balance of the reactive power (kvar). Since voltage control is regional, the reactive power is the most significant source for voltage control to compensate for the mismatch between generation and demand. In the balancing process, the reactive power is responsible for regulating the voltage in the system, where voltage is directly proportional to the kvar in the grid. The graphical representation among the bus voltage and the reactive power is shown in Figure B-1, where the Q-V droop characteristic of the synchronous generator is presented. V_{nl} and V_{fl} denotes the no load and full load considerations where Q_{fl} refers to the full load operation of reactive power. When the power flow is high in the network, there is a need to consume reactive power. Counter wise, when the power flow is low, the electric networks tend to generate more reactive power. This concern reveals the need for more reactive power consuming units in the distribution systems [171].

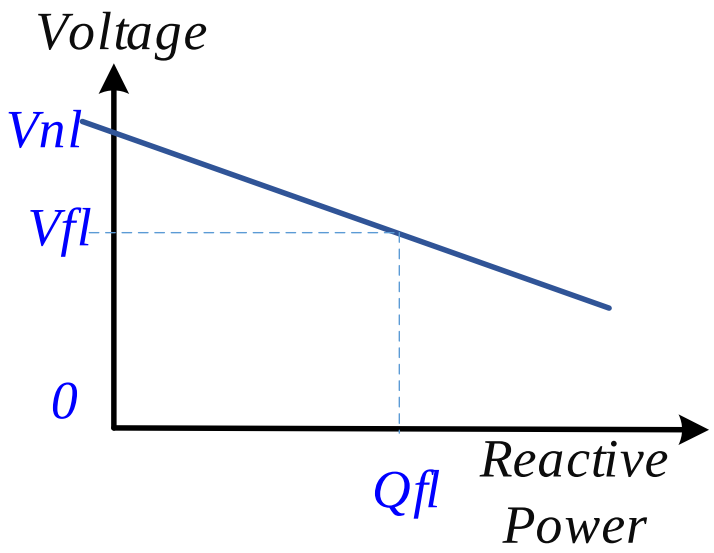

Figure B-1. Bus voltage alteration with reactive power for a SG

As mentioned in the introduction section, synchronous generation is declining in the future network, causing a reduction in the voltage support. Synchronous generators are those directly coupled to the electricity system and not through an inverter (e.g. thermal and hydroelectricity generation). That means the voltage control capabilities are also limited due to deprivation from the inherent dynamic overload capability of synchronous machines.

The future distribution system contains high renewable distributed generation, namely non-synchronous, which have more generation/demand imbalances due to their forecast uncertainty (e.g. wind speed and solar radiation). While both synchronous and non-synchronous providers can provide reactive power, synchronous providers contribute to the overall stability of the network is higher.

The static and dynamic voltage control devices are mostly used in the transmission network. Compared to the transmission network, fewer controllable sources of reactive power are present within the distribution networks. Therefore, the role of the DG inverters is very crucial to take over the part of synchronous units in the system to provide voltage support. By considering all the challenges, the voltage control capabilities within the control units must be detained in reserve during normal operation to be able to provide a dynamic response when a disturbance occurs.

B2. Sensitivity studies on the 33 bus test system

In this section, the sensitivity studies in previous section is extended to the studies on the considered 33 node test system. Another way of determining the sensitivity, the voltage sensitivity matrix, is identified. The radial distribution networks are mostly considered to be analysed under unbalanced load flow simulations due to the characteristic of loads (e.g., single or three-phase loads). Unbalances are regular in DNs since household electrical and PV units are usually single-phase [172]. In this study, the unbalanced load-flow studies are performed in the distribution network to verify the effectiveness of the proposed approach. This part of the study demonstrates sensitivity studies on the selected 33 node distribution network illustrated in Figure 5-1.

Load flow studies are performed for defining the voltage sensitivity matrix S, constituted by solving two nonlinear load flow equation using Newton– Raphson algorithm. Iterations update the system Jacobian matrix till convergence tolerance is fulfilled, and the inverse of Jacobian matrix is used to calculate S matrix. In equations (B.1) - (B.4) where P, Q, U, δ, Y and θ represent the active power flow, reactive power flow, phasor bus voltage, voltage angle, line admittance, and impedance angle, respectively.

$$P_i = |U_i| \sum_{(j=1)}^{n} |U_j| |Y_{ij}| cos(\theta_{ij} - \delta_i + \delta_j)| \tag{B.1}$$

$$Q_i = -|U_i| \sum_{(j=1)}^{n} |U_j| |Y_{ij}| \sin(\theta_{ij} - \delta_i + \delta_j)| \tag{B.2}$$

$$\begin{bmatrix} \Delta\theta \\ \Delta U \end{bmatrix} = \begin{bmatrix} S_{\theta P} S_{\theta Q} \\ S_{UP} S_{UQ} \end{bmatrix} \tag{B.3}$$

$$S = J^{-1} = \begin{bmatrix} S_{\theta P} & S_{\theta Q} \\ S_{UP} & S_{UQ} \end{bmatrix} \quad \text{(B.4)}$$

The focus of the studies are emphasised on the active and reactive power variations with voltage magnitude variation S_{UP} and S_{UQ} , respectively. The voltage sensitivity of the system to active power ($S_{UP} = dv / dP$), the voltage variations at each PV output terminal due to the active power changes of all the PV inverters in the system is investigated.

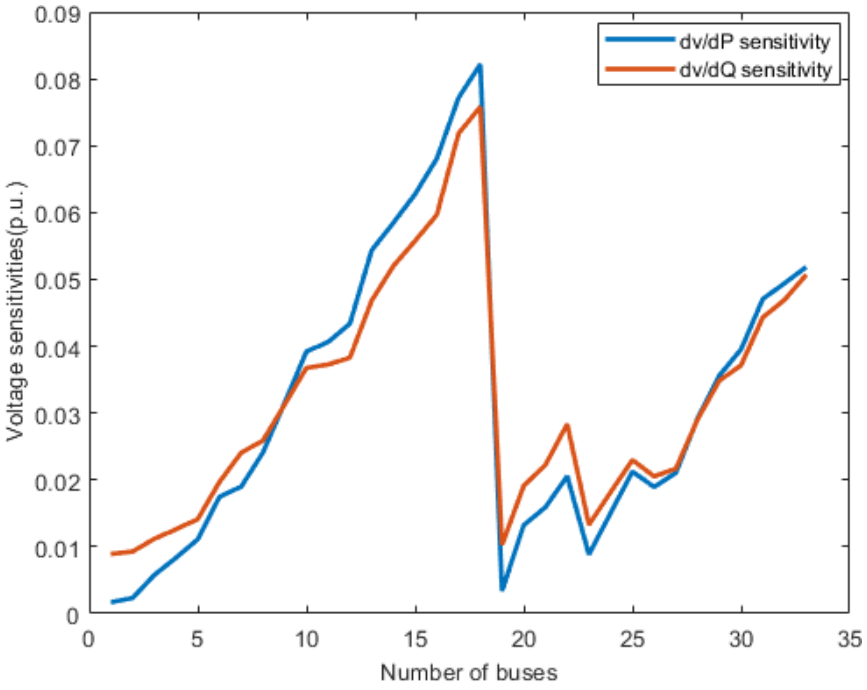

Figure B-2. Bus Voltage sensitivities to active and reactive power injection

Figure B-2, illustrates the voltage sensitivity of the system to active power ($S_{UP} = dv / dP$) and reactive power ($S_{UQ} = dv / dQ$). S_{UQ} is higher when PV is closer to the transformer. The effect of the injections of P and Q at each bus bar is evaluated for the bus bar itself. It is obvious that the sensitivity increases along the line until the end of the feeder. Therefore, it attracts more consideration and voltage regulation studies to be performed at the end of the feeder.

Figure B-3, illustrates the voltage profile of the system with different local control strategies. From the figure, the proposed control strategy has the most superior voltage value at the end of the feeder and while the voltage increment with the Power Factor-P control is higher compared Q-voltage and proposed strategy. If the voltage upper limit is considered as 1.05 *p.u.*, all standard control methods have overvoltage nodes whereas the proposed control strategy has only one node to surpass the voltage limit.

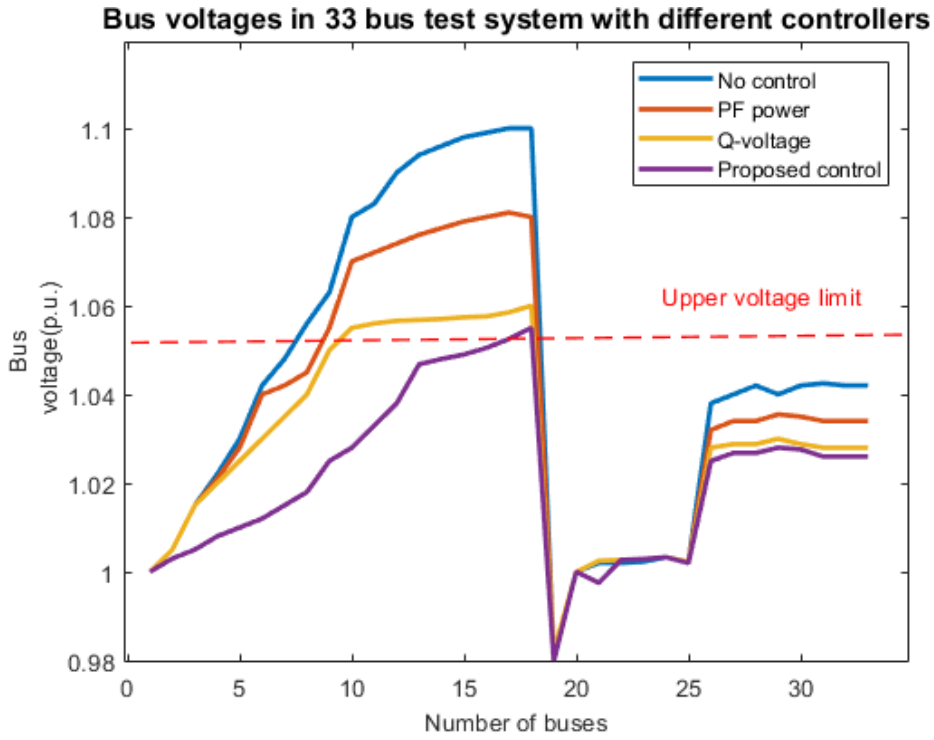

Figure B-3. Voltage profile of the network buses with studied voltage control methods

As can be observed, the proposed controller can enhance the voltage profile of the system considerably in compare to other local voltage control techniques. Noticeably, when the generation is peak during the day times, the voltage would be high as explained in the mathematical equations for ADNs.

Q-voltage strategy improves the voltage at the end of feeder, by reducing the voltage level. Supporting the sensitivity studies in Section 3.3.1. Standard Reactive Power Strategies (PF-

power and Q-voltage strategies), the voltage sensitivity matrix proves that Q-Voltage control should be taken into consideration for the use in the proposed local control, as the supporting voltage control method.

B3. Fundamental approaches to solve uncertainties

Approximate methods: Simplifies the stochastic environment using approximate formulas in the process of computing the statistical moments of random variables. One of the well-known application of approximate methods is their use with point estimate method [56].

Fuzzy methods: In fuzzy methods the characteristic of random variables can be modelled by expert linguistic expressions. The fuzzy models proposed so far are not able to model interdependency of random variables [173], [174].

Robust optimization method: The strategy of robust optimization is to minimize or maximize the objective function under the worst-case bounds of random variables. In robust optimisation, uncertainty is described in given interval uncertainty sets to optimize PV against risk and worst-case scenarios [175]. In [176], a two-stage adaptive robust optimization method is considered for microgrid energy management considering renewable generation uncertainties. Robust optimisation is appropriate when limited information is available, and low computation complexity is requested. It doesn't need probabilistic information, whereas it only uses a set-based representation for uncertainty. Ref. [177] uses the convex approximation of chance-constrained optimal power flow to compute PV reactive power set points with considering uncertainties, resulted in improvement in terms of grid losses. Hence, robust optimisation doesn't match the needs of representing decentralised energy systems such as, PV, WT, BESS, because of the variable and independent input profiles and are not suitable for long term applications.

Interval optimization: Minimizes or maximizes the objective function under the predefined bounds of random variables by decision-maker. Nevertheless, this method is the lack of modelling the correlations between the intervals [178].

Appendix C: Microgrid Test System

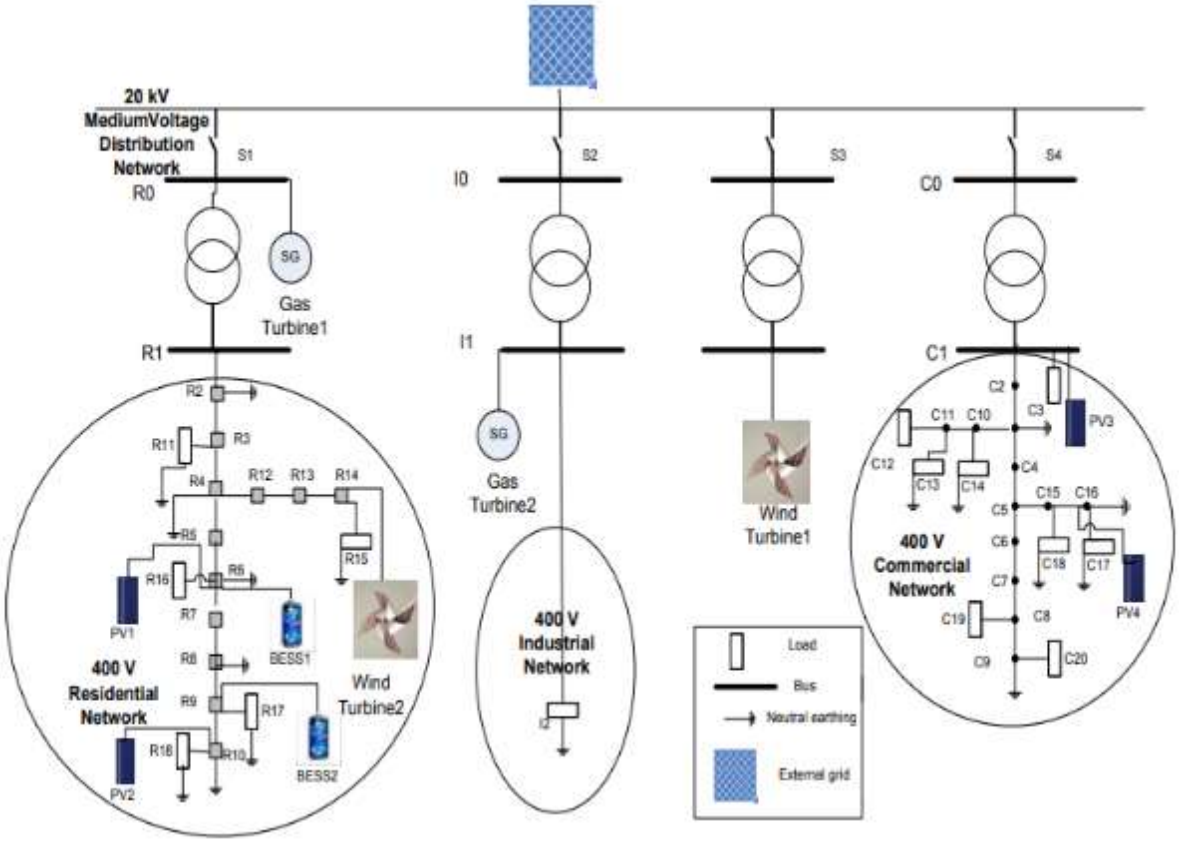

Figure C-1. CIGRE MV/LV Distribution Network- Benchmark model for microgrid studies

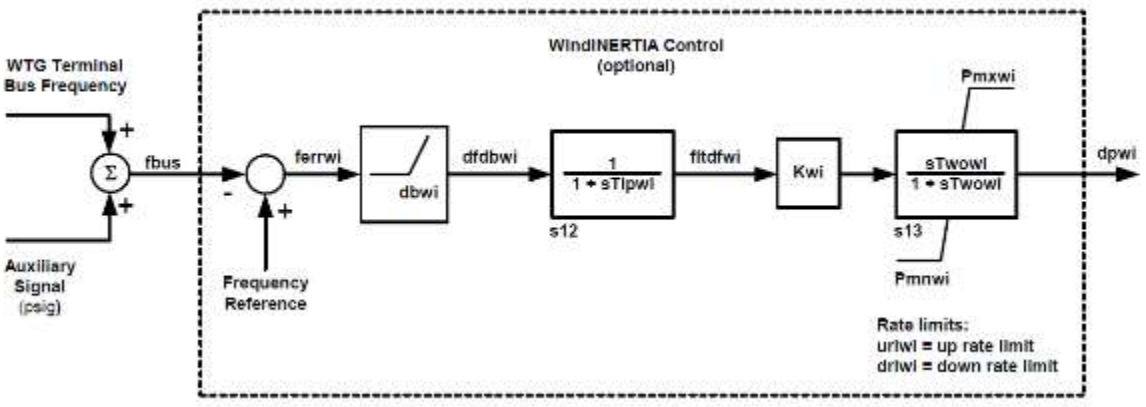

Figure C-2. GE Wind Turbine inertial emulator model[179]

Table C-1. Connections and line parameters of residential feeder of European distribution network Benchmark

Line segment	Node from	Node to	Conductor ID	L (m)	Installation
1	R1	R2	UG1	35	UG 3-ph
2	R2	R3	UG1	35	UG 3-ph
3	R3	R4	UG1	35	UG 3-ph
4	R4	R5	UG1	35	UG 3-ph
5	R5	R6	UG1	35	UG 3-ph
6	R6	R7	UG1	35	UG 3-ph
7	R7	R8	UG1	35	UG 3-ph
8	R8	R9	UG1	35	UG 3-ph
9	R9	R10	UG1	35	UG 3-ph
10	R10	R11	UG3	35	UG 3-ph
11	R11	R12	UG3	35	UG 3-ph
12	R12	R13	UG3	35	UG 3-ph
13	R13	R14	UG3	35	UG 3-ph
14	R14	R15	UG3	35	UG 3-ph
15	R15	R16	UG3	35	UG 3-ph
16	R16	R17	UG3	35	UG 3-ph
17	R17	R18	UG3	35	UG 3-ph

Table C-2. Connections and line parameters of commercial feeder of European distribution network benchmark

Line segment	Node from	Node to	Conductor ID	L (m)	Installation
1	C1	C2	OH1	30	OH 3-ph
2	C2	C3	OH1	30	OH 3-ph
3	C3	C4	OH1	30	OH 3-ph
4	C4	C5	OH1	30	OH 3-ph
5	C5	C6	OH1	30	OH 3-ph
6	C6	C7	OH1	30	OH 3-ph
7	C7	C8	OH1	30	OH 3-ph
8	C8	C9	OH1	30	OH 3-ph
9	C3	C10	OH2	30	OH 3-ph
10	C10	C11	OH2	30	OH 3-ph
11	C11	C12	OH3	30	OH 3-ph
12	C11	C13	OH3	30	OH 3-ph
13	C10	C14	OH3	30	OH 3-ph
14	C5	C15	OH2	30	OH 3-ph
15	C15	C16	OH2	30	OH 3-ph
16	C15	C17	OH3	30	OH 3-ph

Table C-3. Connections and line parameters of industrial feeder of European distribution network Benchmark

Line segment	Node from	Node to	Conductor ID	L (m)	Installation
1	I1	I2	UG2	200	UG 3-ph

Table C-4. Primitive impedance matrices of overhead lines of European distribution network benchmark

Conductor ID/ Installation		**The primitive impedance matrix [Ω/km]**			
		A	**B**	**C**	**D**
OH1 / 3-ph	A	0.540 + j0.777	0.049 + j0.505	0.049 + j0.462	0.049 + j0.436
	B	0.049 + j0.505	0.540 + j0.777	0.049 + j0.505	0.049 + j0.462
	C	0.049 + j0.462	0.049 + j0.505	0.540 + j0.777	0.049 + j0.505
	N	0.049 + j0.436	0.049 + j0.462	0.049 + j0.505	0.540 + j0.777
OH2 / 3-ph	A	1.369 + j0.812	0.049 + j0.505	0.049 + j0.462 0.	049 + j0.436
	B	0.049 + j0.505	1.369 + j0.812	0.049 + j0.505	0.049 + j0.462
	C	0.049 + j0.462	0.049 + j0.505	1.369 + j0.812	0.049 + j0.505
	N	0.049 + j0.436	0.049 + j0.462	0.049 + j0.505	1.369 + j0.812
OH3 / 3-ph	A	2.065 + j0.825	0.049 + j0.505	0.049 + j0.462	0.049 + j0.436
	B	0.049 + j0.505	2.065 + j0.825	0.049 + j0.505	0.049 + j0.462
	C	0.049 + j0.462	0.049 + j0.505	2.065 + j0.825	0.049 + j0.505
	N	0.049 + j0.436	0.049 + j0.462	0.049 + j0.505	2.065 + j0.825

Table C-5. Primitive impedance matrices of underground lines of European distribution network benchmark

Conductor ID/ Installation		**The primitive impedance matrix [Ω/km]**			
		A	**B**	**C**	**D**
UG1 / 3-ph	A	0.211 + j0.747	0.049 + j0.673	0.049 + j0.651	0.049 + j0.673
	B	0.049 + j0.673	0.540 + j0.747	0.049 + j0.673	0.049 + j0.651
	C	0.049 + j0.651	0.049 + j0.673	0.211 + j0.747	0.049 + j0.673
	N	0.049 + j0.673	0.049 + j0.651	0.049 + j0.673	0.540 + j0.747
UG2 / 3-ph	A	0.314 + j0.762	0.049 + j0.687	0.049 + j0.665	0.049 + j0.687
	B	0.049 + j0.687	0.314 + j0.762	0.049 + j0.687	0.049 + j0.665
	C	0.049 + j0.665	0.049 + j0.687	0.314 + j0.762	0.049 + j0.687
	N	0.049 + j0.687	0.049 + j0.665	0.049 + j0.687	0.314 + j0.762
UG3 / 3-ph	A	0.871 + j0.797	0.049 + j0.719	0.049 + j0.697	0.049 + j0.719
	B	0.049 + j0.719	0.871 + j0.797	0.049 + j0.719	0.049 + j0.697
	C	0.049 + j0.697	0.049 + j0.719	0.871 + j0.797	0.049 + j0.719
	N	0.049 + j0.719	0.049 + j0.697	0.049 + j0.719	0.871 + j0.797

Table C-6. Transformer parameters of European distribution network benchmark

Node from	**Node to**	**Connection**	**V1 (kV)**	**V2 (kV)**	**Ztr (Ω)**	**Srated (kVA)**
R0	R1	3-ph Dyn1	20	0.4	0.0032+j0.0128	500
I0	I1	3-ph Dyn1	20	0.4	0.0107+j0.0427	150
C0	C1	3-ph Dyn1	20	0.4	0.0053+j0.0213	300

Table C-7. Load Parameters for European Network

Node	Apparent Power, *S* [kVA]	Power Factor, *pf*
R1	200	0.95
R11	15	0.95
R15	52	0.95
R16	55	0.95
R17	35	0.95
R18	47	0.95
I2	100	0.85
C1	120	0.90
C12	20	0.90
C13	20	0.90
C14	25	0.90
C17	25	0.90
C18	8	0.90
C19	16	0.90
C20	8	0.90

Table C-8. GE wind inertia model parameters [179]

Variable	Value
K	10
db	0.0025
Tlp	1
Two	5.5
Pmax	0.1
Pmin	0